THE EFFECTS OF P22PHOX GENETIC POLYMORPHISMS AND NATURAL COMPOUNDS ON REACTIVE OXYGEN SPECIES FORMATION

by

Scott David Whitehouse

Submitted in partial fulfilment of the requirements
for the degree of Master of Science

at

Dalhousie University
Halifax, Nova Scotia
February 2013

DALHOUSIE UNIVERSITY

DEPARTMENT OF PATHOLOGY

The undersigned hereby certify that they have read and recommend to the Faculty of Graduate Studies for acceptance a thesis entitled "THE EFFECTS OF P22PHOX GENETIC POLYMORPHISMS AND NATURAL COMPOUNDS ON REACTIVE OXYGEN SPECIES FORMATION" by Scott David Whitehouse in partial fulfillment of the requirements for the degree of Master of Science.

Dated: February 21, 2013

Supervisor: _____

Readers: _____

_____

_____

DALHOUSIE UNIVERSITY

DATE: February 21, 2013

AUTHOR: Scott David Whitehouse

TITLE: THE EFFECTS OF P22PHOX GENETIC POLYMORPHISMS AND NATURAL COMPOUNDS ON REACTIVE OXYGEN SPECIES FORMATION

DEPARTMENT OR SCHOOL: Department of Pathology

DEGREE: MSc CONVOCATION: May YEAR: 2013

_____

Signature of Author

Were I to await perfection, it would never be finished.

— Chinese Proverb

Table of Contents

LIST OF TABLES

LIST OF FIGURES

ABSTRACT

Reactive oxygen species (ROS) have a role in cardiovascular health and disease. This study was undertaken to determine if ROS formation is influenced by either common genetic variations in $p22^{phox}$, a subunit of the ROS generating enzyme NOX1, or by natural plant compounds with cardiovascular benefits. Hydrogen peroxide production was measured using Amplex Red, and superoxide generation was measured using NBT and MCLA. Each of seven $p22^{phox}$ variants supported ROS generation by NOX1. No differences were found in the rate of ROS production; however, unequal transfer of the $p22^{phox}$ gene may be a confounding factor. A variation in the 3'UTR of the $p22^{phox}$ gene led to lower $p22^{phox}$ protein levels, whereas none of the other variations affected mRNA or protein expression. The natural compound resveratrol acts as an antioxidant towards hydrogen peroxide, but not superoxide. Resveratrol does not inhibit NOX1 activity.

LIST OF ABBREVIATIONS AND SYMBOLS USED

2K7	Two Cassette
3' UTR	Three Prime Untranslated Region
°	Degrees
$^{\bullet}O_2^-$	Superoxide
$^{\bullet}OH$	Hydroxyl Radical
ADP	Adenosine Diphosphate
α	Alpha
AR	Amplex Red
Ab	Antibody
Abs	Antibodies
ANOVA	Analysis of Variance
AP-1	Activator Protein 1
AT1R	Angiotensin II Type 1 Receptor
ATCC	American Tissue Culture Collection
AU	Arbitrary Units
β	Beta
β-ME	Beta-Mercaptoethanol
bp	Base Pair
BSA	Bovine Serum Albumin
B-LCL	B-Lymphoblastoid Cell Line
C	Celsius
cm	Centimeter
cPPT	Central Polypurine Tract
CuZnSOD	Copper-Zinc Superoxide Dismutase
CVD	Cardiovascular Disease
cDNA	Complementary Deoxyribonucleic Acid
CMV	Cytomegalovirus
cDNA	Complementary DNA
DNA	Deoxyribonucleic Acid
DAG	Diacylglycerol

DPI	Diphenyleneiodonium
ddH_2O	Double-distilled Water
DMEM	Dulbecco's Modified Eagle's Medium
DMSO	Dimethyl Sulfoxide
dNTP	Deoxyribonucleotide Triphosphate
DUOX	Dual Oxidase
EDTA	Ethylenediaminetetraacetic Acid
EGTA	Ethylene Glycol Tetraacetic Acid
eNOS	Endothelial Nitric Oxide Synthase
ECL	Enhanced Chemiluminescence
ERK	Extracellular-Signal-Regulated Kinase
EtOH	Ethanol
FACS	Fluorescence-Activated Cell Sorting
FAD	Flavin Adenine Dinucleotide
FBS	Fetal Bovine Serum
GPx	Glutathione Peroxidase
GSH	Glutathione
GSSG	Glutathione Disulfide
g	Gravity
GFP	Green Fluorescent Protein
GTP	Guanosine Triphosphate
GR	Glutathione Reductase
H^+	Hydrogen Cation
H_2O_2	Hydrogen Peroxide
HBSS	Hank’s Buffered Salt Solution
HEK293T	Human Embryonic Kidney 293T
HEPES	4-(2-Hydroxyethyl)-1-Piperazineethanesulfonic Acid
HeBS	HEPES-buffered Saline Solution
HRP	Horseradish Peroxidase
PFA	Paraformaldehyde
ONOO-	Peroxynitrite

PSI	Pound-force Per Square Inch
PHOX	Phagocytic Oxidative
IC50	Inhibitory Concentration Half Maximal
IκB	Inhibitor of Kappa B
IKK	IκB Kinase
JNK	c-Jun N-Terminal Kinase
κ	Kappa
kb	Kilo Base Pairs
kDa	Kilodaltons
LB	Lysogeny Broth
LPS	Lipopolysaccharide
MAPK	Mitogen-Activated Protein Kinase
MCLA	Methyl Cypridina Luciferin Analog
MEK	MAPK/ERK Kinase
mETC	Mitochondria Electron Transport Chain
MIB	Mitochondrial Isolation Buffer
min	Minute
µg	Microgram
µL	Microlitre
µM	Micromolar
mg	Milligram
mL	Millilitre
mM	Millimolar
min	Minute
MAPK	Mitogen Activated Protein Kinsae
MMPs	Matrix Metalloproteinases
MnSOD	Manganese Superoxide Dismutase
mRNA	Messenger RNA
NADPH	Nicotinamide Adenine Dinucleotide Phosphate
NBT	Nitro Blue Tetrazolium
NF-κB	Nuclear Factor κ-Light-Chain-Enhancer of Activated B Cells

nm	Nanometer
nM	Nanomolar
NO	Nitric Oxide
NOX	NADPH Oxidase
NOXA1	NOX Activating Subunit 1
NOXO1	NOX Organizing Subunit 1
Prxd	Peroxiredoxin
PAGE	Polyacrylamide Gel Electrophoresis
PBS	Phosphate Buffered Saline
PCR	Polymerase Chain Reaction
PDGF	Platelet-Derived Growth Factor
PHOX	Phagocytic Oxidase
PIP_3	Phosphatidylinositol Triphosphate
PVFD	Polyvinylidene Difluoride
PKC	Protein Kinase C
PMA	Phorbol 12-Myristate 13-Acetate
PMSF	Phenylmethylsulfonyl Fluoride
PTP	Protein Tyrosine Phosphatases
PI	Protease Inhibitors
qPCR	Quantitative Polymerase Chain Reaction
qRT-PCR	Quantitative Reverse Transcription Polymerase Chain Reaction
RNA	Ribonucleic Acid
RNS	Reactive Nitrogen Species
ROS	Reactive Oxygen Species
RPMI	Roswell Park Memorial Institute
RT	Reverse Transcription
SD	Standard Deviation
SDS-PAGE	Sodium Dodecyl Sulphate Polyacrylamide Gel Electrophoresis
Sec	Second
SEM	Standard Error of the Mean
SH3	SRC Homology 3

SNP	Single Nucleotide Polymorphism
SO	Superoxide
SOC	Super Optimal Broth with Catabolite Repression
SOD	Superoxide Dismutase
TrxR	Thioredoxin Reductase
TNF	Tumor Necrosis Factor
VEGF	Vascular Endothelial Growth Factor
VSMC	Vascular Smooth Muscle Cells
WPRE	Woodchuck Hepatitis Virus Post-transcriptional Regulatory Element
XO	Xanthine Oxidase

ACKNOWLEDGEMENTS

I am happy to thank my supervisor, Dr. Karen Bedard, for her endless enthusiasm and support over the years. Her guidance and teachings have encouraged my love of research. I would also like to extend gratitude to my co-supervisor, Dr. David Hoskin, for his prudent advice and insight, and to my committee members, Dr. Brent Johnston, and Dr. David Waisman for their caring assistance.

I am indebted to my lab-mates in the Bedard lab for their unwavering support, positive attitudes, and for helping me improve my techniques. The stories and laughs we have shared have made my time in the lab a tremendously enjoyable experience.

I would also like to offer thanks Anna Greenshields, Emilie Lefort for supplying reagents and compounds, and to Barry Kennedy for instruction on mitochondrial isolation.

Finally, I would like to thank my friends and family for their endless understanding and support. Without you, none of this would have been possible.

CHAPTER 1: INTRODUCTION

1.1 Reactive Oxygen Species

Reactive oxygen species (ROS) are strong oxidizing agents derived from oxygen, and include two major groups: free radicals exhibiting an unpaired electron, such as superoxide ($^{\bullet}O_2^-$), nitric oxide (NO), and the hydroxyl radical ($^{\bullet}OH$), and non-radicals, such as hydrogen peroxide (H_2O_2) and peroxynitrite ($ONOO^-$), among others (reviewed Bedard, 2007; Paravicini & Touyz, 2008). The initial observation of ROS dates back to 1932, and was first described as a respiratory phenomenon resulting from phagocytic leukocytes (Baldridge & Gerard, 1932). Approximately thirty years later this rapid increase in ROS concentration became known as a respiratory burst or phagocytic oxidative (PHOX) burst, and it soon became apparent that superoxide and hydrogen peroxide were involved in these burst events (Iyer et al., 1961; Babior et al., 1973). There are now many known sources of ROS in mammalian cells: peroxisomes, NADPH oxidase (NOX), mitochondrial respiration, endothelial nitric oxide synthase (eNOS), xanthine oxidase (XO), and drug metabolism to name a few (Boveris et al., 1972; O'Donnell & Azzi, 1996; Starkov, 2008; Kukreja et al. 1986; McNally et al., 2003; Paravicini & Touyz, 2008). While initially thought of as harmful byproducts of cellular respiration, it has become apparent that ROS are crucial components of cellular signaling and of the immune system (Sundaresan et al., 1995; Quie et al., 1967; Ray et al,. 2012, Reuter et al., 2011).

One of the most basic forms of ROS is superoxide, which is a free radical that forms when molecular oxygen is reduced through the transfer of an electron from a source such as nicotinamide adenine dinucleotide phosphate (NADPH). Reactions involving the creation of various ROS are depicted in Figure 1. When superoxide is further reduced and interacts with hydrogen ions, it forms H_2O_2, a more stable and potent ROS molecule (Bielski, 1985). Due to the spin behavior of superoxide's valence electrons it is unable to react with non-radical molecules, resulting in superoxide mainly interacting with other superoxide radicals, but it can also interact with other radicals, or transition metals, such as those found in the various forms of the superoxide dismutase (SOD) enzyme (Cadenas, 1989; Klotz, 2002; Apel & Hirt, 2004). Although superoxide can be converted to H_2O_2 through interaction with SOD, it can also create H_2O_2 nonenzymatically through rapid and spontaneous dismutation. Unlike H_2O_2, superoxide does not readily cross cellular membranes, thereby creating distinct concentrations of superoxide in vesicles, extracellularly, and even in mitochondria, depending on the source (Doonan et al., 2008). Superoxide can also interact with nitric oxide (NO) to form the highly reactive molecule peroxynitrite ($ONOO^-$). Another highly reactive molecule, the hydroxyl radical, can be created by the reduction of H_2O_2 by superoxide, and by the Fenton reaction, the second step in the Haber−Weiss reaction (Apel & Hirt, 2004; Lloyd et al., 1997) (Figure 1). The hydroxyl radical is responsible for much of the oxidative damage, with lipids being a prime target (Cabiscolet al., 2010). The main effect of lipid oxidative damage is ultimately a reduction in membrane fluidity, which has a negative effect on membrane bound proteins. The hydroxyl radical can also damage DNA by causing breaks in the phosphate-deoxyribose backbone, which has the negative effect of

preventing replication. The hydroxyl radical can also target proteins, causing dysfunction through peptide fragmentation, protein cross-linking, and reactions with parts of the protein, to name a few (Cabiscolet al., 2010). The superoxide radical is not itself a strong reductant or oxidant, unlike the downstream hydroxyl and peroxynitrite molecules (Bielski, 1985). In order to prevent harmful buildups of these highly reactive molecules, mammalian cells have methods of scavenging them before they cause oxidative damage.

The importance of the balance between ROS production and ROS removal with regards to proper cell function has become more apparent. The regulatory process that keeps the concentrations of ROS and reactive nitrogen species (RNS) in check is known as redox homeostasis (reviewed in Dröge, 2002). At concentrations that are typically considered low, ROS can facilitate cell signalling, but consistently high concentrations can trigger signalling cascades that ultimately cause an increase in the production of antioxidant enzymes (Trachootham et al., 2008). As such, the proportion of oxidants to antioxidants is crucial to stable cell function. Superoxide is able to bind with the vasodialator nitric oxide, and a lack of appropriate superoxide scavenging can dramatically decrease levels of nitric oxide, thereby causing a hypertensive situation in the vasculature (Morrell, 2008). There are enzymatic antioxidants: SOD, glutathione peroxidase, catalase, and nonenzymatic antioxidants: glutathione, α-tocopherol (vitamin E), and ascorbate (vitamin C), to name a few (reviewed in Dröge, 2002).

SOD, catalase, thioredoxin reductase (TrxR), peroxiredoxin (Prxd), and glutathione peroxidase (GPx) are some of the many forms of ROS scavengers present in mammalian cells (Nordberg & Arnér, 2001; Sies, 1993). A ROS scavenger is also referred to as an antioxidant, with the term applying to compounds and enzymes alike.

Since ROS are capable of activating signaling pathways, the enzymes listed above are important in homeostasis, as they influence cellular signal transduction by altering the concentration of ROS within the cell (Nathan, 2003).

First discovered by McCord and Fridovich in 1969, SOD are metal-containing enzymes that catalyze the conversion of superoxide to oxygen and H_2O_2 (Reviewed in Abreu & Cabelli, 2010). The two main types of SOD in humans are manganese SOD (MnSOD), and copper-zinc SOD (CuZnSOD), of which there are two forms: SOD1, a homodimer mainly found in the cytosol, and SOD3, a homotetramer mainly found extracellularly. SOD2 is a manganese-based homotetramer, and is mainly found in mitochondria.

Glutathione peroxidase has many isoforms found throughout the human body: GPx-1 is found in the cytosol, GPx-2 is found in the colon, GPx-3 is found extracellularly, and GPx-4 is found in mitochondria, the cytosol, and in the nucleus (Buettner & Wagner, 2011). Glutathione peroxidase catalyzes the reaction of H_2O_2 with glutathione (GSH) to produce water and also glutathione disulfide (GSSG), which is then reduced through the actions of glutathione reductase (GR) and nicotinamide adenine dinucleotide phosphate (NADPH) to produce $NADP^+$ and glutathione (Makino et al., 2004; Antunes & Cadena, 2000). A basic representation of the breakdown of H_2O_2 by catalase and glutathione is shown in Figure 1C and 1E.

Catalase, also known as hydroperoxidase, is a robust enzyme that catalyzes the breakdown of two H_2O_2 molecules to water and oxygen at a remarkably high rate, and for extended periods of time (Chelikani et al., 2003). In humans, catalase has been identified as the dominant mechanism of H_2O_2 removal, as it is approximately 12 times more

effective than GPx for the same concentration of H_2O_2 (Mueller et al., 1997). The steady-state levels of H_2O_2 in human tissues are considered to be between 1 x 10^{-9} and 1 x 10^{-6} M, a range at which neither catalase nor GPx are saturated (Mueller et al., 1997). It has been recently suggested that catalase is capable of producing the hydroxyl radical, but further testing is required (Goyal & Basak, 2012).

1.2 Molecular Targets of Reactive Oxygen Species

The acid constant, which indicates the extent to which an acid will dissociate in solution, is represented by the abbreviation Ka, with the negative base-10 logarithm being pKa. Typically cysteine, one of the least abundant amino acids within proteins, has a pKa of approximately 8.5 and is less readily oxidized; however, low pKa (4.5 – 5.5) regions within a protein, such as those found within certain cysteine residues, are highly susceptible to oxidation by ROS (Meng et al., 2006; Denuet al., 1998). This is an important factor within the cell, as many proteins involved in cell signaling and various other processes have cysteine residues that are susceptible to reversible and irreversible activation and deactivation through ROS oxidation. The behaviour of cysteine within proteins is complex, as it changes in response to physiological states and environmental conditions, such as protein surface exposure and the pH of the surrounding environment (Reviewed in Marino & Gladyshev, 2012). The high reactivity of the sulfur group within cysteine makes it an especially likely target of ROS-based oxidation. As a result, cysteine can have many effects within the cell, including catalytic activity, post-translational modification, and structural stabilization. ROS can be described as second messenger molecules, as they are intracellular molecules that work to amplify information

transmission from the membrane to the nucleus or cytoplasm (Forman et al., 2002). Furthermore, ROS have the required characteristics of a second messenger: ROS production is tightly regulated through enzymatic processes, ROS signalling actions are reversible through degradation or disassociation, and ROS have affinities for specific targets (Forman et al., 2004). While the signalling process carried out by ROS is often reversible, there are conditions in which the ROS-mediated oxidation transitions from reversible to irreversible. This can occur when there is an abundance or inability to remove ROS within a system, and when ROS are present for an extended period of time. A reversible situation occurs after cysteine oxidation forms sulfenic acid or disulfide bonds, but prolonged formation can result in an irreversible transition to sulfinic and finally sulfonic acids, which trigger cellular repair mechanisms (Forman et al., 2004; Lim et al., 2008). However, in 2003 it was suggested that sulfinic acids can be reversibly oxidized by sulfiredoxin, but little research has since been conducted in support of this notion (Woo et al., 2003; Rhee et al., 2007). Disulfide bonds can occur between oxidized cysteines and either other cysteines or glutathione, both of which can prevent the activity of ROS-specific targets. One of the best-studied targets of ROS regulation is protein tyrosine phosphatases (Morgan and Liu, 2011).

Protein tyrosine phosphatases (PTP) are enzymes that are involved in the regulation of cell signal transduction through the dephosphorylation of tyrosine residues. An influential area of cysteine oxidation is found within the protein tyrosine phosphatase protein, with H_2O_2 being the molecule responsible for oxidation (Meng et al., 2006). Oxidation of this cysteine residue promotes inactivation of PTP, thereby providing a plausible mechanism by which ROS can influence signaling pathways (Rhee et al.,

2000). Reversible oxidation of this functionally essential cysteine residue renders PTP inactive, disrupting cell signaling and influencing complex processes such as cell growth (Tonks, 2006). In a similar fashion, ROS can target cysteine residues on other important protein complexes.

ROS are involved in many cellular processes where they act as second messengers and influence cell proliferation and death (Martindale & Holbrook 2002; Menon & Goswami, 2007). As such, the localization and activity of ROS is tightly regulated (Terada, 2006; Bokoch, 1994). Transcriptional factors/activators are a major target of ROS, with some prominent targets being tumor suppressor protein 53 (p53), nuclear factor kappa-light-chain-enhancer of activated B cells (NF-κB), and activator protein 1 (AP-1) (Sun & Oberley, 1996). By targeting these proteins ROS can stimulate or inhibit gene expression, and affect cell survival. The p53 protein plays a crucial role in many organisms, where it regulates cell death through gene transcription in response to DNA-damaging cellular stresses, such as oxidative stress (Liu et al., 2008). NF-κB proteins also respond to DNA stress by controlling transcription, but are also tightly linked to cell growth and proper function of the immune system (reviewed by Morgan & Liu, 2011). ROS can interact with NF-κB in a number of ways, one of which is oxidation of a cysteine within the p50 subunit of NF-κB, which prevents binding with DNA. However, ROS-mediated regulation of NF-κB appears complex and cell-specific, as H_2O_2 is also capable of activating NF-κB in T-cells, and inhibiting NF-κB in lung epithelial cells (Schreck et al., 1991; Li & Karin, 1999; Korn et al., 2001). Like p53 and NF-κB, AP-1 is a transcription factor involved in cell proliferation and apoptosis (Shaulian, 2002). ROS can activate AP-1, as there are cysteine residues in its DNA binding region which are

highly susceptible to ROS oxidation (Abate et al., 1990; Aharoni-Simon et al., 2006). Given the effect ROS have on transcription factors involved in cell death and proliferation, it would be interesting to investigate if genetic polymorphisms in ROS-production enzymes have an effect on ROS production.

1.3 NADPH oxidase

Initially discovered in neutrophils and macrophages, the only known enzyme family that generates ROS as its sole function are the nicotinamide adenine dinucleotide phosphate oxidases (NOX)(Royer-Pokora et al., 1986). The NADPH cofactor required for NOXs biological activity is involved in many anabolic pathways (making molecules from smaller units) (Babior, 1999; Altenhöfer et al., 2012). There are seven members of the NOX family in mammalian cells: NOX1, NOX2, NOX3, NOX4, NOX5, DUOX1, and DUOX2 (reviewed in Bedard & Krause, 2007). The NOX homologues are depicted in Figure 5. While there are differences amongst the NOX enzymes, there are conserved portions found in all: the NADPH-binding site, FAD-binding site, six transmembrane domains, and four heme-binding histidines (reviewed in Bedard & Krause, 2007). In the case of NOX enzymes, the orientation of the enzyme is such that the electron derived from NADPH in the cytosol is transferred to an oxygen molecule the opposing side of the membrane.

Many factors can alter the amount of ROS produced by NOX, some of which will upregulate gene expression, while others will activate the enzyme system directly (Jiang *et al*., 2011). These factors include chemical (e.g. heavy metals), inflammatory (e.g. angiotensin II), and physical factors (e.g. ultra violet B radiation). Unique among the

NOX enzymes, NOX5 and DUOX activation are regulated by Ca^{2+} influx (reviewed in Bedard & Krause, 2007). NOXs 1-4 require subunits to function properly: NOX1-4 all require the co-expression of $p22^{phox}$ for stabilization in the membrane, and NOX1-3 require additional cytosolic subunits (Hanna, et al., 2004; Ueno et al., 2005; Ambasta et al., 2004; Cheng & Lambeth, 2004a; Cheng et al., 2004b; Volpp et al., 1988). These enzymes can require activator proteins like $p47^{phox}$ or NOXA1, and organizer proteins like $p67^{phox}$ or NOXO1. Their activity may also be influenced by other cytosolic proteins including $p40^{phox}$. Rac GTPases also influence NOX1-3 complexes, and while they are required for full NOX activation, are not considered true subunits since they control other cellular functions (Miyano & Sumimoto, 2012). The phosphorylation of $p47^{phox}$ is thought to disrupt an inhibitory intramolecular interaction, thereby exposing $p47^{phox}$ SH3 domains capable of binding to other NOX components (Sumimoto et al., 1994; Sumimoto et al., 1996; de Mendez et al., 1997). Phosphorylated $p47^{phox}$ or NOXO1 subunits will move to the cell surface and interact with membrane subunits to generate ROS in the extracellular space. In the case of NOX2, this can happen in intracellular vesicle membranes to produce ROS in the vesicle. Vesicles can then move to the extracellular membrane to release the ROS into the extracellular space where they can destroy pathogens (Reviewed in Bedard & Krause, 2007).

1.4 Cardiovascular Disease has a Genetic Component & Involvement of ROS in Hypertension

Cardiovascular disease (CVD), including ischemic heart disease, stroke, and myocardial infarction, is a deadly and costly disease, accounting for approximately 29% of all deaths in Canada, and costing the Canadian economy approximately $20.9 billion

in associated costs each year (Statistics Canada, 2011; Conference Board of Canada, 2010). Hypertension, a condition of chronically elevated blood pressure (≥140/90 mmHg), is a significant risk factor cardiovascular disease (Mancia et al., 2007; Kanne, 1996). Regulation of blood pressure is a complex process that involves numerous genetic and environmental factors involved (van Rijn et al., 2007; Vinck et al., 2001). Based on the results of a genome-wide association study of over 34 000 subjects of European ancestry, hypertension was associated with genetic components (Ehret, 2010). The possibility exists that genetic and environmental factors are linked, and therefore converge to some degree. One of these potential convergence points may be ROS, as NOX-derived ROS can influence CVD, including hypertension (Paravicini & Touyz, 2008; Cuzzocrea et al., 2004).The production of ROS is at least partially determined by genetics, but environmental factors that influence CVD risk, such as exercise, drugs, and diet can also influence ROS production (Forman et al., 2009; Minder et al., 2012). If it can be determined that cardiovascular risk is even minutely affected by genetic variation in ROS-production enzymes, this would be highly informative regarding CVD, and would support the hypothesis that controlling ROS would be therapeutically beneficial in CVD with a variety of underlying contributing factors. Previous studies have aimed to link genetic variations in ROS-producing enzymes with CVD risk; however, the missing link in these studies was any evidence that the genetic variations being examined influenced ROS production (San Jose et al., 2008; Brandes et al., 2010). This study aims to investigate the factors that determine ROS generation by first considering candidate genetic factors, and then by considering a number of biologically active compounds. NOX, a major source of ROS, is genetically variable (Lacey et al., 2000).

1.5 NOX and $p22^{phox}$ genetic variation

There are many forms of NADPH oxidase in the vasculature, with NOX1, NOX2, and NOX4 being the predominant forms, although the involvement of NOX5 is becoming more apparent, especially in diseased vessels (reviewed in Bedard and Krause, 2007; Guzik et al., 2008). A study involving NOX1 knockout mice demonstrated a role for NOX1 in blood pressure regulation and the vascular response to angiotensin II (Gavazzi et al., 2005). The NOX1-deficient mice had decreased basal blood pressure, and lost the ability to sustain an elevated blood pressure in response to angiotensin II, when compared to the control mice. The same group demonstrated that NOX1-deficient mice are protected from aortic dissection in response to angiotensin II (Gavazzi et al., 2007). Spontaneously hypertensive rats exhibited an increase in NOX1 and NOX2 expression, and a subsequent increase in vascular levels of ROS (Wind et al., 2010). As a direct result of increased ROS sequestering of NO, the rats had less NO in their vasculature, and more vasoconstriction as a result. In a swine model of hypertension induced by banding of the pulmonary artery, an increase in NOX1, NOX2, and NOX 4 expression was observed, and once again an increase in vascular ROS was observed (Lu et al., 2011). While the role of NOX in cardiovascular disease is becoming more apparent in animals models, the effect of NOX-based ROS on human cardiovascular risk is not well understood. Furthermore, the roles of the NOX isoforms throughout the body are even more poorly defined.

A genome-wide association study indicated that the phenotypic variation in H_2O_2 production by lymphoblastoid cells among individuals is at least partially controlled by genetics (Attar et al., 2008). In an attempt to further understand the role genetics has in

ROS production, and the connection between NOX-produced ROS and CVD, a candidate gene approach was taken to narrow down the number of potential genes responsible for ROS variations based on the known gene function (Bedard et al., 2009; Wyche et al., 2004; Zafari et al., 2002). The $p22^{phox}$ subunit forming a heterodimer with the main NOX subunit is essential for protein stability (Reviewed in Bedard & Krause, 2007). There exist NOX 2-deficient patients, and $p22^{phox}$-deficient who exhibit chronic granulomatous disease (CGD), which entails life-threatening infections as a result of phagocytes being unable to produce the ROS that destroy pathogens (Clark et al., 1989; Roos, 1994, Roos et al., 2010). These patients have been studied with regards to their immune system, yet little information exists regarding their cardiovascular health. There may be genetic variations within the NOX subunits that are directly affecting the ability of the NOX enzymes to produce ROS.

1.6 $p22^{phox}$ is a likely candidate as ROS influencer due to high genetic variability compared to other subunits

The level of ROS production from person to person varies greatly, with one potential explanation being high genetic variability within one or more of the enzymes responsible for the production of ROS (Bedard, 2009; Lacy et al., 1998). Single nucleotide polymorphisms (SNPs) are genetic variations found at a frequency of 1% or more in the human population. Examination of the main NOX subunits as well as the activating and organizing subunits reveal relatively low numbers of SNPs, which may be insufficient to explain the high variability of ROS production. However, the $p22^{phox}$ subunit is described

as having a relatively high number of SNPs, thus making is a suitable candidate for study with regards to ROS production and CVD.

1.7 $p22^{phox}$ single nucleotide polymorphisms are in areas that could compromise NOX integrity and ROS production

When studies attempted to determine the association of $p22^{phox}$ polymorphisms with cardiovascular disease the results were varied and conflicting (San Jose et al., 2008). Even within the same disease model a single $p22^{phox}$ polymorphism (c.214T>C) was found to protect from the disease, exacerbate the disease, and have no effect on the disease. These conflicting results may be explained by the altered functionality of the NOX enzymes when other $p22^{phox}$ SNPs are taken into account. Other potentially influential SNPs are c.521T>C, and c.*24G>A. A representation of $p22^{phox}$ and the three common polymorphisms included in the current study are depicted in Figure 6. The amino acid shifts caused by the three SNPs are as follows: c.214T>C = tyrosine > histidine; c.521T>C = valine > alanine; c.*24G>A = 3' UTR region (reviewed in Bedard & Krause, 2007). The "c" in c.*24G>A indicates a variation in the coding region, the asterisk indicates nucleotides located 3' of the translation stop codon, and the greater-than symbol indicates a substitution (den Dunnen and Antonarakis, 2000). It is important to note that the sequence variants described here as 214 and *24 are based on a newer nomenclature, and the mutations were previously referred to as 242 and 612, respectively. Mutations within the 3'UTR can result in decreased expression of associated sequences, most likely by decreasing mRNA stability (Bedard et al., 2009). The mutation at *24 resulted in a significant reduction in associated protein expression (Bedard et al., 2009). Neglecting to include the c.521T>C, and c.*24G>A SNPs in their

CVD association studies may explain the conflicting results. Investigating the SNPs as a grouping called a haplotype may allow one to more easily study the effects of the polymorphisms on cellular function. The effect the three SNPs have on NOX2 ROS production was examined, and it was determined that the haplotype containing all three SNPs resulted in a significantly lower level of ROS generation and lower $p22^{phox}$ expression (Bedard et al., 2009). These haplotypes were examined in NOX2, but NOX1 plays a more prominent role in cardiovascular physiology, therefore it may prove useful to examine these same haplotypes in a NOX1 system to determine their effect on NOX1-based ROS production.

1.8 NOX1

NOX1 is mainly expressed in colonic epithelium, but is also present in vascular smooth muscle cells (VSMC) and endothelial cells, among others (reviewed in Bedard & Krause, 2007). The subcellular localization of NOX1 is still up for debate, but there is evidence that NOX1 can be found alongside $p22^{phox}$ in the plasma membrane, as well as in the cytoplasmic compartment to a lesser extent, most likely within the membranes of certain organelles (Helmcke et al., 2008; Block & Gorin, 2012; Liu et al., 2012).

In order to function, NOX1 requires the NOXA1 activating subunit, the NOXO1 organizing subunit, the $p22^{phox}$ stabilizing subunit, and a GTPase Rac. NOX1 can also interact with the NOXA1 and NOXO1 homologues, $p67^{phox}$ and $p47^{phox}$, respectively, although the level of activation will be relatively lower (Banfi et al., 2003; Cheng & Lambeth, 2004). NOX1 differs from NOX2 in that the NOXO1 organizing subunit does not have an autoinhibitory loop, as is found on $p47^{phox}$ subunit. This, combined with the

fact that NOXO1 is usually already membrane bound, results in a higher basal level of NOX-based ROS generation (Brandes & Kreuzer, 2004). Activators of NOX1 in VSMCs include platelet-derived growth factor, prostaglandin F, and angiotensin II (Brandes & Schroder, 2008; Cave, 2009).

NOX1 plays a crucial role in VSMCs, as NOX1-deficient mice exhibit a significant decrease in VSMC migration and proliferation, as well as a decrease in vascular ROS levels and the angiotensin II blood pressure response (Matsuno et al., 2005; Lee et al., 2009). Also related to vascular health, NOX1-deficient mice demonstrate a lack of angiotensin II type 1 receptor (AT1R) cell surface localization in smooth muscle (Basset et al., 2009). NOX1 deficiency prevents AT1R surface localization through interference of caveolin phosphorylation, as the ROS typically produced by NOX1 seems to be required for proper phosphorylation of caveolin, and subsequent surface localization of the AT1R. In this scenario the AT1R instead localizes to the endoplasmic reticulum and Golgi apparatus. Given the relationship between NOX1, blood pressure control, and hypertension, these studies indicate that NOX1 is a desirable therapeutic target for the treatment of CVD.

1.9 Natural Compounds as ROS Inhibitors

Antioxidants are molecules that can scavenge ROS, and/or prevent the production of ROS by either reducing O_2 levels, or by directly binding and inhibiting ROS-producing systems (reviewed in Brewer, 2011). When a molecule directly prevents the production of ROS by binding to systems, it is often referred to as an inhibitor. Plants are a varied and plentiful source of natural antioxidants, such as flavonoids, phenolic acids,

carotenoids, and tocopherols (Khanduja, 2003; Ozsoy et al., 2009; Aqil et al., 2006). Many clinical trials have demonstrated that attempting to exploit antioxidant compounds for their ROS scavenging will end in disappointment (Bjelakovic et al., 2012), and as such we are interested in antioxidant compounds that have the ability to inhibit ROS-producing systems.

1.10 Resveratrol

Resveratrol, a form of phenol known as a stilbenoid that is found in grapes and various other plants, has gained attention since it was discovered that it can extend the life span of certain organisms by influencing a family of enzymes known as sirtuins, and through affecting genes related to aging (Lekli et al., 2010; Xia et al., 2010; Della-Morte et al., 2009; Markus & Morris, 2008; Finley & Haigis, 2010). Resveratrol is an antioxidant that has cardioprotective, anti-cancer, and anti-diabetic effects in mice (Bhat & Pezzuto, 2002; Wu et al., 2011; Szkudelski & Szkudelska, 2011). While there is much evidence that resveratrol is an effective treatment in rodents, following the Resveratrol 2010 Conference, held in Helsingør, Denmark, it was concluded that there is insufficient evidence to recommend human supplementation of resveratrol beyond what is obtained from a normal diet (Vang et al., 2011). In addition to being a protein kinase C (PKC) inhibitor, resveratrol is able to scavenge H_2O_2 in cellular systems, yet cannot scavenge superoxide in cell-free systems (Deby-Dupont et al. 2005; Leiro et al. 2004; Poolman et al. 2005). PKC is typically activated by diacylglycerol (DAG) released by the cleavage of phospholipid phosphatidylinositol 4,5-bisphosphate (PIP2) by phospholipase C (PLC) (Figure 3)(Brandes, 2004). Also, PKC can be activated by phorbol myristate acetate

(PMA), and, potentially by superoxide as well. This makes the behaviour of resveratrol relevant to NOX enzymes, as NOX enzymes can be activated by the PKC-mediated phosphorylation of the organizing subunits, $p47^{phox}$ or NOXO1. Representation of PKC-mediated activation of a NOX enzyme is shown in Figure 4.

With regards to resveratrol being a NOX inhibitor, there is evidence that resveratrol can reduce the level of superoxide in intact human umbilical vein endothelial cells at a concentration of approximately 16.0 uM ± 4.7 uM, yet no effect was seen by resveratrol on the cell-free, superoxide-generating xanthine/xanthine oxidase system (Steffen et al., 2007). This suggests that resveratrol may be a NOX inhibitor, but does not reveal if it is a direct or indirect inhibitor. Aside from study noted above, there is scant evidence of resveratrol as a direct NOX inhibitor; however, there is evidence that phenols can inhibit PKC-mediated activation of NOX enzymes (Pignatelli et al., 2000). As such, resveratrol remains as a natural compound of interest as a potential NOX inhibitor.

1.11 Celastrol

Celastrol is a triterpenoid quinone methide compound extracted from the root of the Thunder God Vine, also known as *Tripterygium Wilfordii*, which is indigenous to Southern China where it has been used as a part of traditional medicine to treat fever, chills, and pain (Allison et al., 2001). By the early 1990's celastrol was shown to inhibit lipid peroxidation and exhibit antioxidant behaviour (Sassa et al, 1990; Sassa et al., 1994). More recently, celastrol was shown to have beneficial effects with regards to autoimmune disease and inflammation (Qiu & Kao, 2003; Canter et al., 2006). Also, celastrol is known to have anti-neurodegenerative effects in mouse models, potentially

due to its antioxidant effects and activation of NF-κB, and has been proposed as a treatment for Alzheimer's Disease (Kiaei et al., 2005; Wang et al., 2005; Cleren et al., 2005; Allison et al., 2001). When human neutrophil-like cells were treated with celastrol, the release of H_2O_2 by NOX1, NOX2, NOX4, and NOX5 was inhibited by interfering with the collaborative binding of the NOX subunits $p47^{phox}$, and NOXO1 with $p22^{phox}$ where applicable, and by a yet to be determined mode (Jaquet et al., 2011). The ability of celastrol to reduce ROS levels through the inhibition of mitochondria has yet to be fully explored; however, celastrol can inhibit complex I of the mitochondria electron transport chain (mETC), resulting in an accumulation of ROS in human lung carcinoma and liver carcinoma cells (Chen et al., 2011). Interestingly, blocking the mETC actually increases ROS production, as inhibiting an individual complex on the mETC causes the electrons normally transferred among the complexes to leak into the surrounding mitochondrial matrix and intermembrane space (Li et al., 2003; Dias & Bailly, 2005). As a result of mETC complex I inhibition and the subsequent ROS accumulation, celastrol indirectly inhibits heat shock protein 90 (HSP90), a molecular chaperone involved in protein stabilization and folding, and activates the transcription factor c-Jun N-terminal kinase (JNK), resulting in increased cell growth inhibition, apoptosis, and necrosis (Chen et al., 2011).

1.12 Natural compounds potentially affecting ROS

There are many compounds extracted from plants or based on plant extracts that are tested for their antioxidant properties and potential against various diseases (Souri et al., 2010; Abdel-Sattar et al., 2010.) Apigenin is a flavinoid plant extract that has been

used in cancer chemoprevention for its antiproliferative effects, which may be achieved by interfering with the NF-κB gene expression pathway (Shukla & Gupta, 2010; Xu et al., 2008). In addition, apigenin may have antioxidant properties (Al-Shaal et al., 2011). Artesunate, a semisynthetic compound based on the plant extract artemisinin, has been successfully used as an anti-malarial agent, and can affect oxidative stress by suppressing prooxidants and activating antioxidants (Ho et al., 2012). Interestingly, it's also been demonstrated that artesunate can suppress expression of NOX enzymes and associated subunits, and can inhibit NF-κB activity (Wong et al., 2012; Gu et al., 2012). Piperine is an alkaloid plant extract that also may have antioxidant effects (Jagdale et al., 2009; Kamaraj et al., 2009). Piperine is cytotoxic to human adenocarcinoma cells through the induction of apoptosis partly via increased ROS production (Yaffe et al., 2012). The natural compounds apigenin, artesunate, and piperine were included in this study due to their similar properties to celastrol or resveratrol with regards to their potential pro or antioxidant effects, and their effect on gene expression pathways, such as NF-κB.

1.13 Do any known compounds affecting ROS production have positive CVD effects?

Based on the connection between ROS and blood pressure, one might expect antioxidants to positively affect CVD risk. Two common antioxidant compounds, vitamin C and E, have been implicated in blood pressure regulation, specifically by having the effect of lowering blood pressure for a short period of time at high dosages (Reviewed by Kaliora & Dedoussis, 2007). However, due to many limitations and oversights within these studies, it is unclear whether vitamin C and E have true antihypertensive capabilities, with the main concern regarding the bioavailability of the compounds, which

represents the rate and extent of a compound's appearance in the blood (Lodge, 2005). Resveratrol has been characterized as having a low bioavailability due to rapid metabolization, but the bioavailability can be improved by reducing cytochrome P450 enzyme activity, as observed with piperine, an alkaloid derived from black pepper that improved resveratrol bioavailability in mice by approximately 1544% (Johnson et al., 2011). Despite the low bioavailability, resveratrol has significant cardioprotective effects, and has even been shown to inhibit mitochondrial ROS production in human endothelial cells (Gurusamy et al., 2010; Csiszar et al., 2009; Ungvari et al., 2009).

1.14 Do NOX-inhibiting compounds have a positive effect on CVD?

Evidence suggests that NOX enzymes are a significant source of oxidative damage in pathologic conditions (Vaziri et al., 2000; Yorek, 2003, Gupta et al, 2010). Therefore, blocking NOX enzymes may be a therapeutic strategy for treating oxidative stress-related diseases. Inhibition of NOX activation by phenols may provide a novel method of CVD risk reduction, as phenols inhibit platelet aggregation and adhesion to collagen, events directly associated with risk factors for CVD (Pignatelli et al., 2000; Sharma & Berger, 2011). Statins are another example of a compound that has positive CVD potential and prevents NOX activation (Antoniades et al., 2010; Zhou & Liao, 2010). In a human vascular environment a statin can directly prevent the Rac1 protein from phosphorylating subunits responsible for NOX activation, thereby lowering vascular superoxide levels (Antoniades et al., 2010). The disadvantage of these compounds and many like them is that they have multiple targets, resulting in multiple potential adverse side effects when used in a clinical setting (Antoniades et al., 2010). It would be beneficial to find inhibitors that are exclusive to NOX enzymes or even particular NOX

isoforms, as the potential for adverse effects decreases as the number of off-target decreases.

Another way to address the question of whether NOXs are involved in cardiovascular disease is to explore the fact that there is a correlation between disease and factors that influence ROS generation by NOX. In addition, there is some evidence that drugs that block NOX are beneficial (Wagner et al., 2000). For example, statins are capable of preventing NOX subunits from assembling properly, thereby affecting subunit-dependent NOX isoforms, and calcium blockers would prevent the proper function of the NOX5 isoform. More specific inhibitors would be beneficial.

1.15 Study hypothesis and objectives

The objectives of my studies were to determine the effect of $p22^{phox}$ genetic polymorphisms on the production of reactive oxygen species by the NOX1 enzyme, and to determine the effect of the natural compounds celastrol and resveratrol on the production of reactive oxygen species by the mitochondria and NOX enzymes respectively. The subunit $p22^{phox}$ exhibits a high level of genetic variability, and this variability results in more non-silent changes than would be expected (Bedard, 2009; Lacy et al., 1998)**.** This type of variation can be found in genes where there is a benefit in diversity that is positively selected for, such as in genes related to antigen presentation and recognition (Nei et al., 2010). Likewise, the high degree of variation in $p22^{phox}$ may have beneficial effects, like allowing for more a nuanced control of protein regulation across multiple cell types, potentially via microRNAs targeting the 3' UTR. We would

like to test the hypothesis that variation of the $p22^{phox}$ protein affects the different NOX isoforms in different ways by considering the effect of these variants on NOX1 function.

Given that celastrol completely inhibited ROS production in B-lymphocytes in which little of the ROS produced is attributable to mitochondria, and given that the inhibition of ROS production in NOX5- or NOX4-transduced HEK cells was incomplete, and less than that of the inhibitor DPI, a gold standard inhibitor of NOXs and mitochondria (Cross, 1987; Morré, 2002), which would be expected to inhibit both NOX and mitochondrial ROS (Jaquet et al., 2011), we hypothesize that the natural compound celastrol will not act as an inhibitor of mitochondrial ROS production. Through *in vitro* investigation using a H661 human lung cancer cell line with functional NOX1 lentivirally inserted, I examined the amount of $p22^{phox}$ mRNA, H_2O_2 generation, and $p22^{phox}$ protein expression by qRT-PCR, Amplex Red assay, and Western blot respectively. Using the same NOX1 cell line, we investigated the antioxidant and ROS inhibition capabilities of celastrol and resveratrol by Amplex Red, methyl cypridina luciferin analog (MCLA), and nitro blue tetrazolium (NBT) assays.

A) $O_2 + NADPH \quad \bullet O_2^- + NADP^+ + H^+$

B) $2\bullet O_2^- + 2H^+ \quad H_2O_2 + O_2$

C) $2H_2O_2 \quad 2H_2O + O_2$

D) $\bullet NO + \bullet O_2^- \rightarrow ONOO^-$

E) $H_2O_2 + 2GSH \quad 2H_2O + GSSG$

F) $GSSG + NADPH + H^+ \quad 2GSH + NADP^+$

G) Haber-Weiss Reaction

Step One:

$Fe^{3+} + \bullet O_2^- \rightarrow Fe^{2+} + O_2$

Step 2 (Fenton Reaction):

$Fe^{2+} + H_2O_2 \rightarrow Fe^{3+} + OH^- + \bullet OH$

Net Reaction:

$\bullet O_2^- + H_2O_2 \rightarrow \bullet OH + OH^- + O_2$

Figure 1. Reactions involving reactive oxygen species or antioxidants. The process of A) NOX-catalyzed formation of superoxide, B) forming hydrogen peroxide, C) catalase-catalyzed breakdown of H_2O_2, D) forming peroxynitrite, E) glutathione peroxidase-catalyzed breakdown of H_2O_2, F) glutathione reductase-catalyzed formation of glutathione. G) The Haber-Weiss reaction involving iron (Fe).

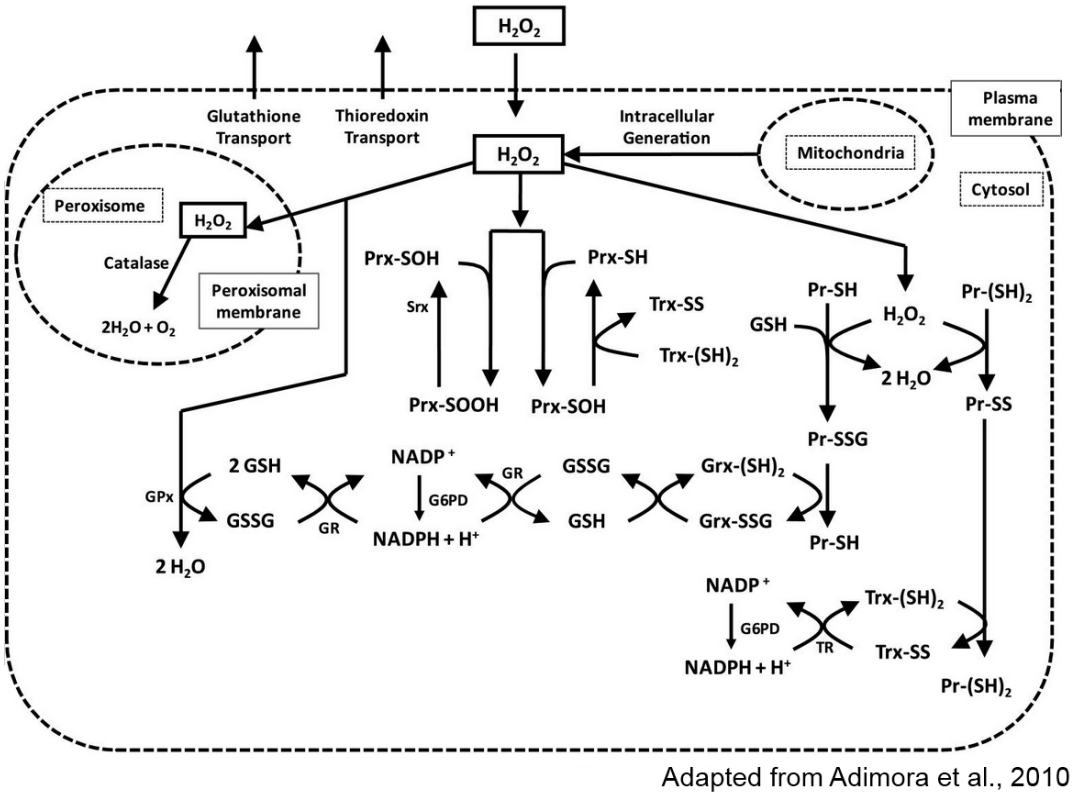

Adapted from Adimora et al., 2010

Figure 2. The breakdown of hydrogen peroxide (H_2O_2) by catalase and glutathione. The levels of hydrogen peroxide are tightly controlled by catalase, glutathione or peroxiredoxin, which metabolize hydrogen peroxide and form water as a byproduct. Adapted from Adimora et al., 2010.

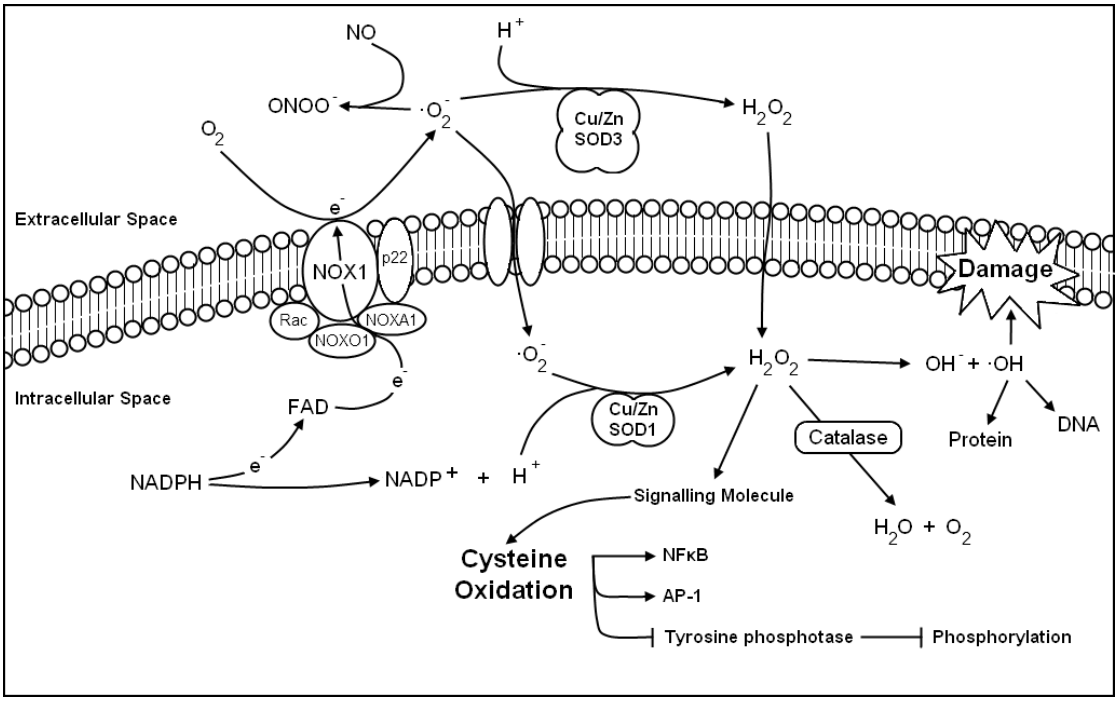

Figure 3. The creation and fate of superoxide. An electron from NADPH is ultimately donated to NOX1, which then uses it to create superoxide. Superoxide ($\cdot O_2^-$) then becomes hydrogen peroxide (H_2O_2) by either spontaneously interacting with another superoxide molecule, or by interaction with superoxide dismutase (SOD). At low concentrations hydrogen peroxide can act as a signalling molecule by oxidizing cysteine residues prior to its breakdown by catalase, glutathione, peroxiredoxins, or other antioxidants. H_2O_2 can also damage proteins, lipids, and DNA, among others.

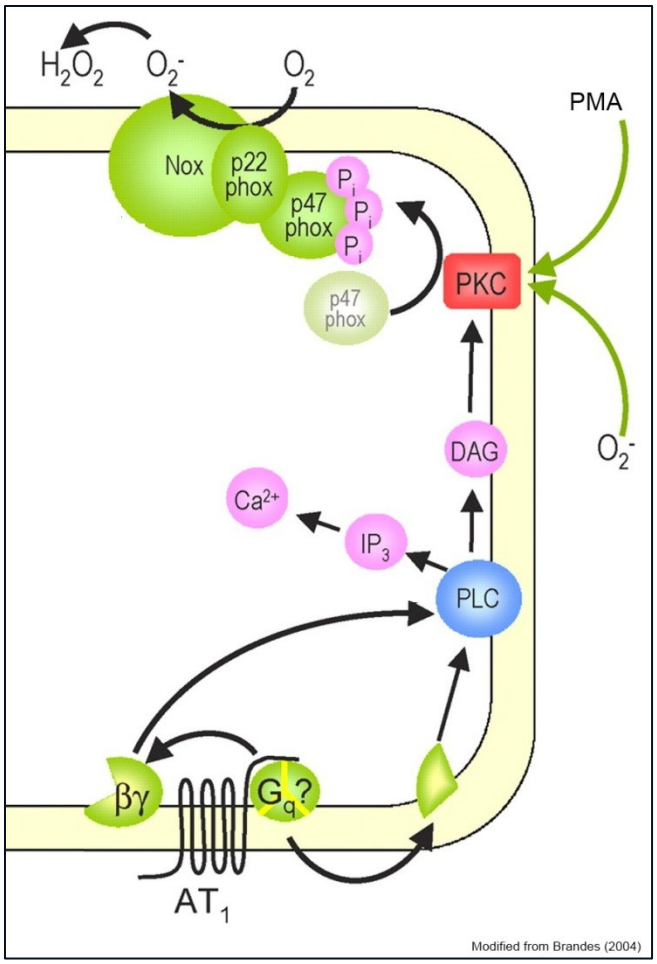

Figure 4. Protein Kinase C activation of a NOX enzyme. Stimulators of protein kinase C (PKC), such as superoxide (O_2^-), diacylglycerol (DAG), and phorbol 1 2-myristate 13-acetate (PMA), can cause phosphorylation of the NOX organizing unit ($p47^{phox}$ or NOXO1), and assembly of the complete NOX enzyme. This process can create superoxide from oxygen and the NADPH electron source, and ultimately create hydrogen peroxide (H_2O_2), a second messenger signalling molecule. Adapted from Brandes, 2004.

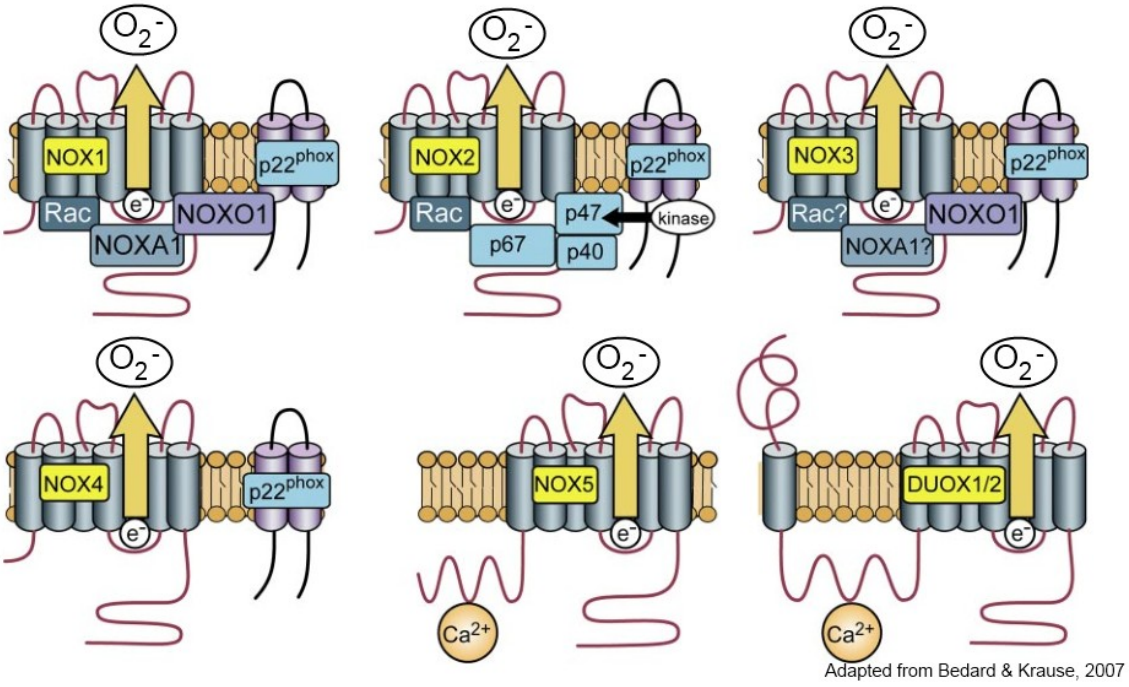

Figure 5. The NADPH oxidase family of enzymes. The NOX enzymes contain a conserved six-transmembrane domain, yet certain forms interact with various subunits, whereas others do not. NOXs are activated to produce superoxide via various mechanisms, such as phosphorylation and calcium binding.

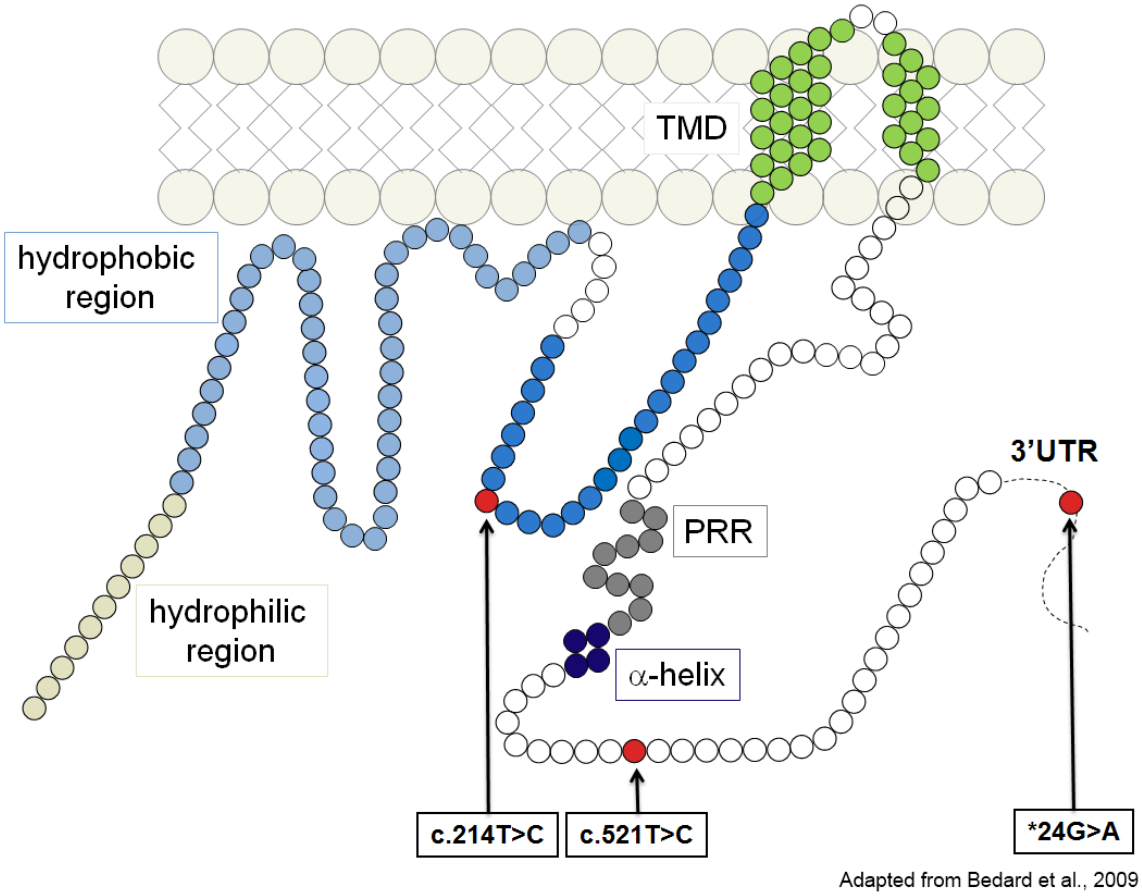

Figure 6. Representation of p22^{phox} and three common polymorphisms. The p22^{phox} subunit of the NOX enzyme contains hydrophobic and hydrophilic regions, a transmembrane domain (TMD), a proline rich region (PRR) that interacts with p47^{phox} or NOXO1, and an alpha-helix. Three common polymorphisms depicted in red occur at c.214, c.521, and at *24.

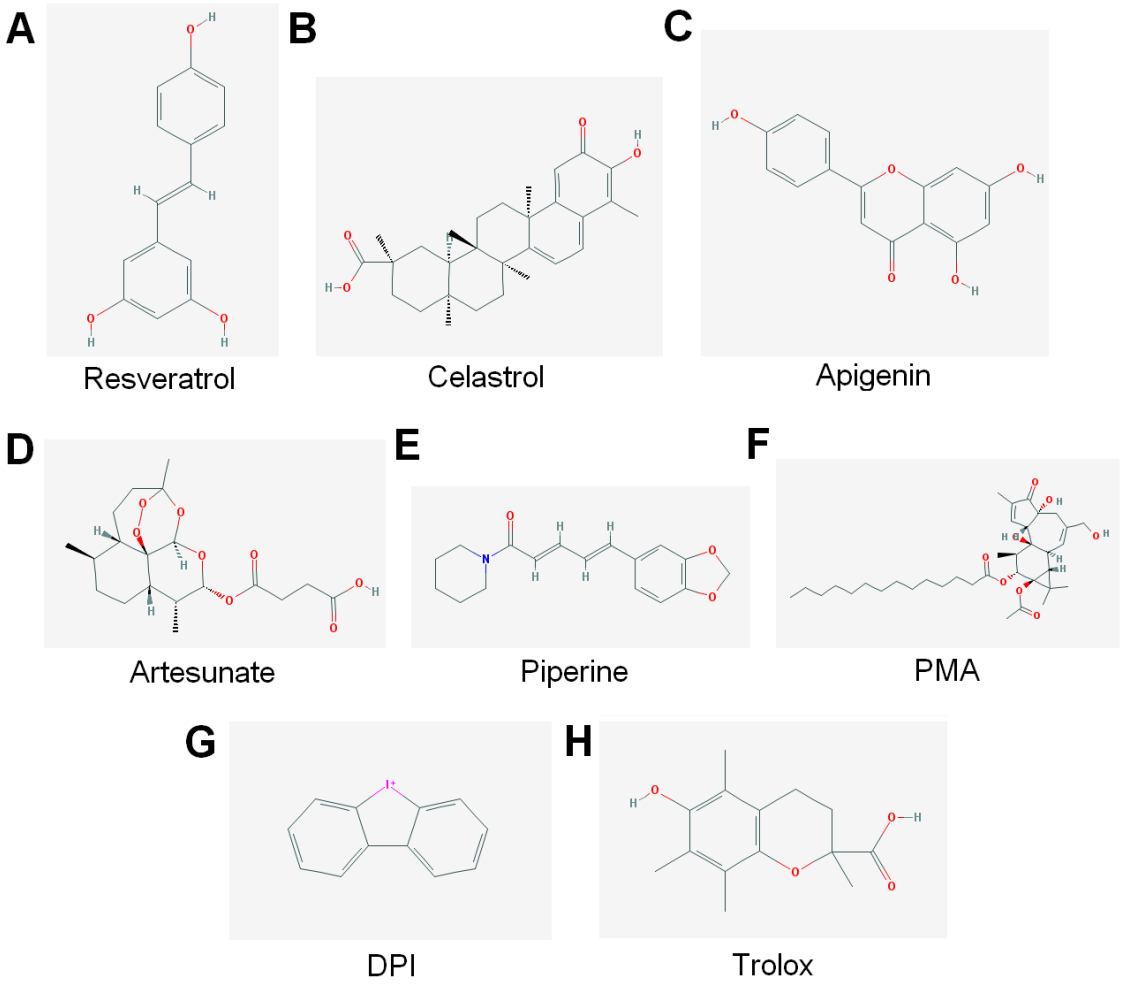

Figure 7. Compound structures. The 2D chemical structure of A) resveratrol, B) celastrol, C) apigenin, D) artesunate, E) piperine, F) phorbol myristate acetate (PMA), G) diphenyleneiodonium (DPI), H) trolox. Structures referenced from NCBI PubChem Compound Database (https://www.ncbi.nlm.nih.gov/pccompound; March, 2013).

CHAPTER 2: MATERIALS

2.1 Cell culture

All cells were cultured at 37°C in a 5% CO_2 atmosphere in a sealed and humidified incubator. The human lung carcinoma cell line H661 (ATCC) and B-lymphocyte cell lines (gift from Dr. Marie Jose Stasia, Centre Hospitalier Universitaire, Grenoble, France) were cultured in 1640 Roswell Park Memorial Institute Medium (RPMI; 2 mM L-glutamine, 10 mM HEPES, 1 mM sodium pyruvate, 4500 mg/L glucose, 1500 mg/L sodium bicarbonate; (Thermo Fisher, Massachusetts, United States) supplemented with 10% fetal bovine serum (FBS) 100 U/mL penicillin, and 100 mg/mL streptomycin. The human embryonic kidney cell line HEK293T (gift from Dr. Chris Sinal, Dalhousie University, Halifax, Canada) cells were cultured in Dulbecco's Modified Eagle Medium (DMEM) (4 mM glutamine, 4500 mg/L glucose, without sodium pyruvate; Thermo Fisher, Massachusetts, United States) supplemented with 10% FBS, 100 U/mL penicillin, and 100 mg/mL streptomycin. For subculture, H661 cells were washed with PBS prior to addition of 0.5% (w/v) trypsin-EDTA (Sigma Aldrich, Missouri, United States). Trypsin was added directly to the less adherent HEK293T cells. B-lymphocytes were subcultured by dilution.

2.1.1 Hank's Buffered Salt Solution (HBSS):

HBSS (0.137 M NaCl, 5.4 mM KCl, 0.25 mM Na_2HPO_4, 0.44 mM $KHPO_4$, 1.3 mM $CaCl_2$, 1% Glucose (w/v), 1.0 mM $MgSO_4$, and 4.2 mM $NaHCO_3$) was used in Amplex Red assays.

2.2 Gateway® Cloning

To generate plasmids of NOX1 and associated subunits, Gateway® cloning was employed. PCR products designed for the NOX1 subunits and flanking terminal *att*B Gateway® sites were amplified from human normal colon cDNA (Invitrogen, California, United States) using Platinum® Pfx (Invitrogen, California, United States) with primers h_gwNOX1F and h_gwNOX1R (NOX1), h_gwNOXA1F and h_gwNOXA1R (NOXA1), h_gwNOX1F1 and h_gwNOX1R3 (NOX1) (Table 1). The *att*B-PCR products were separated via 1% agarose gel electrophoresis at 100 V for 1 hr. The bands containing the DNA of NOX1 subunits were isolated and then purified using the QIAquick Gel Extraction Kit following the manufacturer's instructions (Qiagen, Venlo, Netherlands). The *att*B-PCR products NOX1 and subunits and the *att*B-PCR product for the CMV promoter were inserted into Entry cloning vectors by BP Clonase recombination into pDONR221, and pDONR-P4-P1R, respectively (Invitrogen, California, United States) (Figure 4A). One Shot® TOP10 (p22 variants) or One Shot® Mach1™ T1 Phage-Resistant (NOX1 subunits) chemically competent *E. coli* (Invitrogen, California, United States) were transformed with 2 µL of each BP reaction into 25 µL of *E.Coli* cells following manufacturer's instructions. Briefly, the mixture was set on ice for 30 min, heat

shocked at 42°C for 30 sec, and placed back on ice for 2 min. Super Optimal broth with Catabolite repression (SOC) medium (250 µL) (Cellgro, Virginia, United States) was added, and the mixture shaken for one h in a 37°C incubator. From this, 100 µL was added to LB agar plates supplemented with kanamycin (50 µg/mL), and incubated at 37°C overnight. Resulting colonies were cultured in 3 mL Lysogeny broth (LB) supplemented with kanamycin (50 µg/mL), and shaken overnight at 37°C. The plasmid DNA of CMV and the NOX1 subunits were then purified using the QIAprep Spin Miniprep Kit (Qiagen, Venlo, Netherlands). The Expression clones were generated by a recombination reaction between the Entry vectors containing the CMV promoter and Entry vectors containing NOX1 or subunits and a modified pDONR vector called a 2K7 cassette Gateway® vector, as previously described (Suter et al., 2006)(Figure 4B). One Shot® Stbl3 Chemically Competent *E. coli* (25 µL) were transformed with 2 µL of each LR reaction into of (CMV with NOX1 or subunits, and selection marker), as per above. From this, 100 µL was added to LB agar plates supplemented with ampicillin (50 µg/mL), and incubated at 37°C overnight. Resulting colonies were cultured in 3 mL LB broth supplemented with ampicillin (50 µg/mL), and shaken overnight at 37°C. The cultured bacteria was transferred into 250 mL LB broth supplemented with ampicillin (50 µg/mL), and shaken overnight in a 37°C incubator. The plasmid DNA of CMV and the NOX1 subunits was then purified using the QIAGEN Plasmid Maxi Kit (Qiagen, Venlo, Netherlands). Sequences of the vectors were confirmed by Sanger sequencing using BigDye® (Life Technologies, California, United States) and primers s_2K7CF1 and s_2K7CR1 (2K7 cassette + CMV), s_NOXA1iF and s_NOXA1iR (NOXA1), s_NOXO1iF and s_NOXO1iR (NOXO1), s_NOX1iF1 and s_NOX1iR1 (NOX1),

M13_forward and M13_reverse (pENTR) (Table 1). The PCR products were amplified using a Biometra® T-gradient thermocycler (Montreal Biotech Inc., Quebec, Canada) with the following cycling conditions: 94°C for 2 min; 35 cycles of 94°C for 30 sec; 58°C for 30 sec, 72°C for 45 sec; and a final elongation step for 5 min at 72°C. The sequencing PCR products then were purified using the BigDye® Terminator™ purification kit using the manufacturer's instructions

(Life Technologies, California, United States), prior to sequencing on a 3130xl Genetic Analyzer (Applied Biosystems, California, United States).

2.3 Preparation of Lentiviral Particles

2.3.1 Transfection for Lentiviral Packaging

HEK293T cells (2 x 10^6 /10 cm tissue culture dish) were cultured in complete DMEM at 5% CO_2 atmosphere in a 10 cm tissue culture dish for 24 hr. Medium was changed and transfection was performed using the Promega® calcium phosphate method. The three vectors collectively encoding the lentiviral packaging system, 2.5 μg envelope plasmid (MD2.G), 3.75 μg packaging plasmid (pCMVDR-8.92), and 3.5 μg REV-expression plasmid (PCMVDR-8.93), were combined in a volume of 10 μL. To this 10 μL of 1 μg/μL plasmid of interest (NOX1, NOXA1, NOXO1, or $p22^{phox}$), and this was brought to 250 μL with room temperature ddH_2O. An equal volume of 250 ul of 2 M $CaCl_2$ was added to the vector mixture. A volume of 500 μL of a $CaCl_2$ and plasmid vector mixture was added dropwise to 500 μL HEPES-buffered saline solution (HeBS) solution while vortexing the HeBS tube. After 30 min at room temperature, 1 mL of the

mixture was added dropwise to the plated HEK293T cells in complete DMEM. The plate was then incubated at 37°C/5% CO_2 atmosphere in a humidified incubator. The following day complete DMEM medium was warmed, medium was changed in each well, and the dish was replaced in a 37°C/5% CO_2 incubator for 24-48 hr.

2.3.2 Transduction

H661 cells were seeded at 1 x 10^4 cells per well in complete RPMI in a six-well plate a day prior to transduction. The medium from the lentivirus vector producing HEK293T cells was filtered through a sterile 0.45 μm filter, and 1 mL of this medium was added directly to the H661 cells to be transduced. The H661 cells were incubated in a 37°C/5% CO_2 atmosphere humidified incubator.

The medium was changed every two days, and antibiotic resistance selection commenced. Selection included blasticidin (5 μg/mL), neomycin (1 mg/mL), and zeocin (100 μg/mL). NOXA1 cells were selected via neomycin, NOXO1 cells were selected via zeocin. NOX1 cells selected via clonal selection of GFP fluorescent colonies of cells plated dilutely on a 15 cm plate. These cells H661 containing NOXA1, NOXO1 and NOX1 were called HOAx1 cells. These HOAx1 cells were then transduced with each of the seven variants of $p22^{phox}$ to create the set of cell lines called S184 and then again to create the set of cell lines called S232. The SNPs contained within each haplotype is represented in Table 2.

2.3.3 RNA and DNA Extraction/ cDNA Synthesis/ Polymerase Chain Reaction

RNA was extracted from pelleted cells using the QIAshredder kit, and RNeasy Mini Kit with DNAse on-column digestion (Qiagen, Venlo, Netherlands). cDNA was prepared using either 0.5 μg or 1 μg of isolated RNA. Reverse-transcription of total RNA into cDNA was performed using the Ready-To-Go T-Primed First Strand Synthesis kit and manufacturer's instructions (GE Healthcare, Glattbrugg, Switzerland).

Genomic DNA was isolated from cells using the DNeasy Blood & Tissue Kit (Qiagen, Venlo, Netherlands).

The H661 cell line was analyzed via polymerase chain reaction. Briefly, 1 μL of cDNA, or 50-100 ng of isolated genomic DNA was combined with 1X KCl PCR buffer, 0.2 mM dNTP, 2 mM $MgCl_2$, 1 μM of the appropriate forward and reverse primers, and 1 unit Platinum® Taq DNA Polymerase High Fidelity enzyme. Primers used for amplification of NOX enzymes and associated subunits are listed in Table 1, primer numbers 15 – 32. The PCR product was amplified using a Biometra® T-gradient thermocycler (Montreal Biotech Inc., Quebec, Canada) with the following cycling conditions: 94°C for 2 min; 35 cycles of 94°C for 30 sec; 58°C for 30 sec, 72°C for 45 sec; and a final elongation step for 5 min at 72°C. Amplified PCR products were resolved on 1% agarose gels stained with SYBR® Safe DNA gel stain (10 000x in DMSO) (Invitrogen, California, United States) by electrophoresis at 100 V for 60 min. Molecular weight marker used was Qiagen Gelpilot 1kb Plus Ladder (Qiagen, Venlo, Netherlands). Nucleic acid bands were visualized by UV light exposure, using the FluorChem M Imager (Protein Simple, California, United States). Primers involved in confirming the

absence of NOX enzymes and associated subunits are as follows: hNOX1F and hNOX1R (NOX1), hNOX2F and hNOX2R (NOX2), hNOX3F and hNOX3R (NOX3), hNOX4F and hNOX4R (NOX4), hNOX5F and hNOX5R (NOX5), hCYBAF and hCYBAR ($p22^{phox}$), hNCF1F and hNCF1R (p47), hNCF2F and hNCF2R (p67) (Table 1).

2.4 Assays

2.4.1 Amplex Red (AR) Assay

H_2O_2 was measured with the Amplex Red® fluorescence assay, using the Infinite M200 Pro microplate reader (Tecan Group Ltd., Männedorf, Switzerland), as previously described (Jacquet et al., 2011). Detached cells were plated in a 96-well plate at a density of 5 x 10^4 in 200 µL of HBSS containing 25 µM Amplex Red™ (Invitrogen, California, United States) and 0.005 U/mL horse radish peroxidase (HRP)(Sigma-Aldrich, Missouri, United States). Cells were stimulated with 100 nM phorbol 12-myristate 13-acetate (PMA)(Sigma-Aldrich, Missouri, United States), and inhibited with 10 µM diphenyleneiodonium (DPI)(Sigma-Aldrich, Missouri, United States). The H_2O_2 (Fisher Scientific, New Hampshire, United States) standard curve ranged from 5000 nM to 0 nM. In order to ensure all superoxide was converted to H_2O_2, Cu/Zn from bovine erythrocytes (100 U/well)(Sigma-Aldrich, Missouri, United States) was added to the appropriate wells. To properly normalize H_2O_2 results with the number of viable cells, calcein (10 µg/mL)(Invitrogen, California, United States) was added to wells of a cellular standard with cell densities ranging from 1 x 10^6 to 0 cells per well. In a cell-free system, 625 nM of H_2O_2 in 200 µL HBSS containing 25 µM Amplex Red™ and 0.005 U/mL HRP was

combined with various natural compounds at final concentrations ranging from 0.5 μM to 100 μM to determine their antioxidant properties. H_2O_2 was determined by measuring the fluorescence every 2 min for 30 cycles at 37°C, with excitation and emission wavelengths of 544 nm and 590 nm respectively.

2.4.2 Nitro Blue Tetrazolium (NBT) Assay

Intracellular cellular superoxide generation was measured with the nitro blue tetrazolium (NBT) fluorescence assay, using the Infinite M200 Pro microplate reader (Tecan Group Ltd., Männedorf, Switzerland). In a 100 μL volume of HBSS, detached S184 or B-lymphocytes were seeded at 4 x 10^4 cells per well in a 96-well plate. Natural compounds, dissolved in DMSO and diluted in PBS, were added to the wells at final concentrations ranging from 0.5 mM to 100 mM. At the final concentrations in wells DMSO was less than 1% of the total solution volume. NBT (Invitrogen, California, United States)(0.66 mg/mL) and PMA (Sigma-Aldrich, Missouri, United States)(100 nM) was added to each well and placed the plate in a sealed 37°C incubator for 3 hr. The plate was removed from the incubator and spun in a centrifuge at 2270 g for 2 min. The well solutions were removed and the cells were washed twice with 100 μL of PBS. The plate was spun again for 2 min at 2270 g between washes. The solution in each well was removed, and the cells were washed with 100 μL methanol, then air dried for 5 min. Next 112 μL 2M KOH, 96 μL DMSO (99%) was added to each well, mixed thoroughly by micropipette, and read the plate was read at 630 nm. Cu/Zn SOD (25 U/mL) was added to control wells.

2.4.3 MCLA Assay

Superoxide generation was measured in a cell-free environment with the methyl cypridina luciferin analog (MCLA)(Invitrogen, California, United States) chemiluminescence assay using the Infinite M200 Pro microplate reader (Tecan Group Ltd., Männedorf, Switzerland), as previously described (Jacquet et al., 2011). The generation of superoxide by the xanthine/xanthine oxidase was performed in PBS supplemented with xanthine oxidase (0.1 U/mL), EDTA (0.3 mM), MCLA (0.1 mM), xanthine (0.5 mM). Natural compounds at various final concentrations ranging from 0.5 mM to 100 mM were added to the wells. Cu/Zn SOD (100 U/mL) and DPI (10 μM) were added as controls and for verification of xanthine oxidase function and superoxide production. Superoxide generation was determined by measuring the MCLA light emission every 90 sec for 30 cycles at 37°C with an integration time of 0.9 sec.

2.5 Vector Quantification

2.5.1 Tissue Culture

HEK293T cells were seeded at 1 x 10^4 cells per well in a six-well dish. One well received undiluted DMEM medium containing lentiviral particles, and four wells received quarter serial dilutions of the original medium down to a 1:256 concentration. The GFP vector contained the blasticidin resistance gene as a selection marker. The remaining well received complete DMEM. Supernatants were harvested and total RNA

was collected from the lentiviral particles using the RNeasy Mini kit (Qiagen, Venlo, Netherlands) in conjunction with QIAshredder and the DNase on-column digestion.

A volume of 175 µL of the lentiviral prep was disrupted with 175 µL of RT buffer from the RNeasy Mini kit. This 350 µL volume was then homogenized using the QIAshredder (Qiagen, Venlo, Netherlands), and the protocol from the RNeasy kit was followed. The final volume from RNA isolation was 61 µL. qRT-PCR performed on cDNA prepared from the diluted virus preparation samples using primers for blasticidin as the gene of interest and primers for kanamycin as the normalization gene found that a decrease in the amount of blasticidin resistance gene could be detected on dilution. (Figure 17). A volume of 5 µL of kanamycin (7.5 pg/µL) was added to the 61 µL RNA isolate to act as a known concentration control for the qRT-PCR experiment.

A volume of 33 µL of the total 66 µL of isolated RNA was used to reverse-transcribe total RNA into first strand cDNA through the use of the Ready-To-Go T-Primed First Strand Synthesis kit and the manufacturer's instructions (GE Healthcare, Glattbrugg, Switzerland).

Final qPCR conditions and concentrations were as follows: 156.25 nM of each forward and reverse primers (KAN F1 and KANR1 (kanamycin resistance gene)), blasticidin F and blasticidin R, (blasticidin resistance gene)), 1-2 ng template, 1X SYBR Green (Applied Biosciences, California, United States). A total volume of 16 µL was used per reaction. The PCR product was amplified using a Roto-Gene Q (Qiagen, Venlo, Netherlands) with the following cycling conditions: 95°C for 2 min; 40 cycles of 95°C for 10 sec, 60°C for 15 sec, 72°C for 20 sec. A final melting step of gradually increasing temperature from 72°C to 95°C to ensure a single product from each reaction. For

normalization, 1 ng of kanamycin resistance gene RNA was used as a known concentration positive control, and used undiluted viral preparation template as calibrator considered '1' during the final qRT-PCR quantification step. The primers used to quantify blasticidin (blasticidin F/blasticidin R), and kanamycin resistance gene (KAN F1/KAN R1) are described in Table 1.

2.5.2 Fluorescence Activated Cell Sorting (FACS)

HEK293T cells transduced with a previously generated lentiviral vector containing GFP under the CMV promoter, and containing the blasticidin resistance gene (2K7-CMV-GFP-blast)(Bedard et al., 2009) were cultured in a six-well plate incubated at 37°C, 5% CO_2 atmosphere in a sealed and humidified incubator for 24 hr. The medium was removed from all wells, the cells were washed with 1X phosphate buffered solution (PBS; Thermo Fisher, Massachusetts, United States), and trypsinized (0.5% w/v)(Sigma, Missouri, United States) for 3 min. The cells were pelleted for 3 minutes at 1500 g, washed with PBS, and fixed with 200 µL of 2% [w/v] paraformaldehyde (PFA; Sigma Aldrich, Missouri, United States) in preparation for fluorescence assisted cell sorting (FACS). The percent of HEK293T cells successfully transduced with GFP was quantified by flow cytometry using the BD FACSCalibur (BD Biosciences, New Jersey, United States) flow cytometer and Cell Quest Pro software (v 5.2.1).

2.6 Protein Immunoblot

Expression of $p22^{phox}$ was determined through Western blotting. Cells containing the $p22^{phox}$ variants were pelleted and lysed (50 mM Tris-HCl, 150 mM NaCl, 2 mM

EDTA, and 0.2% Triton X-100). Protein was quantified using a Bradford-based assay with pre-diluted solutions containing bovine gamma globulin protein to generate the standard curve (Thermo Fisher, Massachusetts, United States). Protein from the cells was heated at 70°C for 10 min, and 40 μg of total protein in a verified linear range was separated on a 12% SDS-PAGE gel, and transferred to a polyvinylidene difluoride (PVFD) membrane using a Bio-Rad Trans-Blot® Turbo™ Transfer system (Bio-Rad Laboratories, California, United States) The Western blots were performed with 1:1000 monoclonal anti-$p22^{phox}$ (Abcam, Cambridge, England; prod#: ab80896), and 1 : 5000 anti-mouse IgG and 1:10 000 anti-biotin HRP-linked antibodies (Cell Signaling, Massachusetts, United States; prod#: 7075 & 7076S). The loading control, β-actin, was probed with 1:5000 anti-β-actin (Cell Signaling; prod#: 51255). The blots were visualized using an enhanced chemiluminescence (ECL) reagent (GE Healthcare, Glattbrugg, Switzerland), and a FluorChem M Imager (Protein Simple, California, United States). The band density was normalized to the β-actin loading control and quantified using National Institutes of Health (NIH) ImageJ software (v 1.47h) (http://rsbweb.nih.gov/ij/index.html)

2.7 Mitochondrial Isolation & Stimulation/Inhibition

2.7.1 Solutions

Mitochondrial Isolation Buffer (MIB):

Mannitol (0.22 M), sucrose (0.007 M), K-HEPES (0.02 M), EGTA (1 mM), pH 7.2

2.7.2 Protease Inhibitors (PI)

PMSF (50 μM), pepstatin A (1 μM), aprotinin (5 μg/mL), leupeptin A (5 μg/mL). Alternatively, a protease inhibitor cocktail was used (sc-29131; Santa Cruz, United States) as per the manufacturer's instructions. A volume of 82 μL of PI cocktail was added to 2 mL of MIB.

2.7.3 Mitochondrial Isolation

When possible, steps were carried out on ice. Trypsinized (0.5% w/v) H661 cells from a total surface area of 1000 cm^2 (Two Nunc® Triple Flasks; Sigma-Aldrich, Missouri, United States) were placed into a 50 mL conical tube. Cells were pelleted at 1300 g for 3 min at 4°C, and resuspended in 2 mL of mitochondrial isolation buffer (MIB). Cells were ruptured by nitrogen cavitation at 1500 psi for 11 min in a model 4639 cell disruption vessel (Parr Instrument Company, Illinois, United States) as previously described (Kristian et al., 2006). Lysed cell contents into a 50 mL conical tube, and spun at 800 g for 10 min in a 4°C centrifuge. Supernatant was collected, pellet discarded, and supernatant spun at 13 000 g for 10 min in a 4°C centrifuge. Supernatant was removed and discarded, and crude pellet was resuspended in MIB supplemented with 1% BSA (w/v).

Positive controls for Amplex Red® assay were a combination of malate/pyruvate at a final concentration of 1mM, and antimycin A (Sigma-Aldrich, Missouri, United States) at a final concentration of 50 μg/mL. Adenosine diphosphate (ADP) was added to all wells at a final concentration of 300 μM. Celastrol (10 μM), dissolved in DMSO and diluted in

PBS, was added to mitochondria at the start of the Amplex Red® assay to determine potential mitochondrial inhibition capabilities. At this concentration DMSO consisted of less than 1% of the total solution volume.

2.8 Statistical Analysis

Experiments were repeated as indicated and error was expressed as standard deviation (SD). Statistical analysis was performed using GraphPad Prism™ software v5.04 (GraphPad Software, Inc, California, United States). Data were analyzed using a T-test, or one-way ANOVA with repeated or non-repeated measure, and Dunnett's or Tukey's post-hoc analysis. Results were considered to be statistically significant when $p<0.05$, denoted as * $p<0.05$; **, $p<0.01$; ***, $p<0.001$; ****, $p<0.0001$. Treatment groups were compared to the untreated control, unless otherwise indicated. Quantitative PCR raw data were analyzed using Roto-Gene 6000 Series software v1.7, build 34 (Corbett Life Science Pty. Ltd, Sydney, Australia).

Table 1. Primers used for PCR, qPCR, and qRT-PCR analysis of NADPH oxidase and subunits

Primer name	Primer Sequence
h_gwkzNOX1F1	GGGGACAAGTTTGTACAAAAAAGCAGGCTTCGCCACCATGGGAAACTGGGTGGTTAAC
h_gwNOX1R1	GGGGACCACTTTGTACAAGAAAGCTGGGTTTCAAAAATTTTCTTTGTTGAAGTAGAA
h_gw kzNOXO1F1	GGGGACAAGTTTGTACAAAAAAGCAGGCTTCGCCACCATGGCAGGCCCCCGATAC
h_gwNOXO1R1	GGGGACCACTTTGTACAAGAAAGCTGGGTTCTTTACTCAGAGGAACAGCAAATGGCC
h_gw kzNOXA1F1	GGGGACAAGTTTGTACAAAAAAGCAGGCTTCGCCACCATGGCCTCTCTGGGGGAC
h_gwNOXA1R1	GGGGACCACTTTGTACAAGAAAGCTGGGTTTTAGGGCTGATCTCCCTGC
h_gwNOX1F1	GGGGACAAGTTTGTACAAAAAAGCAGGCTTCATGGGAAACTGGGTGGTTAAC
h_gwNOX1R3	GGGGACCACTTTGTACAAGAAAGCTGGGTTTGGGGTTCTCGGTAATTTTG
h_gwNOX4F1	GGGGACAAGTTTGTACAAAAAAGCAGGCTTCATGGCTGTGTCCTGGAGG
hNOX1F	TTAACAGCACGCTGATCCTG
hNOX1R	CACTCCAGTGAGACCAGCAA
hNOX2F	AAATGGTGGCATGGATGATT
hNOX2R	GGGATTGGGCATTCCTTTAT
hNOX3F	CCAGGGCAGTACATCTTGGT
hNOX3R	CCGTGTTTCCAGGGAGAGTA
hNOX4F	AACCGAACCAGCTCTCAGAA
hNOX4R	CCCAAATGTTGCTTTGGTTT
hNOX5F	TACCTCCTCGTGTGGCTTCT
hNOX5R	GCTCAG AGGCAAAGATCCTG
hCYBAF	GTTTGTGTGCCTGCTGGAGT
hCYBAR	TGGGCGGCTGCTTGATGGT
hNCF1F	CCCAGCCAGCACTATGTGTA
hNCF1R	CCCAGGTCTTCTCGTAGTCG
hNCF2F	CGAGGGAAC CAGCTGATAGA
hNCF2R	CATGGGAACACTGAGCTTCA
KAN F1	GCCATTCTCACCGGATTCAGTCGTC
KAN R1	AGCCGCCGTCCCGTCAAGTCAG
s NOXA1iF	AGCCACAGGGACCAGGAG
s NOXA1iR	ACCGACCTCTGTCTCTGCAT
s NOXO1iF	AGAACGAAGACCGGCAGAC
s NOXO1iR	CGGGAAGCACAGAACTGG
s NOX1iF1	CATTGCTGGTCTCACTGGAG
s NOX1iR1	CACGATCATCCCACATCTCA
blasticidin F	ACAGCATCCCCATCTCTGAAGA
blasticidin R	TGCGGCCGTCGCTAGA

PCR Thermal Cycle: : 94°C for 2 min; 35 cycles of 94°C for 30 sec; 58°C for 30 sec, 72°C for 45 sec; and a final elongation step for 5 min at 72°C

Table 2. $p22^{phox}$ single nucleotide polymorphisms in humans

	Single Nucleotide Polymorphism			
Haplotype	c.214T>C	c.521T>C	c.*24G>A	Allelic Frequency
A	X			0.39
B		X	X	0.20
C	X	X	X	0.22
D		X		0.11
E	X		X	0.40
F				0.20
G	X	X		0.20

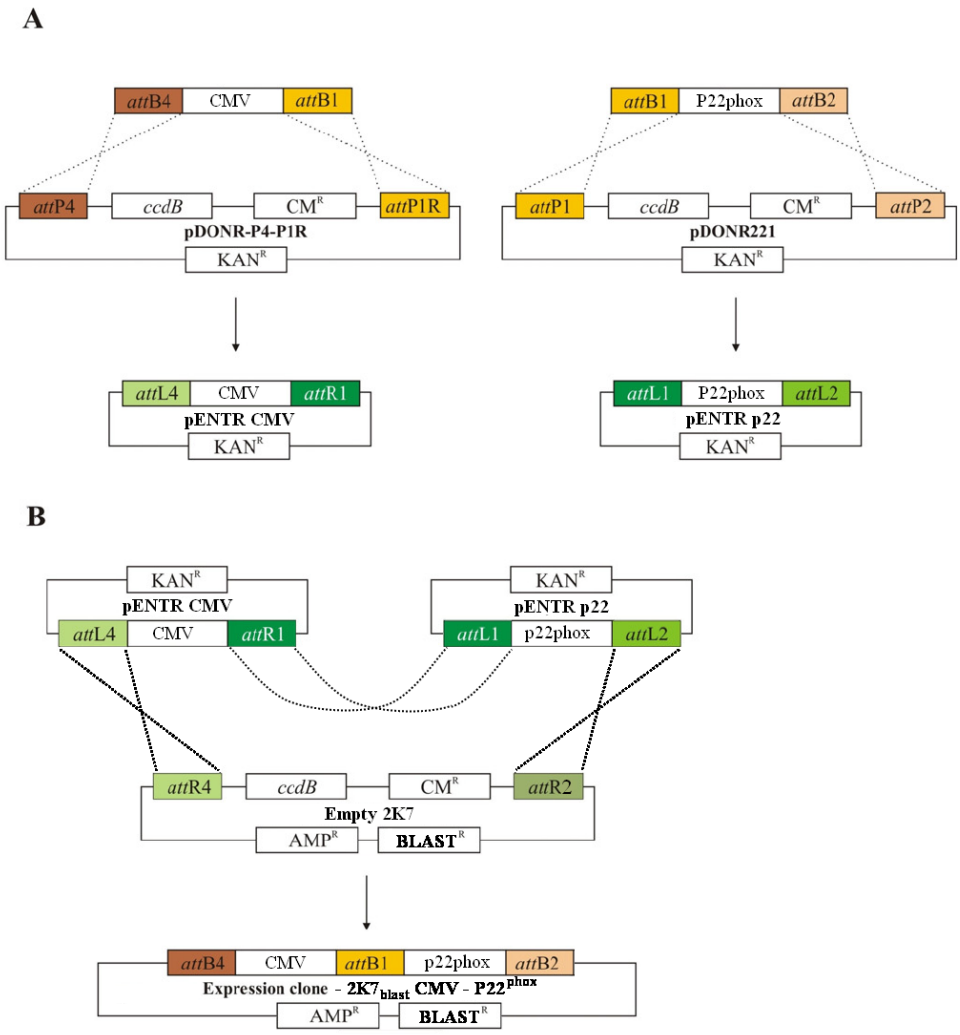

Figure 8. Multisite Gateway® Cloning. The generation of NOX1 and the associated plasmids was achieved using Gateway® cloning. **A**. The Entry vectors were created using the PCR products flanked with recombination sites targeted by the BP recombination reaction (Where B sites recombine with P sites). **B**. The Expression clones were generated by a recombination reaction between the Entry vectors containing the CMV promoter and Entry vectors containing NOX1 or subunits, and a modified pDONR vector called a 2K7 cassette Gateway® vector. This was achieved by using the LR recombination reaction (Where L sites recombine with R sites). Figure modified from Magnani et al., 2006.

CHAPTER 3: RESULTS

3.1 Creation of a model cell line for the study of the effect of $p22^{phox}$ variation on NOX1

This research required a suitable cell line for studying the effect of variations in $p22^{phox}$ on the behavior of NOX1. To obtain this, we selected a cell line reported to be devoid of all endogenous NOX isoforms and associated subunits (Löhneysen et al., 2008; personal communication with Dr. Ulla Knaus, UCD Conway Institute of Biomolecular and Biomedical Research, Dublin), and then used this cell line to introduce the components required for a functional NOX1 enzyme. The chosen cell line, a human lung carcinoma cell line identified as H661, was verified to be devoid of endogenous NOX isoforms through RT-PCR followed by agarose gel electrophoresis (Figure 9).

3.1.1 Generation of the HOAx1 cell line

A foundation cell line was created with the insertion of NOX1 (with GFP as a selection marker), NOXA1 (with neomycin resistance as a selection marker), and NOXO1 (with zeocin resistance as a selection marker). The cell line was made isogenic by dilution and clonal selection, and was verified to contain the desired components by RT-PCR followed by agarose gel electrophoresis (Figure 10). This foundation cell line, hereafter referred to as HOAx1, contained the necessary components for NOX1-based ROS generation, with the exception of $p22^{phox}$.

3.1.2 Confirming lack of interference between GFP and calcein

Green fluorescent protein (GFP) was used as a selection marker for successful NOX1 transduction. Calcein, a green fluorescent marker of viable cells, was used during some plate assays as an indicator of the number of viable cells plated in the well. Calcein has an excitation wavelength of 495 nm, and an emission wavelength of 515 nm. GFP has an excitation wavelength of 488 nm, and an emission wavelength of 507 nm. We would expect the fluorescent from the GFP protein to interfere with the calcein assay. In order to confirm the magnitude of the GFP signal was not interfereing with the calcein the fluorescence was measured from both human lung cancer cells devoid of NOXs (H661), and human lung cancer cells transduced with NOX1 subunits (HOAx1) treated and untreated with calcein. There was a negligible contribution by GFP in fluorescence between the H661 cell line treated with calcein, and the GFP-containing HOAx1 cell line treated with calcein. (Figure 11).

3.2 Assessment of effect of genetic variation in the $p22^{phox}$ subunit on ROS generation

3.2.1 Analyzing H_2O_2 generation following PMA stimulation of S184 A – G cell lines

Seven different genetic variants of $p22^{phox}$ were introduced into the HOAx1 cell line to create seven different cell lines called S184-A to S184-G. An Amplex Red assay was performed to measure the H_2O_2 in these cells at rest and following stimulation with the phorbol ester PMA. The results of the Amplex Red™ test revealed there was little

ROS generated by the HOAx1 cells either at rest or when stimulated with PMA. Further, all seven PMA-stimulated variants of $p22^{phox}$ generated significant levels of ROS compared to the HOAx1 control, indicating that all seven variants support functional NOX1 activity (Figure 12). Compared to the HOAx1 control, there was a significant increase in ROS generation in the absence of PMA for variants E and G, and there was a significant increase after the addition of PMA for all variants. Consistent with NOX1 being the source of the ROS, the PMA stimulated ROS generation was inhibited by the addition of DPI down to a level that was not significantly different from the HOAx1 control. Although the Amplex Red assay indicated that all seven variants of $p22^{phox}$ were able to support NOX1-mediated ROS generation, there was not a significant difference in the rate of ROS generation by NOX1 among these seven variants. The haplotypes were then grouped based on a single nucleotide polymorphism, and the rate of ROS production was examined (Figure 13). This comparison indicates that none of the three single nucleotide polymorphisms have a significant effect on the rate of ROS production.

3.2.2 Determining mRNA levels of $p22^{phox}$ in S184 A – G cell lines

The seven $p22^{phox}$ variants were introduced into the HOAx1 cells by lentiviral transduction. It is possible for cells to incorporate more than one copy of a gene during the lentiviral gene transfer. Differences in the number of copies could influence the amount of $p22^{phox}$ protein present in the cell, and this is a potentially confounding factor in interpreting the effect of genetic variations in the $p22^{phox}$ gene. In order to determine if each of the seven cell lines received the same number of copies of the vector, quantitative polymerase chain reaction (qPCR) was performed on DNA collected from the cells.

Quantifying $p22^{phox}$ directly would be confounded by the fact that the background cell line, H661, would have endogenous $p22^{phox}$ at the DNA level. The blasticidin resistance gene is present on the plasmid that was used to introduce the $p22^{phox}$ gene, and is not present endogenously; therefore, the amount of blasticidin resistance gene indicates the amount of the plasmid that was introduced during transduction. S184 cell line genomic DNA was analyzed for blasticidin expression via qPCR, Expression was normalized to the housekeeping gene GAPDH. Amongst the variants there were significant differences in blasticidin selection marker expression. (Figure 14)

The level of message for $p22^{phox}$ was assessed by quantitative RT-PCR. No significant differences were observed in the level of $p22^{phox}$ expression. With the exception of haplotype B, there were no significant differences between the amount of blasticidin DNA present, and the matching $p22^{phox}$ expression within a variant. However, another possible mechanism by which $p22^{phox}$ variations may exert an effect on NOX-based ROS generation is through decreased stability**.**

Expression of $p22^{phox}$ mRNA was compared when the seven haplotypes were grouped based on a single nucleotide polymorphism (Figure 15). The results of this comparison indicate none of the three single nucleotide polymorphisms have a significant effect on expression of $p22^{phox}$ mRNA.

3.2.3 Western Blot Analysis of $p22^{phox}$ from S184 A – G cell lines

Immunoblotting of the $p22^{phox}$ subunit within the S184 cell line revealed a significant increase in protein expression of haplotypes D and G compared to the control, haplotype A (Figure 16). Haplotypes A, B, C, and E exhibited consistently low levels of

protein expression in comparison to the other haplotypes. When the haplotypes are grouped and examined based on a single nucleotide polymorphism, it appears haplotypes containing the allelic variant at *24 in the 3'UTR exhibit a significantly lower level of $p22^{phox}$ protein expression, whereas the other two allelic variations do not result in a significant difference (Figure 17).

3.3 Development of assay to quantify lentiviral particles to achieve equal copy numbers across cell lines

3.3.1 Quantification of vector (GFP & qPCR)

In order to address the issue of unequal gene transfer among the seven cell lines transduced with $p22^{phox}$ variants, a method was needed to quantify the amount of lentiviral particles present in the virus preparation prior to adding this to the HOAx1 background cells. The quantification method was developed using a 2K7 vector with a CMV promoter and with GFP as the gene of interest. HEK293T cells were transfected with this vector along with the three vectors (8.92, 8.93, and MD2G) encoding the viral packaging components. These cells then create a viral vector containing the GFP gene, and as this is a retroviral based packaging system, the GFP gene is therefore encapsulated as RNA. The virus preparation was collected and then serially diluted using a 4 fold dilution series. The diluted vector preparation was then divided into two parts. One was used to transduce HEK293T cells to determine transduction efficiency. RNA was isolated via an RNeasy kit (Qiagen, Venlo, Netherlands) from the other sample fraction to determine the amount of virus present by combining equal parts viral preparation, and a buffer RLT solution containing beta-mercaptoethanol. The RNA from the virus

preparation was spiked with a fixed quantity of a purchased RNA encoding the kanamycin resistance gene to be used as a normalizer. RNA isolated from each of the virus prep dilutions was spiked with the same amount of kanamycin (7.5 pg/μL). The GFP vector contained the blasticidin resistance gene as a selection marker. qRT-PCR performed on cDNA prepared from the diluted virus preparation samples using primers for blasticidin as the gene of interest and primers for kanamycin as the normalization gene found that a decrease in the amount of blasticidin resistance gene could be detected on dilution. (Figure 18). The percent of HEK293T cells successfully transduced with GFP was quantified by flow cytometry using the BD FACSCalibur (BD Biosciences, New Jersey, United States) flow cytometer and Cell Quest Pro software (v 5.2.1)(Figure 19 and Figure 20). Undiluted virus preparation resulted in transduction efficiency ranging from 48% to 62%. There was a decrease in the number of cells expressing the GFP gene as the virus preparation was diluted, and this relationship was linear (Figure 21).

3.3.2 Using a novel technique to generate new cell line with equal $p22^{phox}$ transduction

The method of detecting the amount of virus present in viral preparations was used to try to create a new set of seven cell lines where the amount of vector encoding $p22^{phox}$ was equal among the cell lines. The blasticidin gene was detected by qRT-PCR on cDNA prepared from RNA isolated from the virus preparations. Six of the seven virus preparations were diluted to match the sample with the lowest concentration. The HOAx1 cells were then transduced with these diluted virus preparations to create the S232 series of cells. Results from the qPCR analysis of the DNA for the blasticidin resistance selection marker within the S232 cell lines indicate the vector quantification

procedure is effective, as equal copy numbers were achieved across all seven variants. Analyses of the corresponding mRNA via qRT-PCR reveal no significant differences in expression of $p22^{phox}$ amongst the variants and in expression of $p22^{phox}$ expression within a variant when compared to the blasticidin expression, despite achieving equal blasticidin resistance copy numbers throughout the cell line at the transduction stage (Figure 22).

3.3.3 S232 cell line with equal $p22^{phox}$ transduction does not produce ROS

Analysis of the Amplex Red™ assay conducted with the seven variants of the PMA-stimulated S232A cell line reveals a lack of ROS generation above basal levels when compared to the control HOAx1 cell line (Figure 23). PCR and gel electrophoresis analyses of the S232 cell line indicate a loss of expression of the subunit NOXA1, as a band of the expected size was absent, while NOX1, NOXO1, and $p22^{phox}$ expression remained (Figure 24).

3.4 Natural plant extracts as NOX or mitochondrial inhibitors

Amplex Red™ assays indicate that 50 μM and 100 μM concentrations of celastrol dramatically increased and rate of H_2O_2 generation in the unstimulated NOX1-based S184 cell line containing haplotype A, whereas concentrations of celastrol ranging from 1 to 10 μM decreased the rate of H_2O_2 production. Furthermore, 50 μM and 100 μM concentrations of resveratrol, and concentrations of piperine between 5 μM and 100 μM significantly decreased the rate of H_2O_2 production by S184 cells (Figure 25). SOD did not have a significant effect on NBT assay superoxide measurements (Figure 26), but SOD and DPI significantly reduce superoxide measurements from MCLA assays (Figure

27). Amplex Red™ assays in PMA-stimulated B lymphocytes (0.1 nM), where NOX2 is the source of ROS, involving celastrol and resveratrol revealed the ability of these compounds to inhibit H_2O_2 production by NOX2 at concentrations ranging from 0.5 μM to 100 μM for celastrol, and 50 μM to 100 μM for resveratrol (Figure 28). Analyses conducted by Amplex Red™ assay indicate celastrol and resveratrol act as significant antioxidants towards H_2O_2 in a dose-dependent manner (Figure 29). Under the same conditions apigenin, artesunate, and piperine do not act as strong antioxidants against hydrogen peroxide. Amplex Red™ analyses of 100 μM compound concentrations in conjunction with 625 nm of H_2O_2 revealed the five natural compounds (apigenin, artesunate, celastrol, piperine, and resveratrol) do not significantly interfere with Amplex Red™ assay readings (Figure 30).

3.4.1 Antioxidant ability of celastrol and resveratrol towards H_2O_2

Amplex Red™ assays with B-LCL cells indicate that resveratrol has an IC50 of approximately 30 μM, while celastrol has an IC50 of approximately 8.6 μM under the same conditions (Figure 31). Amplex Red™ analysis revealed the hydrogen peroxide scavenging activity of celastrol and resveratrol with IC50s of approximately 22 μM and 42 μM, respectively (625 nM H_2O_2 and equal volumes for all drug concentrations)(Figure 32).

3.4.2 Celastrol and resveratrol do not affect NOX2 superoxide production but inhibit NOX1 superoxide production

Analyses of celastrol and resveratrol by the nitro blue tetrazolium test indicate these compounds do not significantly inhibit production of superoxide by NOX2 (Figure 33). The compounds, apigenin, artesunate, and piperine also do not have a significant effect on NOX2 superoxide production at concentrations of 100 μM and below. Analyses by nitro blue tetrazolium assay indicate that celastrol significantly inhibits production of superoxide by NOX1 at concentrations ranging from 5 μM to 100 μM. The compounds resveratrol, apigenin, artesunate, and piperine do not have a significant effect on NOX1 superoxide production at concentrations of 100 μM and below. (Figure 34) Analyses via the methyl cypridina luciferin analog (MCLA) chemiluminescence assay in conjunction with a cell-free xanthine/xanthine oxidase system indicate celastrol and resveratrol can act as significant antioxidants towards superoxide at concentrations ranging from 0.5 μM to 100 μM for celastrol, and 0.5 to 50 μM for resveratrol (Figure 35).

3.4.3 Effect of celastrol on mitochondrial H_2O_2 generation

Analysis conducted by Amplex Red™ assay indicate that celastrol (10 μM) causes a minor, yet insignificant increase in the rate of H_2O_2 generation from mitochondria isolated from H661 cells (Figure 36). This result is observed when using a malate/pyruvate combination as the electron donor for the mitochondrial electron transport chain. Antimycin and malate/pyruvate positive controls did not work as expected, and DPI did not inhibit ROS generation as expected.

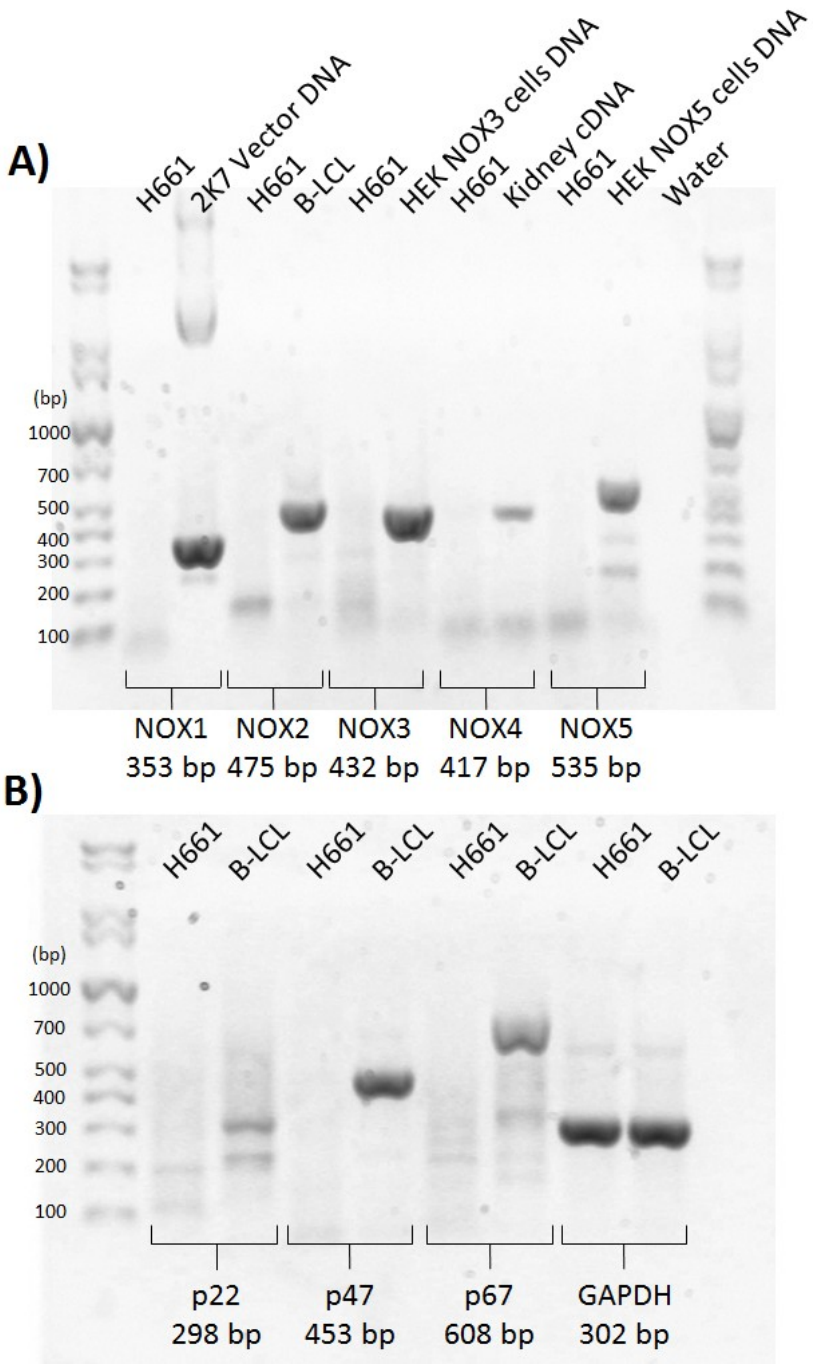

Figure 9. Characterization of the (A) expression of NOX isoforms and (B) subunits in H661 cells. PCR (NOX1 positive control) or RT-PCR (all other samples) was performed on H661 cells and on positive control samples. A 2K7 vector containing the NOX1 gene was used as a positive control for the NOX1 gene. RNA isolated from previously established HEK cells expressing NOX3 or NOX5 were used for those genes. Purchased human kidney cDNA was used for a positive control for NOX4. cDNA prepared from human B-lymphocyte cell lines was used as a positive control for all other genes. PCR products were visualized on a 1% agarose gel.

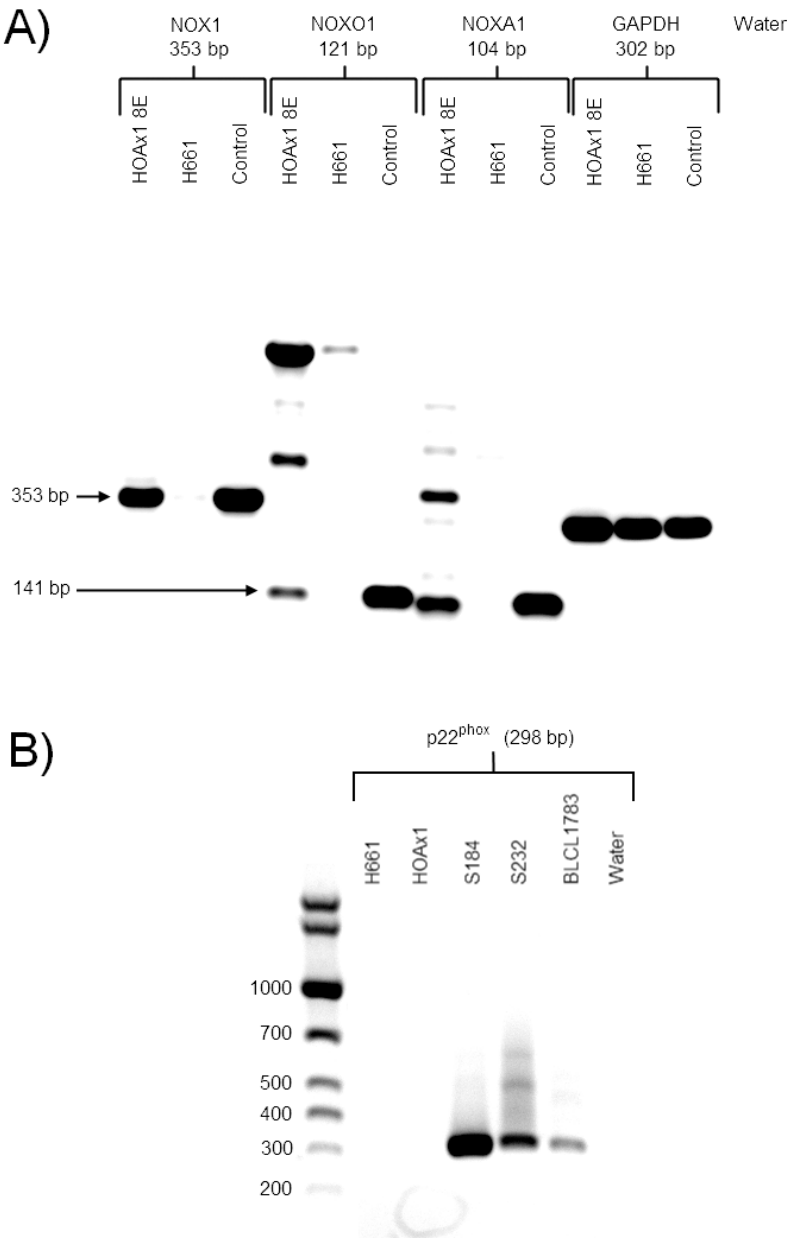

Figure 10. Characterization of the HOAx1 cell line. PCR and agarose gel electrophoresis visualization of the NOX enzyme and associated subunits following their insertion into the H661 human lung cancer cell via lentiviral transduction. The resulting HOAx1 cells appear to contain (A) the main NOX1 unit, and the associated NOXO1, NOXA1 subunits, and (B) the $p22^{phox}$ subunit.

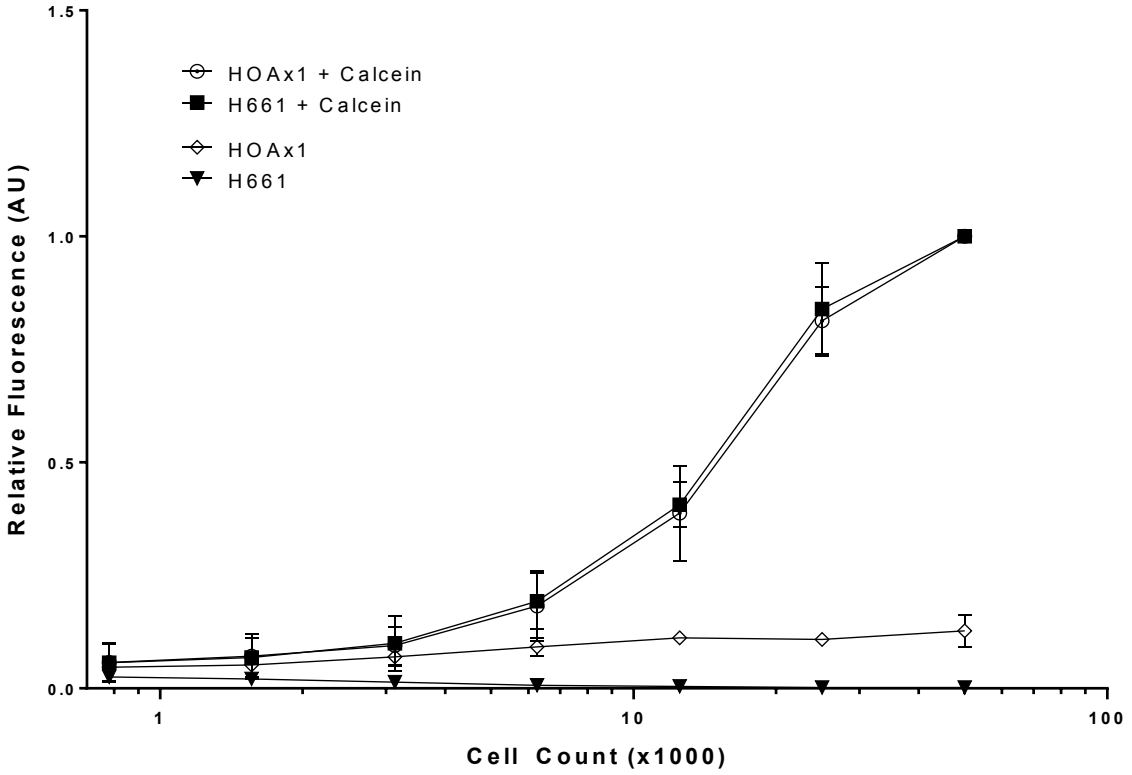

Figure 11. GFP and calcein measurements in human lung cancer cells transduced with NOX1 subunits. The fluorescence was measured from both human lung cancer cells devoid of NOXs (H661), and human lung cancer cells transduced with NOX1 subunits (HOAx1) treated and untreated with calcein to determine if the GFP selection marker found within HOAx1 interferes with calcein assay measurements. Bars indicate standard deviation. n = 3.

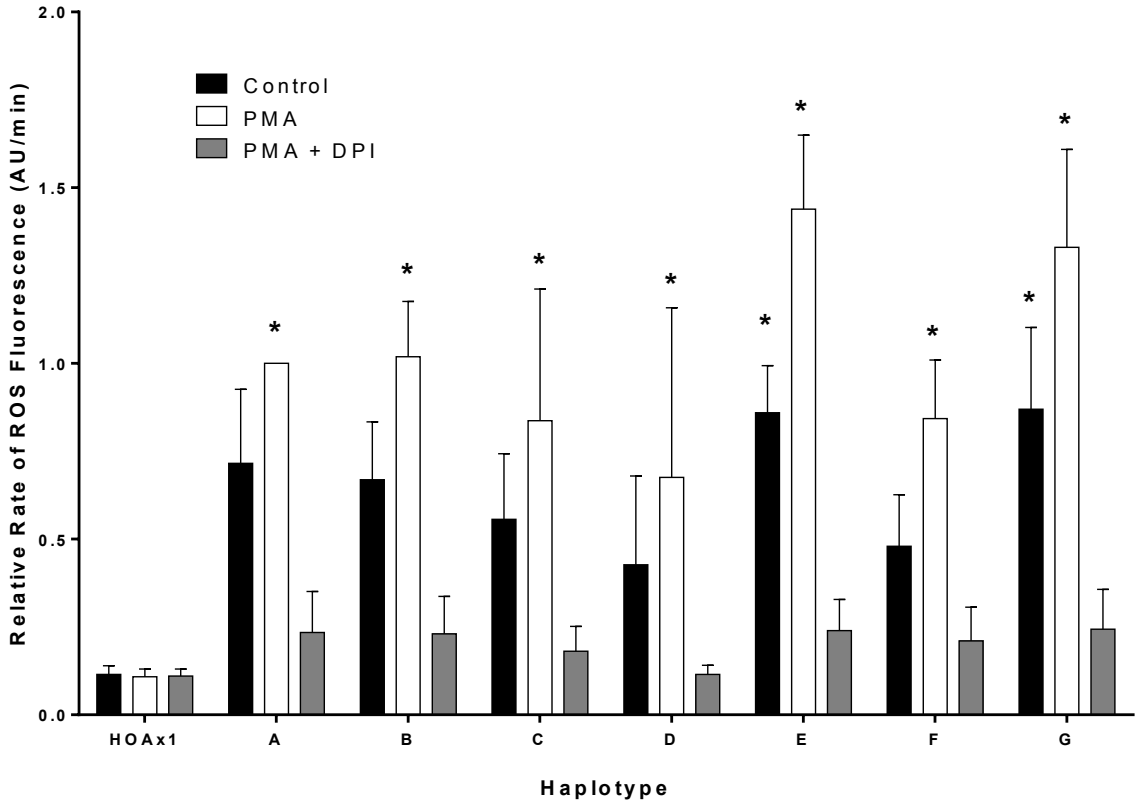

Figure 12. ROS generation in p22^{phox}-deficient human lung cancer cells transduced with seven different haplotypes. The rate of ROS generation was measured using the Amplex Red assay in a H661 human lung cancer cell line devoid of endogenous NOXs that was transduced with each of the seven haplotypes. Plotted according to haplotype and normalized to the PMA treatment of haplotype A. The asterisk indicates significant difference from the PMA treated, p22^{phox}-absent control, HOAx1 (ANOVA, Dunnett post hoc analysis). Bars indicate standard deviation. n = 3.

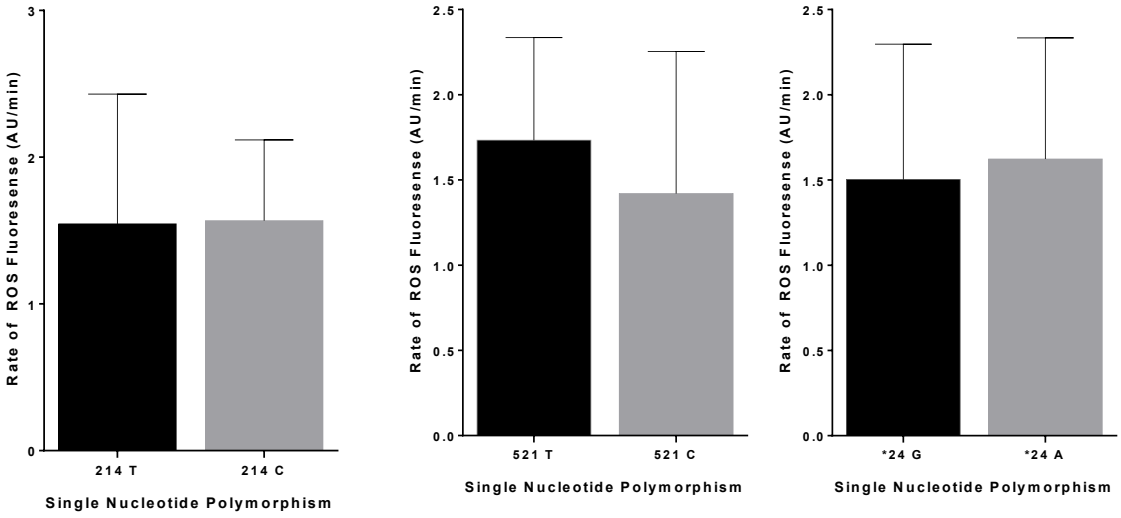

Figure 13. ROS generation of S184 cell line sorted by polymorphism. The rate of ROS generation was measured using the Amplex Red assay in a H661 human lung cancer cell line devoid of endogenous NOXs that was transduced with each of the seven haplotypes. Plotted according to single nucleotide polymorphism. No significant differences were noted (Unpaired, two tailed T-test). Bars indicate standard deviation. n = 3.

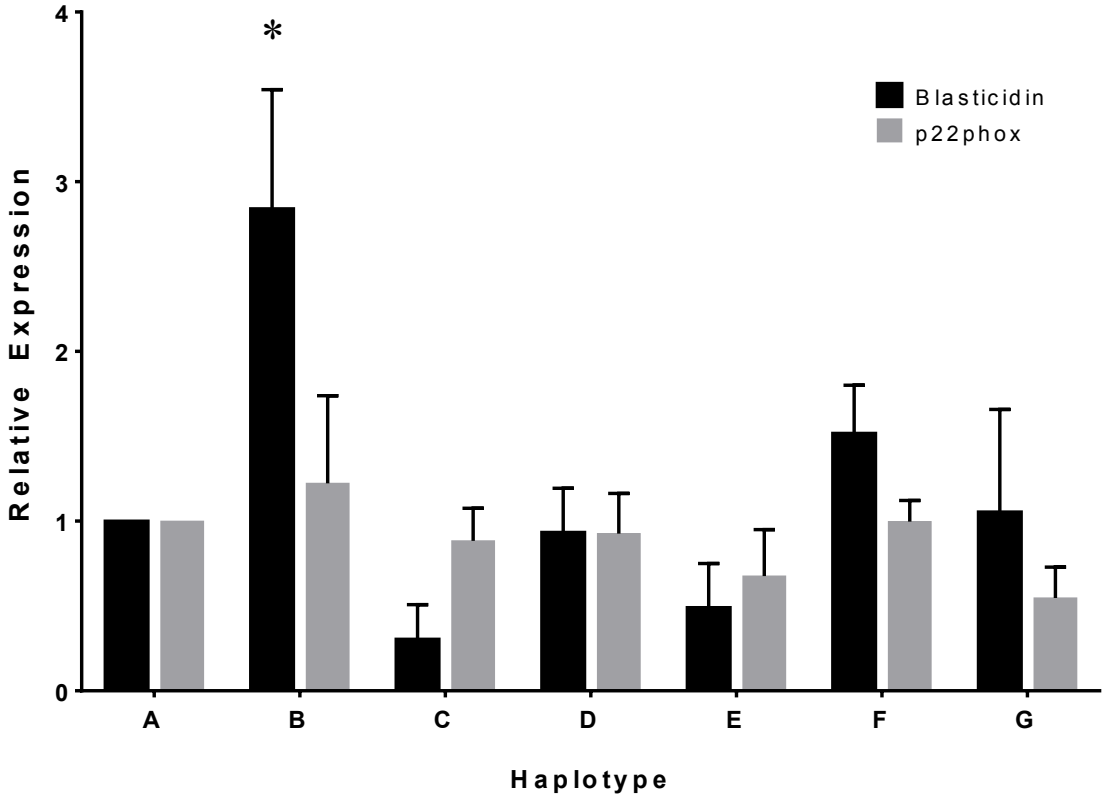

Figure 14. Unequal vector copy numbers of blasticidin following transduction. Blasticidin, which is not endogenous to the cell line, was inserted alongside the $p22^{phox}$ haplotypes as a selection marker, and as a way for determining relative copy numbers of the inserted haplotypes. Quantitative PCR (qPCR) of the blasticidin DNA, and quantitative reverse transcriptase PCR (qRT-PCR) of the $p22^{phox}$ mRNA reveal unequal copy numbers across the haplotypes, and that expression of the blasticidin within one haplotype does not consistently correlate with the relative $p22^{phox}$ expression. qPCR and qRT-PCR results are plotted according to haplotype and normalized to their respective haplotype A result. No significant differences were measured among blasticidin or $p22^{phox}$ from all haplotypes (ANOVA, Tukey multiple comparisons post hoc analysis). Bars indicate standard deviation. n = 3.

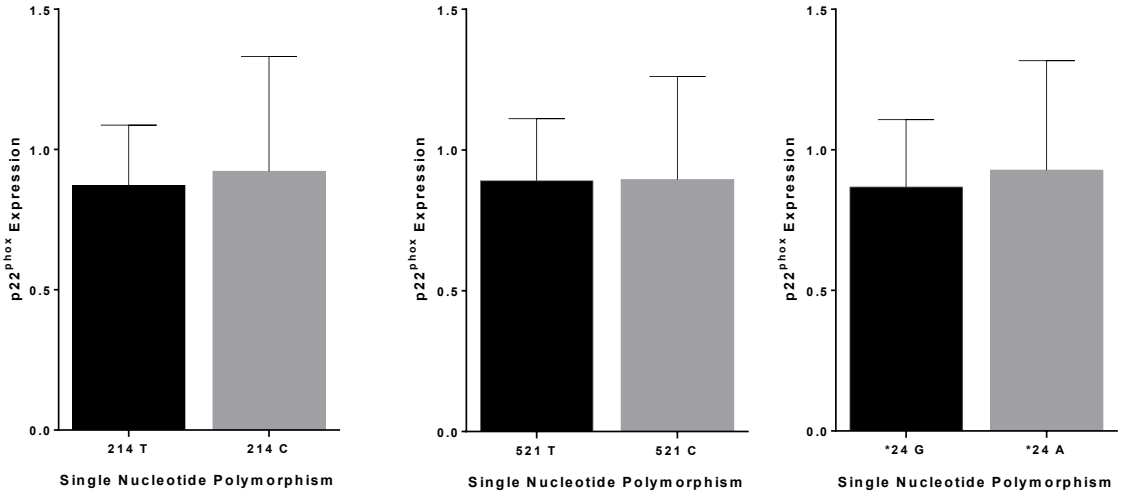

Figure 15. Comparison of p22^{phox} mRNA expression from three single nucleotide polymorphisms. The expression of p22^{phox} mRNA was measuring using qRT-PCR in a H661 human lung cancer cell line devoid of endogenous NOXs that was transduced with each of the seven haplotypes. All haplotypes were plotted according to single nucleotide polymorphism. No significant differences were noted (Unpaired, two tailed T-test). Bars indicate standard deviation. n = 3.

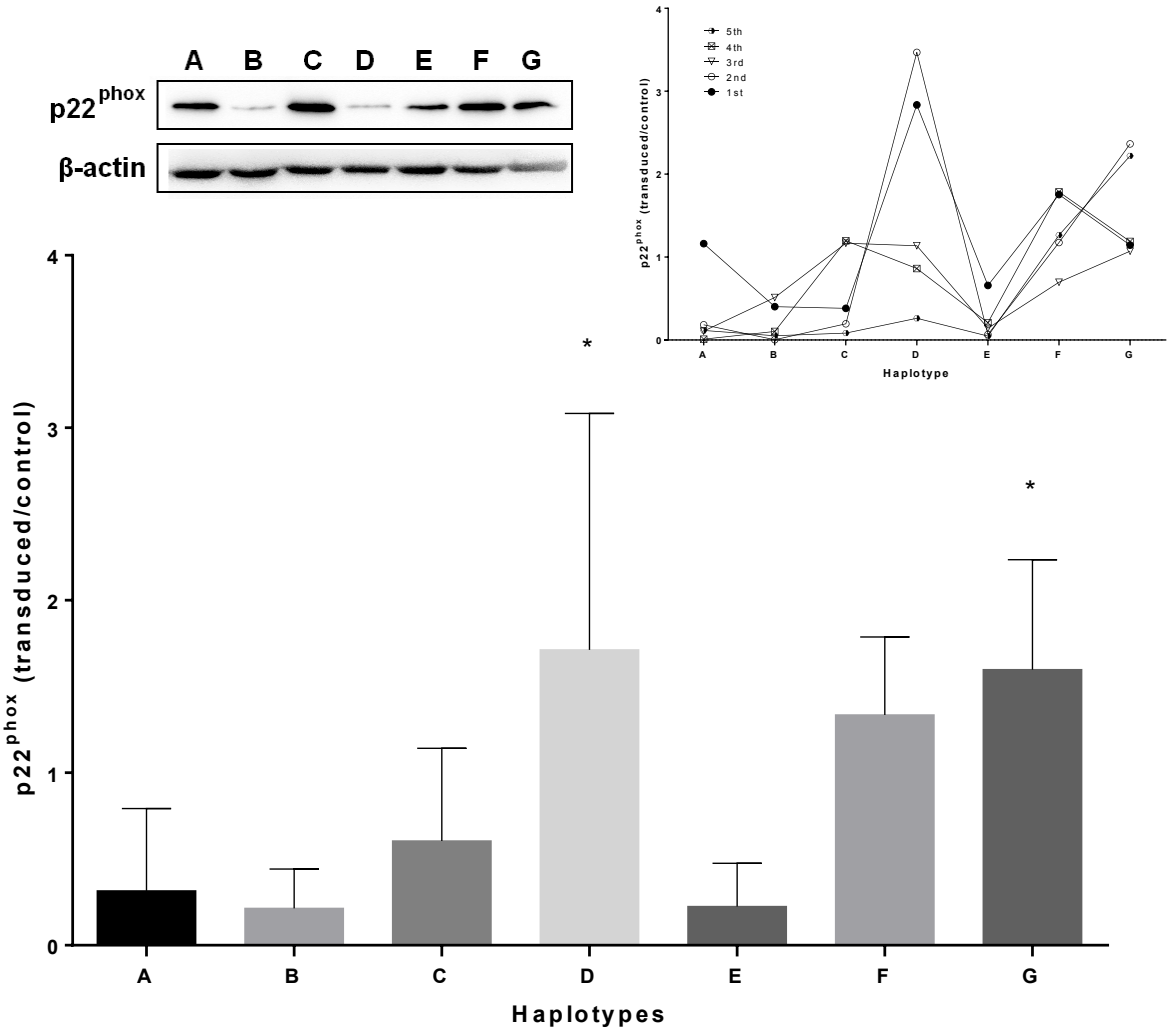

Figure 16. p22^{phox} protein level in human lung cancer cells transduced with NOX1 and each of the seven p22^{phox} haplotypes. The amount of p22^{phox} protein expression in transduced H661 human lung cancer cells was assessed by Western blotting. The Western blot results were quantified by densitometry and plotted according to haplotype. To control for equal loading of protein, bands were normalized to β-actin. **Inset:** Normalized p22^{phox} expression of each individual trial of protein immunoblotting. An asterisk indicates a significant difference from the overall mean (ANOVA, Dunnett post hoc analysis). Bars indicate standard deviation. n = 5.

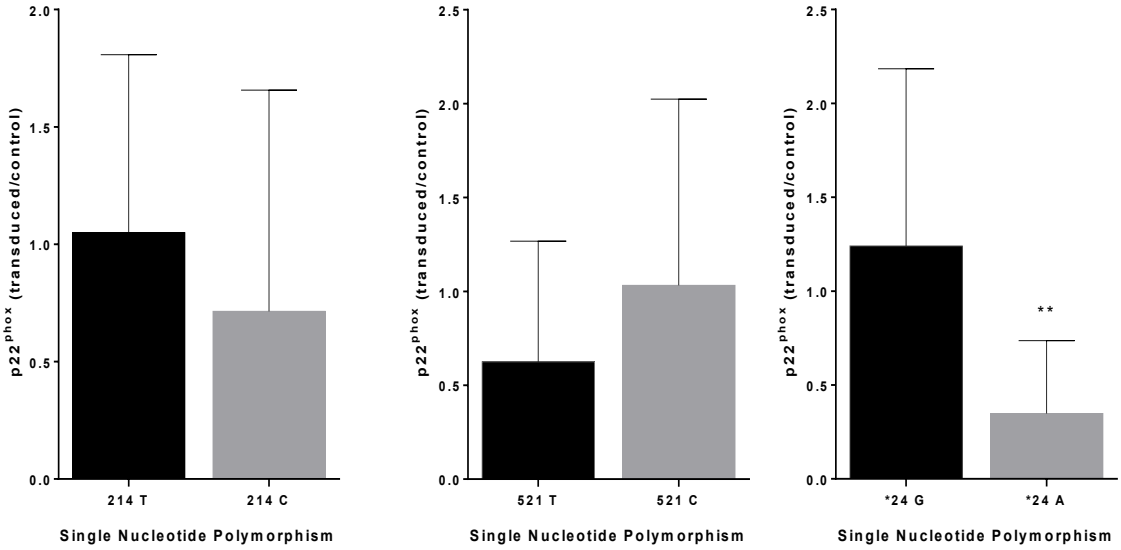

Figure 17. Comparison of p22^{phox} protein expression from three single nucleotide polymorphisms. The amount of p22^{phox} protein expression in transduced H661 human lung cancer cells was assessed by Western blotting. The Western blot results were quantified by densitometry and plotted according by single nucleotide polymorphism. To control for equal loading of protein, bands were normalized to β-actin**.** An asterisk indicates a significant difference from the overall mean (Unpaired, two tailed T-test). Bars indicate standard deviation. n = 3.

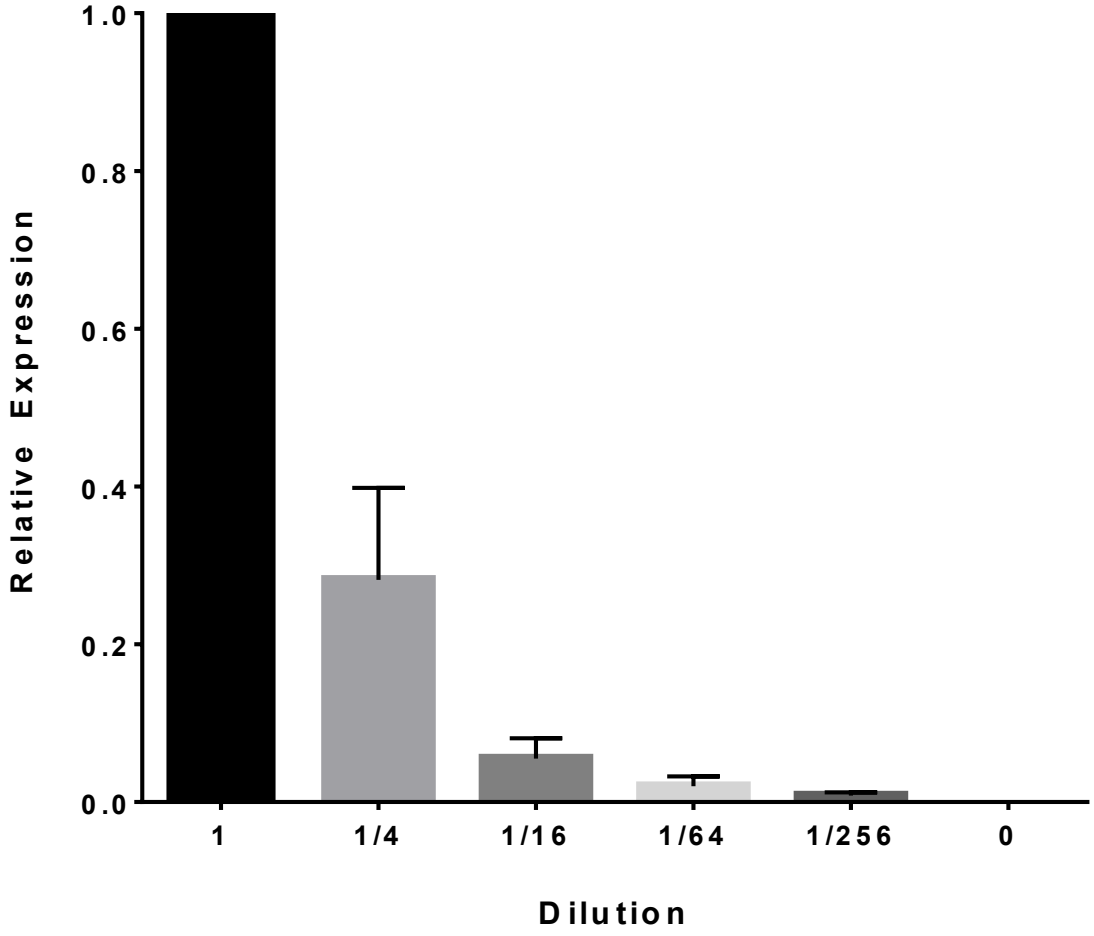

Figure 18. qRT-PCR quantification of lentiviral particles containing blasticidin DNA. The GFP vector contained the blasticidin resistance gene as a selection marker. qRT-PCR performed on cDNA prepared from the diluted virus preparation samples using primers for blasticidin as the gene of interest and primers for kanamycin as the normalization gene found that a decrease in the amount of blasticidin resistance gene could be detected on dilution. Bars indicate standard deviation. n = 3.

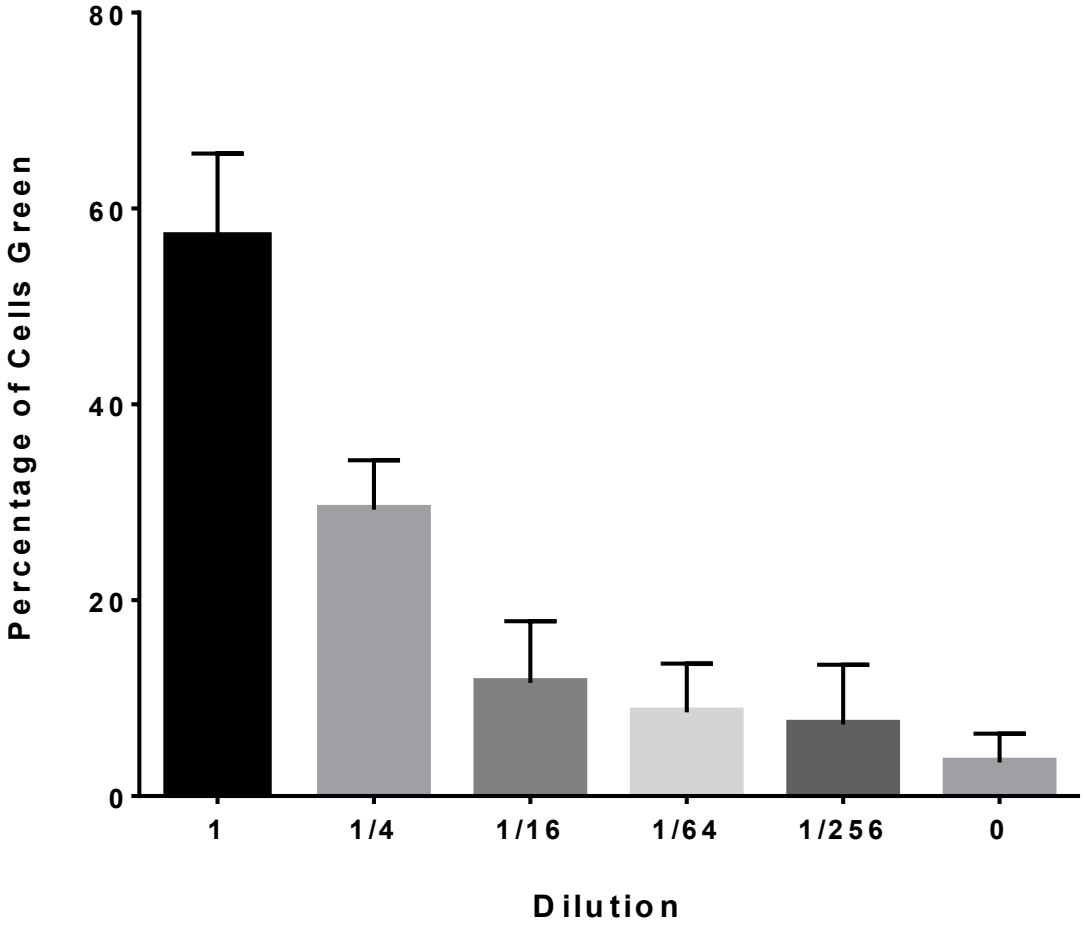

Figure 19. Quantification of HEK293T cells fluorescing green. The percentage of cells fluorescing green following transduction with diluted viral particles containing the GFP message was quantified via flow cytometry. Bars indicate standard deviation. n = 3.

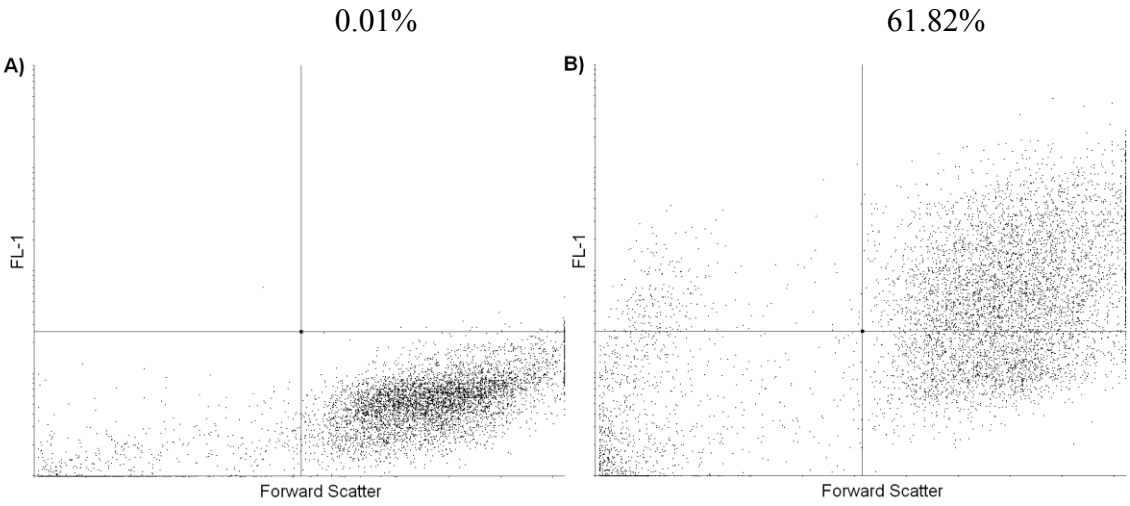

Figure 20. Percentage of cells fluorescing green following serially-diluted lentiviral transduction. HEK293T cells were transduced with diluted amounts of viral particles containing a GFP message and quantified via flow cytometry. A) The percentage of cells fluorescing green following no viral treatment of cells. B) The percentage of cells fluorescing green following treatment of cells with full strength viral preparation.

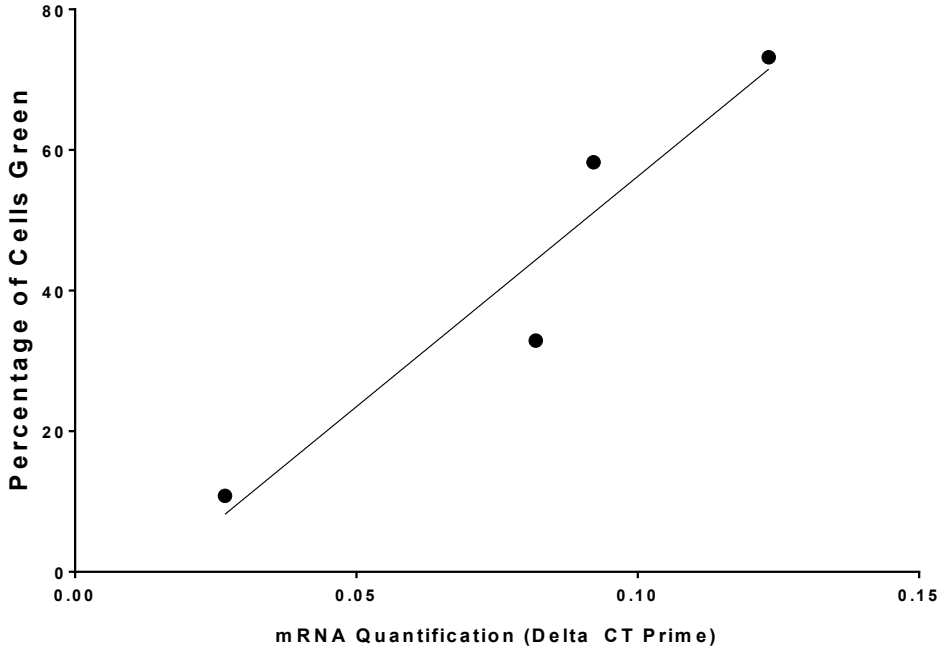

Figure 21. Percentage of green fluorescent cells compared to the relative mRNA quantification following serially-diluted lentiviral transduction. Relationship between the quantification of the GFP-containing viral particles, and the resulting percentage of cells fluorescing green as determined via qRT-PCR and flow cytometry, respectively**.**

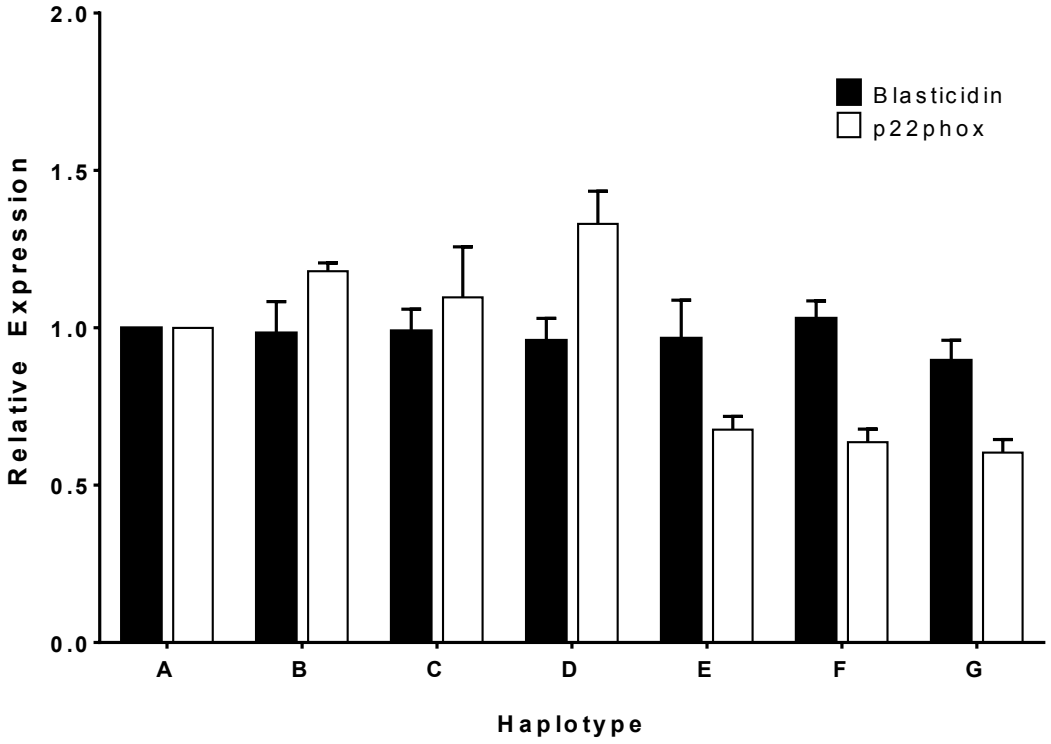

Figure 22. Equal copy numbers of blasticidin achieved with S232 cell line. Quantitative PCR (qPCR) of the blasticidin DNA, and quantitative reverse transcriptase PCR (qRT-PCR) of the $p22^{phox}$ mRNA reveal equal copy numbers across the haplotypes, following a novel vector quantification technique. qPCR and qRT-PCR results are plotted according to haplotype and normalized to their respective haplotype A result. No significant differences were measured among blasticidin or $p22^{phox}$ from all haplotypes (ANOVA, Tukey multiple comparisons post hoc analysis). Bars indicate standard deviation. n = 3.

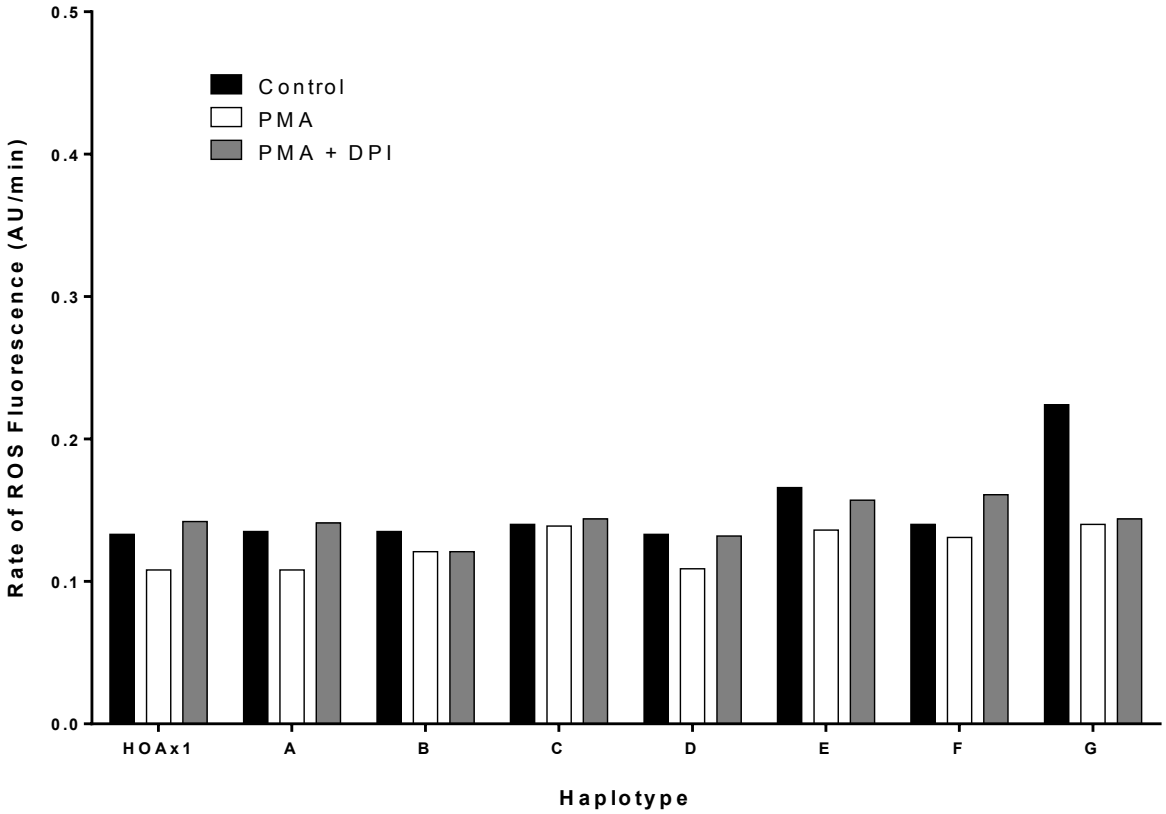

Figure 23. ROS generation in p22^{phox}-deficient human lung cancer cells equally transduced with seven different haplotypes. The rate of ROS generation was measured using the Amplex Red assay in a NOX-devoid H661 human lung cancer cell line that was transduced with each of the seven haplotypes via a vector quantification method to achieve equal vector transduction efficiency. Results are plotted according to haplotype. n = 2.

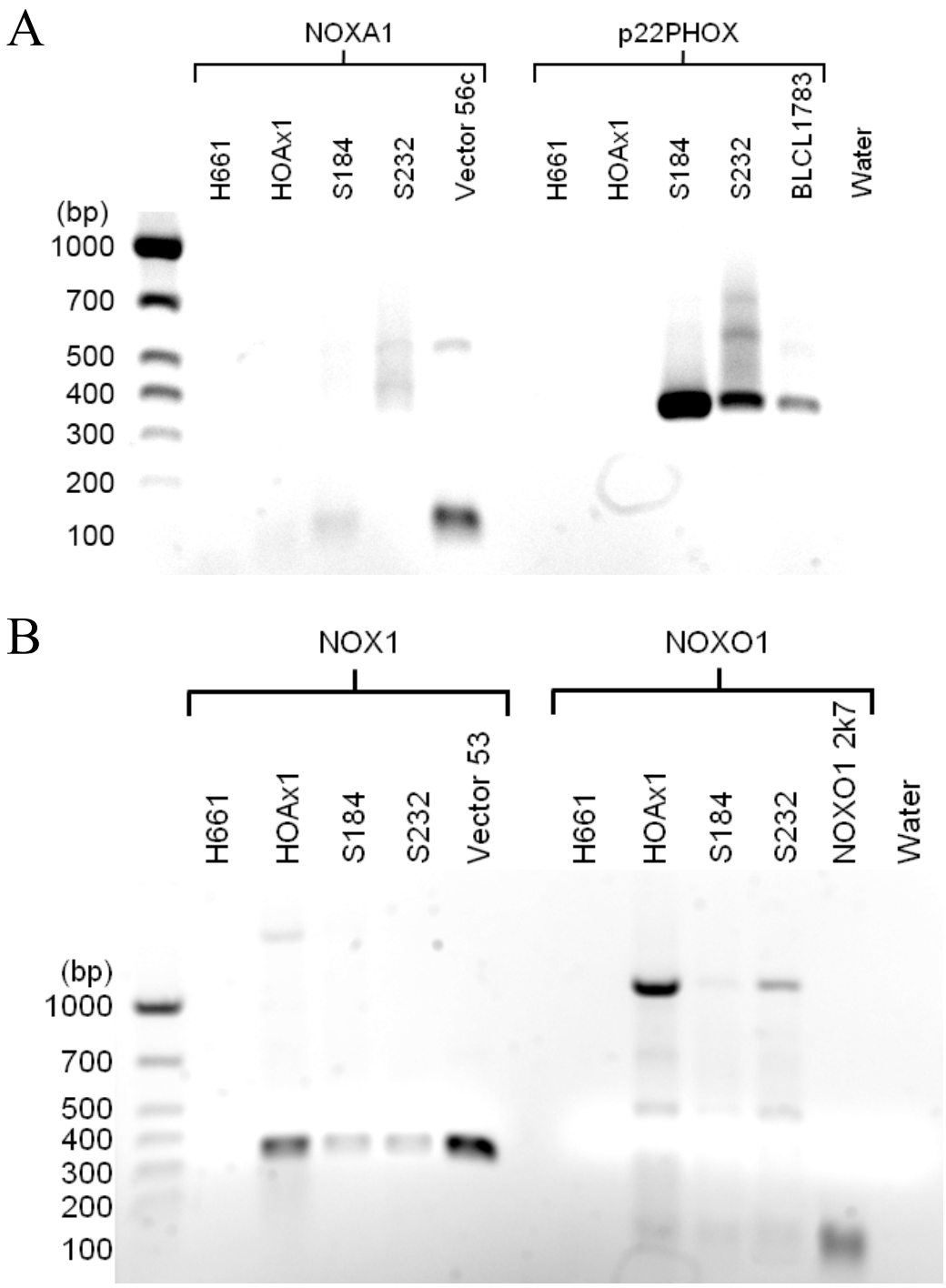

Figure 24. Examining presence of NOX1 subunits. Successful transduction of H661 cells with NOX1 and associated subunits was verified using various selection markers. **A)** RT-PCR and 1% agarose gel electrophoresis indicate the presence of $p22^{phox}$ in the appropriate cell lines, but an absence of the NOXA1 (104 bp) subunit in the S232 cell line. **B)** The NOX1 (353 bp) and NOXO1 (121 bp) subunits were present in the appropriate cell lines. Vector 56c is the NOXA1 positive control, Vector 53 is the NOX1 positive control, and NOXO1 2k7 is the NOXO1 positive control.

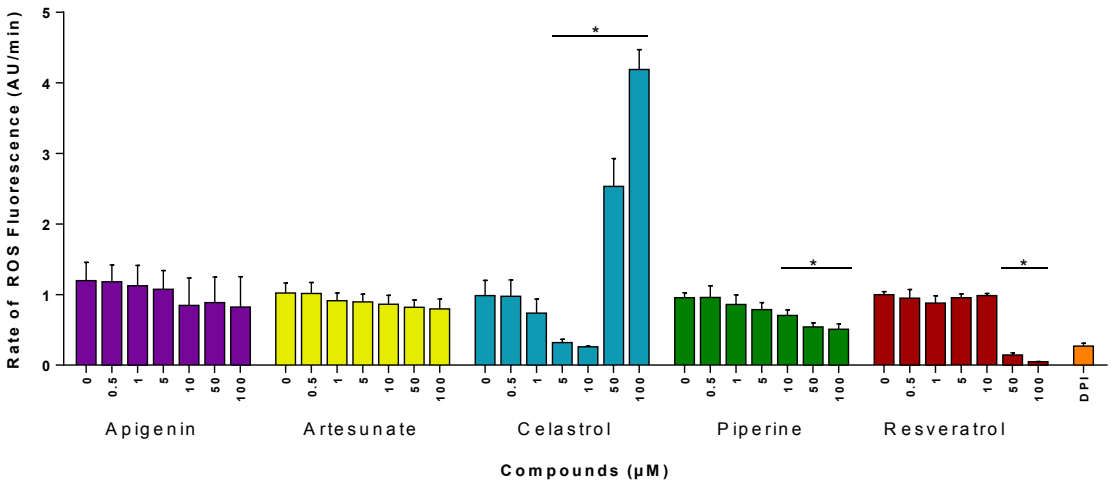

Figure 25. The effect of natural compounds on the rate of NOX1-based ROS production. The rate of H_2O_2 generation by the S184 cell line treated with natural compounds was measured over a two hour period using the Amplex Red assay. An asterisk indicates a significant difference from the 0 µM control within a group (ANOVA, Dunnett post hoc analysis). Bars indicate standard deviation. n = 3.

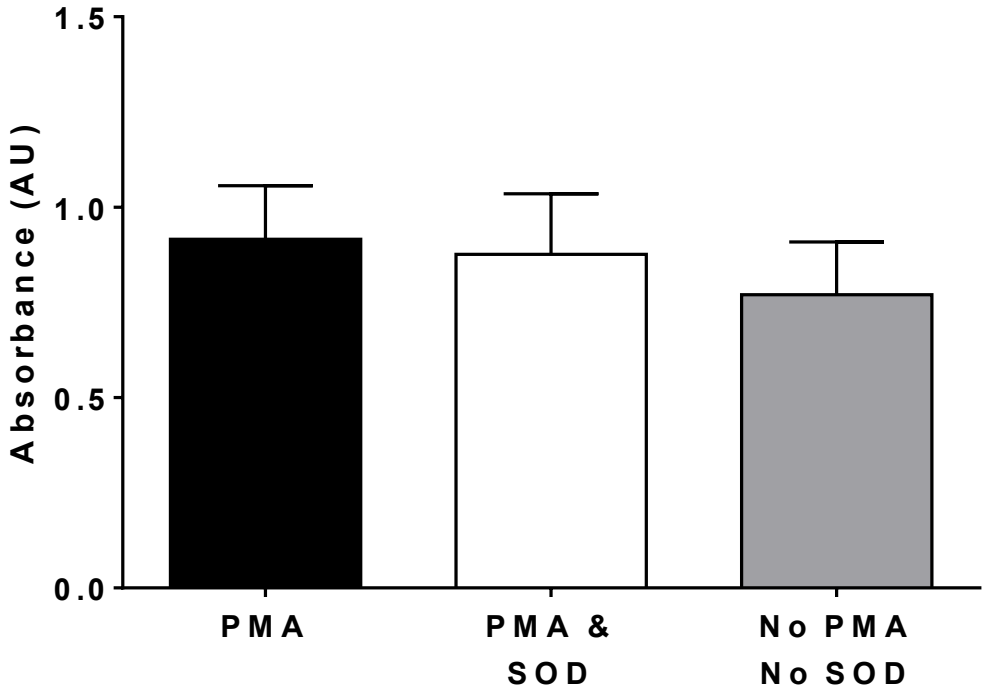

Figure 26. Superoxide generation by S184 cells treated with PMA and SOD. The rate of ROS generation was measured using the NBT assay in a H661 human lung cancer cell line devoid of endogenous NOXs that was transduced with haplotype A, and stimulated with PMA (50 U/mL), treated with Cu/Zn superoxide dismutase (SOD; 100 U/well), or both. Addition of SOD does not affect measurements of superoxide during an NBT assay. No significant differences amongst the treatments (ANOVA, Dunnett post hoc analysis). Bars indicate standard deviation. n = 3.

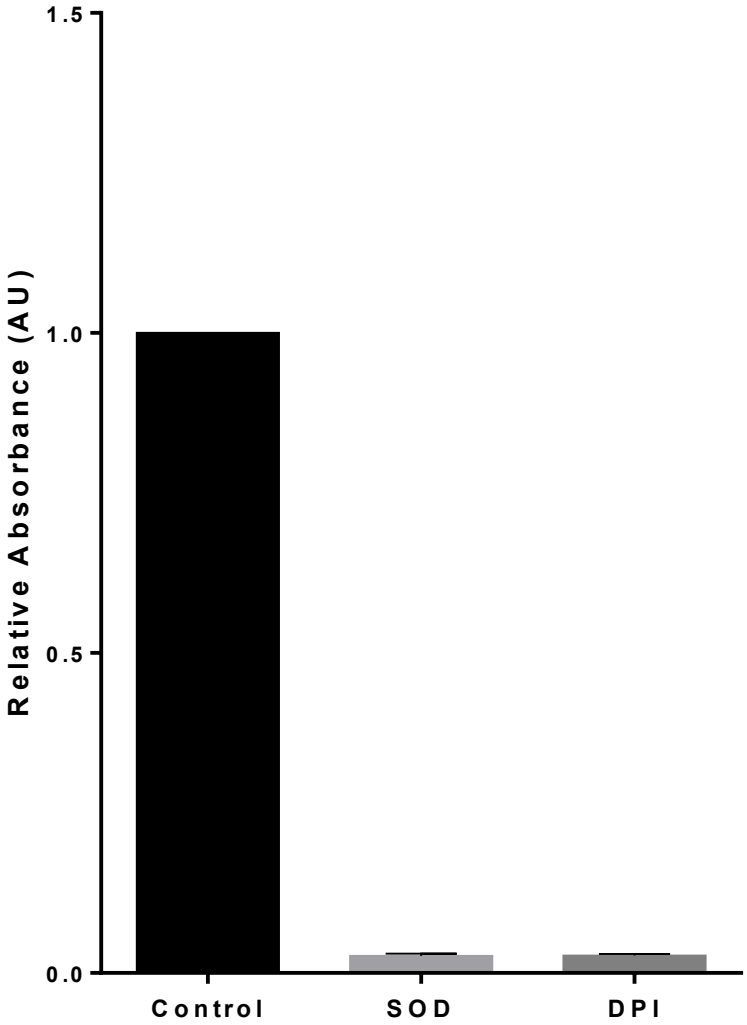

Figure 27. Superoxide generation by a cell-free xanthine/xanthine oxidase system treated with PMA and SOD. The relative amount of superoxide generated was measured using the NBT assay in a cell-free xanthine/xanthine oxidase system treated with either the inhibitor DPI (10 µM) or SOD (100 U/well). Bars indicate standard deviation. n = 3.

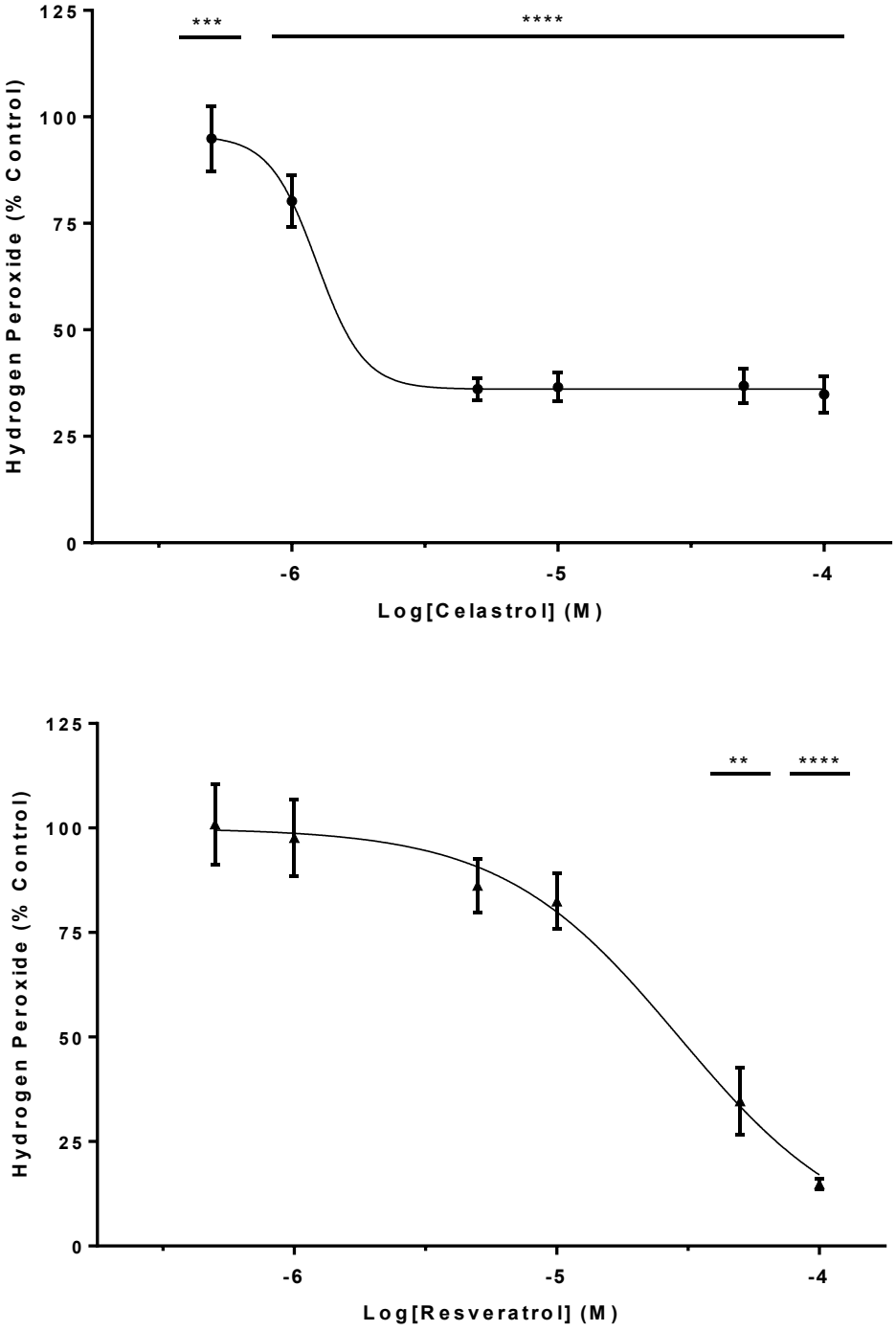

Figure 28. H_2O_2 generation in B-lymphocytes treated with natural compounds. The amount of ROS generation was measured using the Amplex Red assay in B-lymphocytes treated with either celastrol or resveratrol, and plotted as a percent of the respective untreated control. The asterisk indicates a significant difference from the untreated control (ANOVA, Dunnett post hoc analysis). Bars indicate standard deviation. n = 3.

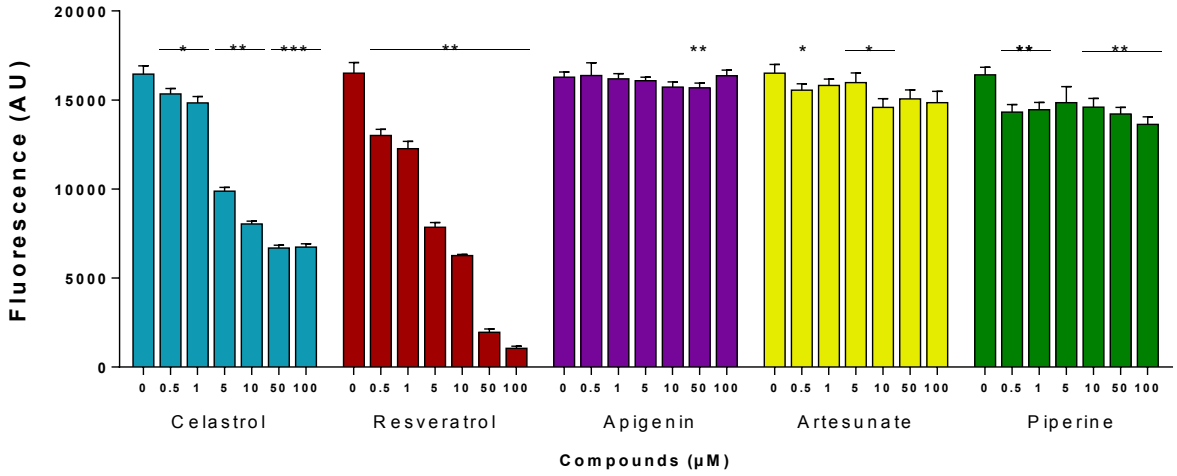

Figure 29. H_2O_2 scavenging in a cell-free system. The amount of ROS remaining was measured using the Amplex Red assay in a 625 nM H_2O_2 solution following treatment with natural compounds at various concentrations. The asterisk indicates a significant difference from the untreated control within a treatment (ANOVA, Dunnett post hoc analysis). Bars indicate standard deviation. n = 3.

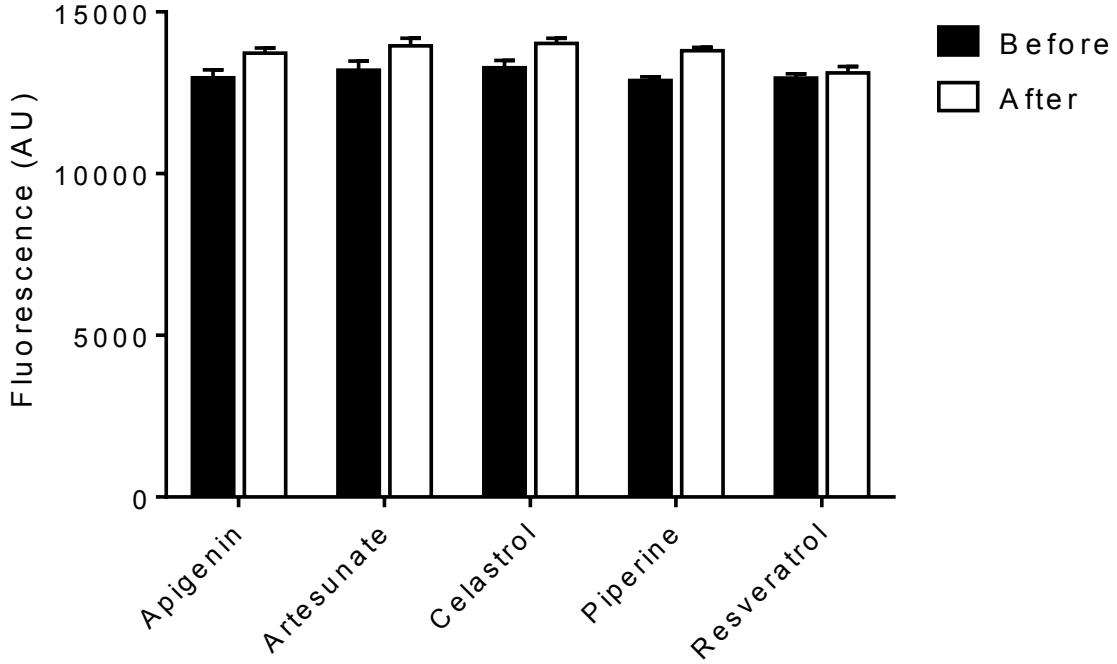

Figure 30. Examining potential drug interference with Amplex Red assay measurements. In order to determine if the natural compounds interfere with the Amplex Red assay measurements, H_2O_2 was added, along with the Amplex Red master mix, and incubated for 10 minutes, at which point the absorbance was read (Before). 1 mM of drug was then added to the wells and incubated for ten minutes prior to a second absorbance reading (After). Addition of the drug after complete conversion of Amplex Red to resorufin does not alter the absorbance reading of the assay. There were no significant differences in the generation in any treatments (ANOVA, Dunnett post hoc analysis). Bars indicate standard deviation. n = 3.

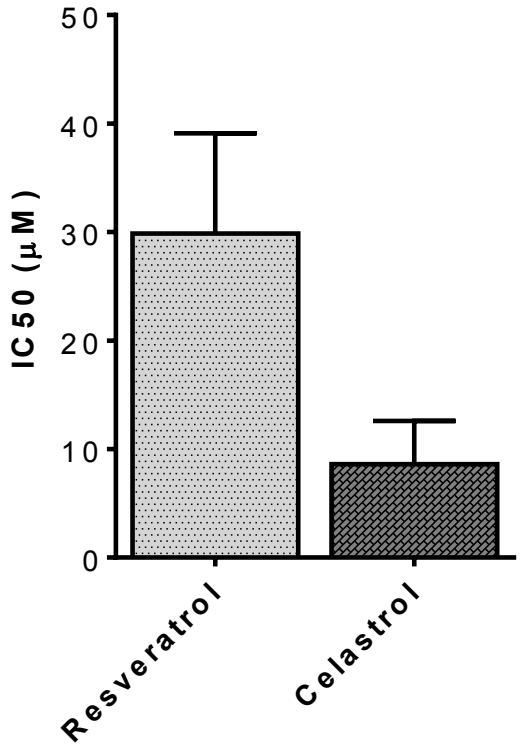

Figure 31. IC50 of natural compounds on superoxide production by lymphoblastoid cells. Biological IC50 of resveratrol and celastrol determined by the Amplex Red assay using B-lymphocytes. Bars indicate standard deviation. n = 3.

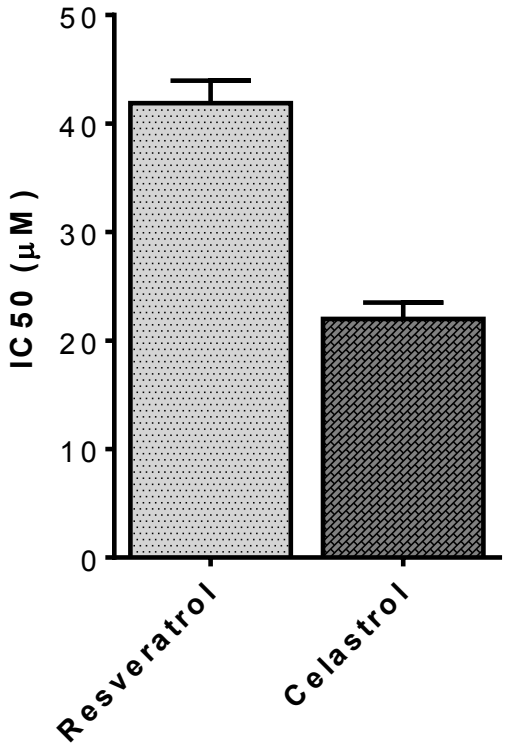

Figure 32. H_2O_2 scavenging by celastrol and resveratrol. The concentration of resveratrol or celastrol required to scavenge 50% of the available 625 nM H_2O_2, as determined by Amplex Red assay. Bars indicate standard deviation. n = 3.

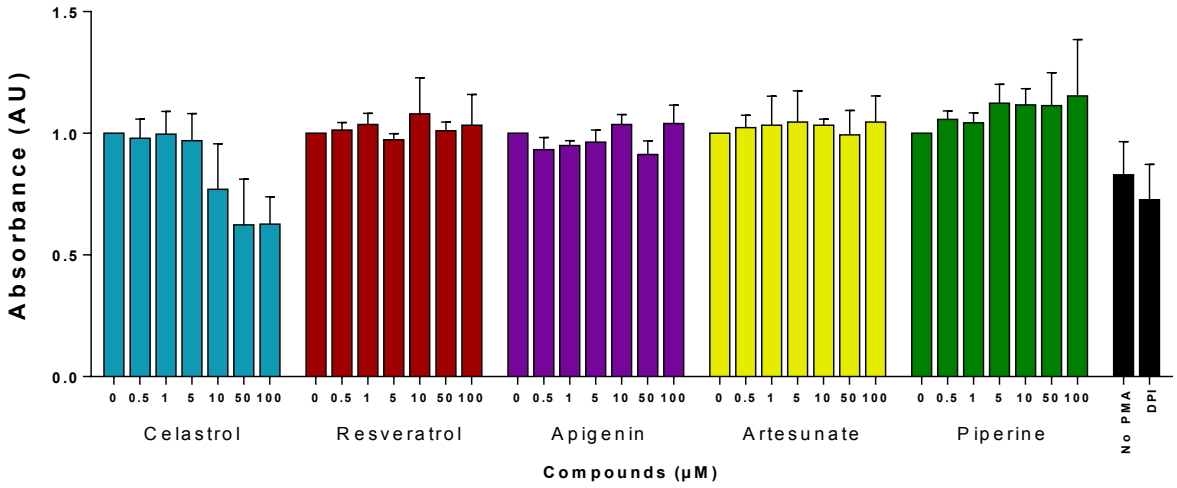

Figure 33. The effect of natural compounds on NOX2 superoxide production. Superoxide generation in B-lymphocytes cells. The amount of superoxide generated was measured using the NBT assay following treatment with natural compounds at various concentrations. No significant differences in superoxide generation were measured amongst the various treatments (ANOVA, Dunnett post hoc analysis). Bars indicate standard deviation. n = 3.

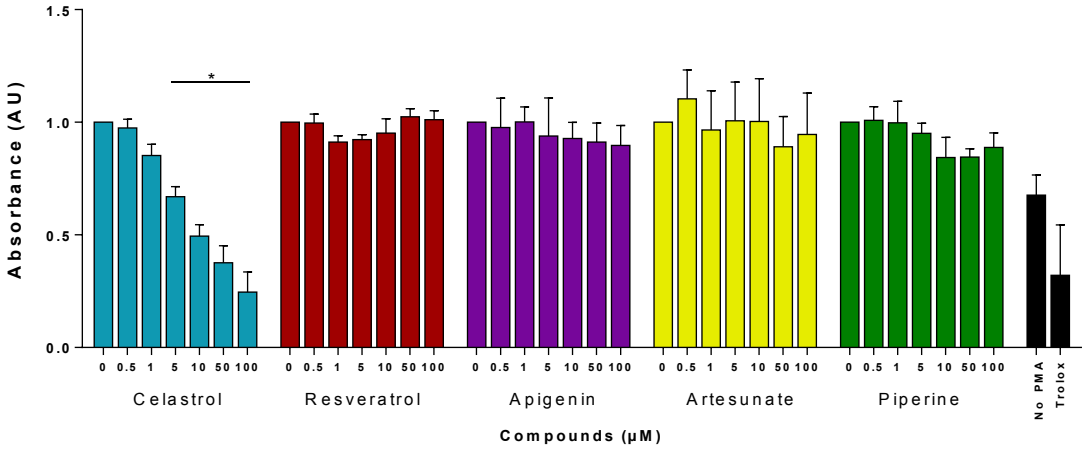

Figure 34. Superoxide generation by NOX1-transduced cells treated with natural compounds. Superoxide generation in the NOX1-transduced S184 cells. The amount of superoxide generated was measured using the NBT assay following treatment with natural compounds at various concentrations. The asterisk indicates a significant difference from the untreated control within a drug treatment (ANOVA, Dunnett post hoc analysis). Bars indicate standard deviation. n = 3.

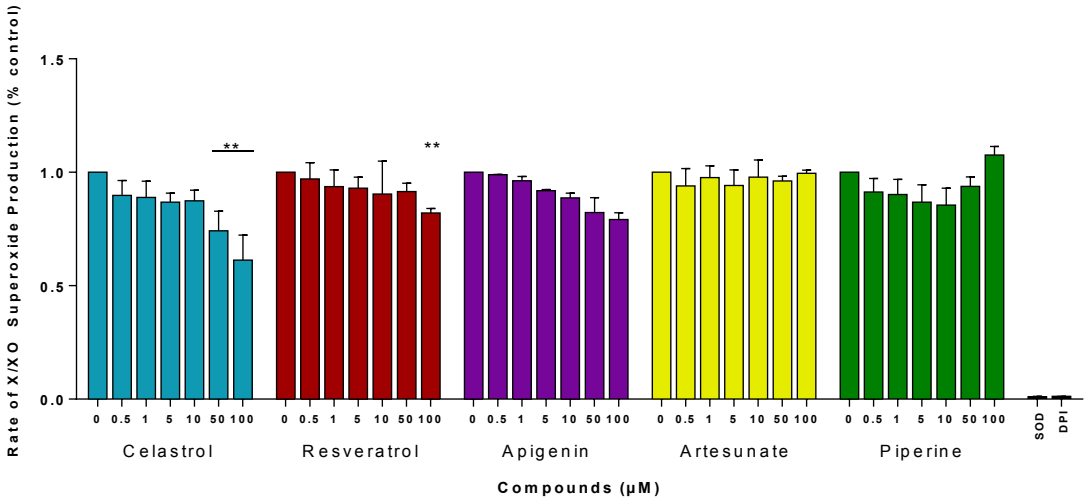

Figure 35. Rate of superoxide generation in a cell-free xanthine/xanthine oxidase system. The amount of superoxide generated was measured using the MCLA assay following treatment with natural compounds at various concentrations. The asterisk indicates a significant difference from the untreated control within a drug treatment (ANOVA, Dunnett post hoc analysis). Bars indicate standard deviation. n = 3.

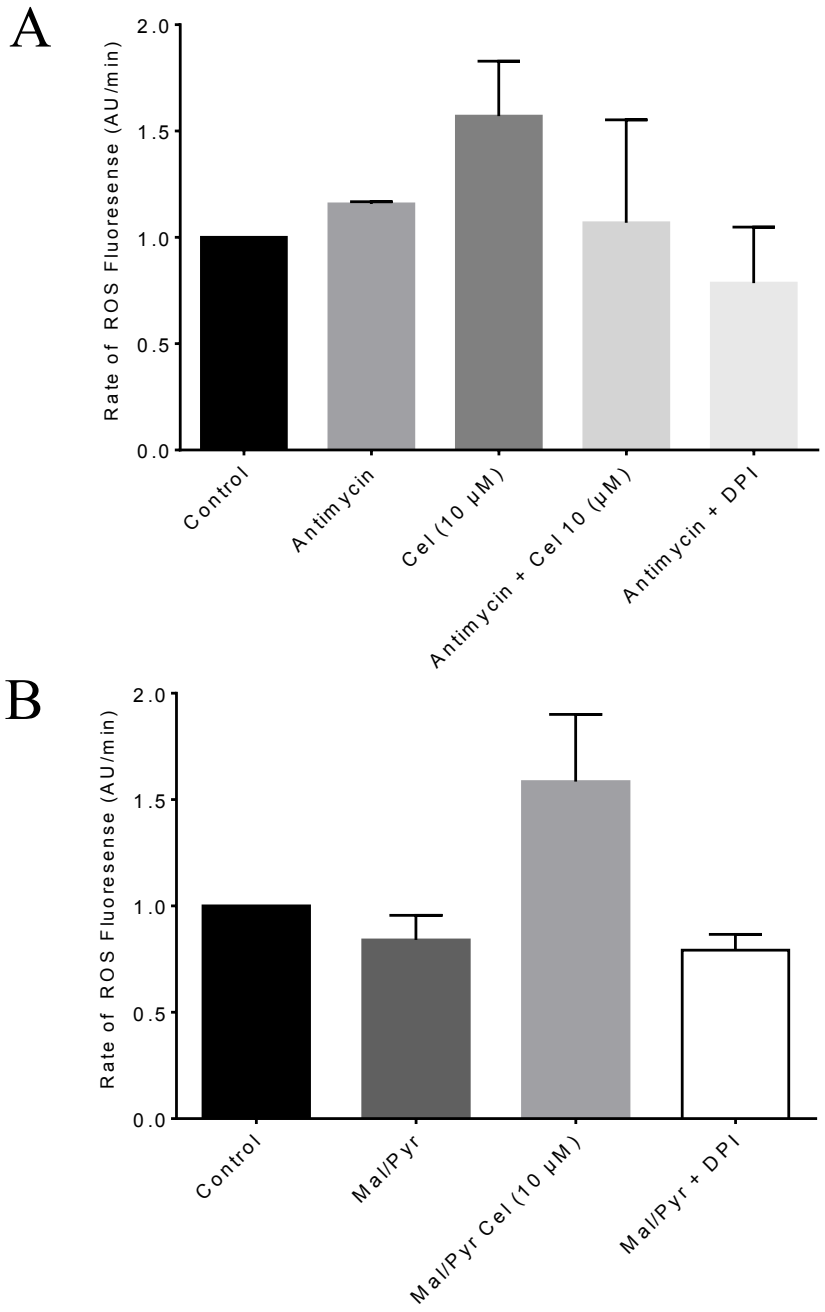

Figure 36. Rate of H_2O_2 generation by mitochondria isolated from human lung cancer cells. The rate of ROS generation was measured using the Amplex Red assay from mitochondria isolated from the H661 human lung cancer cell line following treatment with celastrol. Data are plotted relative to the unstimulated control, and compared to the positive controls **A)** antimycin, and **B)** malate/pyruvate. There were no significant differences in the rate of ROS generation in any treatments (ANOVA, Dunnett post hoc analysis). Bars indicate standard deviation. n = 3.

CHAPTER 4: DISCUSSION

The objective of the current study was to determine the effect of $p22^{phox}$ genetic polymorphisms on ROS generation by the NOX1 enzyme, and to determine the effect the compounds celastrol and resveratrol have on NOX and mitochondrial ROS generation.

4.1 The 7 novel S184 A – G cell lines produced ROS, but varied in the number of $p22^{phox}$ gene copies introduced

The NOX1 enzyme has multiple subunits, all of which are required for generation of ROS (reviewed in Bedard and Krause, 2007). After verifying by RT-PCR that all required subunits were present in the generated NOX1-containing S184 cell line, we examined the levels of ROS generated by the cell line. Each of the $p22^{phox}$ haplotypes permitted the NOX1 enzyme to function since when compared to the control we observed significant increases in ROS generation from each cell containing one of the seven haplotypes.

Previously, groups have attempted to associate the $p22^{phox}$ sequence variant c.214T>C with CVD, but the results were varied and conflicting (San Jose et al., 2008). In response to those results, we attempted to assess the effects of the c.214T>C alteration, and others, on the functional behaviour of the NOX enzymes involved in CVD. Although many $p22^{phox}$ polymorphisms exist, mainly within the promoter region, we focused on SNPs within exons that are also the three most common polymorphisms found in the population: c.214T>C, c.521T>C, and c.*24G>A. The fact that $p22^{phox}$ is highly polymorphic is interesting, as this might indicate that the p22 protein is not particularly sensitive to variation. However, given that $p22^{phox}$ interacts with four NOX isoforms, this

tolerance to variation may result from some $p22^{phox}$ variants performing better with certain NOX isoforms. This enhanced performance could potentially occur through more efficient enzymatic activity or increased membrane stability, which may result in improved cell signalling and function.

Blasticidin resistance, which is not endogenous to human cells, was inserted alongside the $p22^{phox}$ haplotypes with the purpose of serving as both a selection marker and as a method of determining transduction efficiency among the cells line. Given that there was a range in the percent of cells that were transduced, and that the original S184 cells were prepared using undiluted virus preparation, it is possible that there were differences in the amount of virus particles among the preparations, and that this contributed to the differences in the amount of vector introduced into the cells. With a transduction efficiency of 20% or less, the probability of having one cell receive two copies of the plasmid is 0.03. Therefore, aiming for a low transduction efficiency would lead to fewer transduced cells, but also to a lower chance of having two or more copies of the gene introduced into some cells. This could have the benefit of preventing overexpression and saturation of the vector message, thereby revealing the effect of potentially subtle differences caused by SNPs. Although the HOAx1 cells were clonally selected, the cells with the $p22^{phox}$ variants were not. As such they are a mixed population, in which some cells had many copies, but most cells may have just one copy. As a result the overall RNA level is the same for the population, because cells containing multiple copies might not actually be able to keep up with the demand making that much $p22^{phox}$ mRNA.

Although this study on the effect $p22^{phox}$ variations on NOX1 has similarities to the NOX2 study conducted by Bedard et al. in 2009, one major difference in the Bedard study compared to ours is that we did not achieve equal vector copy numbers at the transduction stage. This is important, as significant differences observed in ROS generation amongst the haplotypes could be explained away by differences in mRNA levels and subsequently protein levels of NOX1 and associated subunits, rather than the effectiveness of the $p22^{phox}$ variant. Similarly, any differences we may have seen in ROS generation are potentially being obscured by the effect of unequal copy numbers within our S184 cell line. Another major difference in this study compared to the 2009 Bedard study is in the usage of cell lines. The 2009 study used NOX2-rich B-lymphocytes that were devoid of the $p22^{phox}$ protein as a result of a $p22^{phox}$ mutation. As such, there was only a requirement to express $p22^{phox}$, as the other required NOX components were intact. In contrast, the H661 cell line that we used required the insertion and expression of each of the four NOX enzyme components. As a result, the strong CMV promoter we used would overexpress each of the NOX components, thereby making it difficult to isolate $p22^{phox}$ as the limiting factor in the ROS production. We took the low transduction efficiency approach when generating the S232 cell line that followed the S184 cell line, and were successful in achieving equal transduction.

4.2 The 7 novel S232 A – G cell lines had an equal number of $p22^{phox}$ copies introduced, but they did not produce ROS

In order to address the issues that unequal copy numbers present, we generated the S232 cell line using a novel vector quantification technique to achieve equal copy

numbers across all haplotypes within the cell line. Upon verification all cell lines had achieved equal, and theoretically low, copy numbers we proceeded to measure $p22^{phox}$-dependent ROS production using the Amplex Red assay.

The novel vector quantification technique used in this study improves upon previous vector quantification techniques not only by reducing the amount of time required to quantify vector preparations, but by also permitting direct quantification of the lentiviral particles in a more accurate manner. Previous techniques required days for completion, as the virus preparation was added to cell cultures in a dilution series, followed by quantification of colony forming units, based either on GFP tags included in the vector, or on RT-PCR of RNA isolated from the transduced cells (Barde et al., 2010*)* The novel technique can be completed within a day, requiring only RNA isolation, cDNA preparation, and qRT-PCR analysis. An alternative technique that has also been used previously quantified the virus particles directly based on the small double stranded segment present in the lentivector; however, this would not distinguish between packaged viral particles and the unprocessed DNA vector what was added to the cells (Scherr et al., 2001). Our technique eliminates the possibility of quantifying unpackaged viral particles, as we isolate only the single-stranded RNA from the viral particles following transfection. As a result, this technique provides a more accurate representation of the number of viral particles. Another advantage of our technique is the large linear range of quantification the qPCR method provides compared to the analysis of GFP transduced cells via flow cytometry. Furthermore, since our technique quantifies RNA it should work with all lentivectors.

4.3 Subunit may have been silenced or population was not isogenic

None of the cells containing any of the seven $p22^{phox}$ haplotypes were able to generate ROS beyond levels seen in the negative control cell line that is devoid of endogenous NOX enzymes. Upon further investigation using gel electrophoresis, it was determined that the NOXA1 subunit was no longer being expressed. This result was surprising, as generation of the cell line involved the neomycin resistance gene at the NOXA1 transduction stage, and any cells that were not successfully transduced should have been selected against. In addition to antibiotic selection, we conducted a monoclonal selection of the cell line once it was successfully transduced with NOX1, NOXA1, and NOXO1. Loss of gene expression transduced using a lentiviral system has been observed (Vroemen et al., 2005). The possibility also exists that there was a failure to generate an isogenic cell line during the GFP-based selection of single colonies, or that contamination with a non-NOXA1 cell line occurred, and that this HOAx1 cell line represented a mixed population. Given that a successfully transduced cell would require more energy and resources to produce the subunits, an unsuccessfully transduced cell may more readily survive and replicate. However, one of the advantages of using a lentivector compared to a retroviral vector is the decreased occurrence of gene silencing (Pfeifer et al., 2002; Lois et al., 2002). To increase copy number of the integrated vector in the host cell and transgene expression, Woodchuck Hepatitis Virus Post-transcriptional Regulatory Element (WPRE), and the HIV-1 central polypurine tract (cPPT) were included in the vector (Suter et al., 2006). Additionally, either blasticidin or neomycin resistance driven by an SV40 promoter were included to allow antibiotic selection of transduced cells.

4.4 All of the variants of $p22^{phox}$ supported NOX1 activity, but the variations did not alter NOX1 activity

Although minor increases and decreases were observed there were no significant differences in the amount of ROS generated among the seven haplotypes within the S184 (NOX1-based) cell lines, which is a surprising result given a difference in ROS generation was observed when the haplotypes were inserted into a NOX2 system (Bedard et al., 2009). Perhaps the manner in which $p22^{phox}$ interacts with NOX1 differs from its interaction with NOX2, thereby negating the potential effects that $p22^{phox}$ polymorphisms might cause. Also, the spread of data within a treatment was large for each condition, so perhaps further testing would reveal that one of the $p22^{phox}$ haplotypes does have a significant effect on NOX1-mediated ROS generation.

4.5 The $p22^{phox}$ mRNA did not correlate with NOX1 activity or $p22^{phox}$ protein expression

The subunit $p22^{phox}$ is required for proper function of the NOX1 enzyme. The levels of $p22^{phox}$ mRNA expression amongst the S184 haplotypes did not correlate with levels of ROS generated by these same cells. The main NOX subunit and the $p22^{phox}$ subunit interact at a 1:1 ratio (Huang et al., 1995). Knowing this, a possible reason as to why more $p22^{phox}$ expression does not result in more ROS generation may be that the $p22^{phox}$ subunit is saturated within the cell system, and that another NOX subunit or other element is acting as a limiting factor of ROS generation. Also, given that one of the $p22^{phox}$ SNPs (c.*24G>A) occurs within the 3'UTR, and that mutations within this region can result in decreased expression of associated sequences, it is possible that proper formation and expression of $p22^{phox}$ is being prevented by increased mRNA instability

(Bedard et al., 2009). While we did not find a significant decrease in mRNA expression of haplotypes containing the SNP in the 3'UTR, we did find a significant decrease in protein expression. The B, C, and E haplotypes containing the 3'UTR SNP exhibit a decrease in $p22^{phox}$ protein expression compared to the other haplotypes. This result is surprising, as one might expect protein expression to remain consistent if mRNA expression is consistent, but this is not always the case (Vogel & Marcotte, 2012). In fact, the levels of $p22^{phox}$ protein expression do not appear to correlate with mRNA expression within haplotypes. Since it appears c.*24G>A had little effect on mRNA stability, the lower protein expression may be explained by changes in translational activity, or post-transcriptional and degradation regulation. Interestingly, haplotype A does not contain the 3'UTR SNP, yet expresses a similarly low level of expression. This could be explained by the sole SNP at c.214 in the NOX maturation region, and yet it does not appear to decrease the $p22^{phox}$ expression of haplotype D.

Focusing on haplotypes rather than individual SNPs may prove to be valuable as it may more accurately predict protein expression, or how a person will respond to certain drug treatments. Considering haplotypes in disease association studies may prove valuable as well, since having a genetic variant linked to a functional effect would allow for large-scale population disease screening. Given that CVD is a complex disease with many factors, including the involvement of ROS, it is unlikely that any single variation can be attributed sole responsibility for the disease. Regardless, if genetic variation in $p22^{phox}$ was determined to be correlated with CVD, it would suggest that NOX-derived ROS contribute minutely to the genetic component. With the genetic component playing a minor role in CVD compared to the environmental component, small genetic

components may prove to be useful starting points when attempting to determine important environmental factors. For example, exhaustive endurance exercise is associated with cardiac dysfunction and injury, resulting from the subsequent elevation in oxidative stress (Knez et al., 2006). Alternatively, the knowledge of a CVD genetic component linked to ROS could be exploited through the use of antihypertension drugs that affect NOX enzymes. An example of such being the class of drugs known as statins, which are tremendously effective in the treatment of coronary heart disease and high cholesterol (Moosmann & Behl, 2004). Statins have positive CVD potential and prevent NOX activation, but have multiple and significant adverse effects, the most notable being muscular and neurological. Many natural forms of statins exist, and while the most popular forms of statins are synthetic, they too cause significant adverse effects. If one could isolate a natural compound that targets NOX enzymes, or even a specific NOX isoform, there could be therapeutic benefits in the treatment of CVD while avoiding the adverse effects associated with other compounds. As such, we chose to examine the effects of celastrol and resveratrol on NOX1 and mitochondrial ROS generation.

4.6 Celastrol was an antioxidant towards SO and H_2O_2, and resveratrol had little effect on superoxide

Celastrol can prevent NOX1-3 ROS generation by binding with the $p47^{phox}$ and NOXO1 organizing subunits, thereby preventing their required interaction with $p22^{phox}$ (Jacquet et al., 2011). In our cell-free systems celastrol was observed to be an antioxidant toward both superoxide and H_2O_2. In the same systems resveratrol was observed to be a significant antioxidant towards H_2O_2, but not intracellular superoxide. This result is surprising since resveratrol (0.131 mM) has been reported as a strong antioxidant toward

superoxide in a cell-free riboflavin illumination system (Gülçin et al., 2010). That same study also suggested that resveratrol is a much stronger antioxidant toward superoxide than trolox, a vitamin E-based compound which is considered the gold standard of antioxidants. This is interesting considering that trolox is able to effectively penetrate cell membranes, and while resveratrol can penetrate membranes, it becomes embedded within the lipid bi-layer, which would theoretically make it less effective as an intracellular antioxidant (McClain et al., 1995; Lancon et al., 2004: Brittes et al., 2010; Lania-Pietrzak et al., 2004). This behaviour of resveratrol might explain why we observed a significant antioxidant effect towards superoxide using the MCLA assay that detects extracellular superoxide, but did not observe a significant effect using the NBT assay that detects intracellular superoxide.

4.7 Resveratrol is not a direct NOX inhibitor

Resveratrol is known to act as an antioxidant toward H_2O_2, superoxide, and the hydroxyl radical. (Ungvari et al., 2007; Leonard et al., 2003; Hung et al., 2003). However, the antioxidant effects of resveratrol are weak compared to strong antioxidants like cysteine (Bradamante et al., 2004). Currently, NOX1 and NOX2 enzymes do not appear to be direct molecular targets of resveratrol, but resveratrol is capable of indirectly affecting NOX activity and expression. For example, resveratrol inhibits LPS-induced NOX1 expression, and inhibits TNF-alpha-induced NOX activation (Park et al., 2009; Zhang et al., 2009). Resveratrol can decrease expression of NOX1, NOX2, and NOX4, in addition to increasing SOD1 and GPx1 expression (Spanier et al., 2009). Protein Kinase-C (PKC) is a strong activator of NOX, and resveratrol is known to directly inhibit PKC

(Poolman et al., 2005). Also, in a human keratinocyte cell resveratrol (10 μM) was documented as increasing that activity of SOD, a strong antioxidant toward superoxide, and GPx, a strong antioxidant towards H_2O_2 (Chen et al., 2006). Resveratrol (0.25 μM) can inhibit PKC activation of $p47^{phox}$ (Shen et al., 2007).

4.8 Celastrol unexpectedly increased mitochondrial H_2O_2 production

Celastrol is an inhibitor of NOX ROS generation (reviewed in Bedard and Krause, 2007); however, celastrol was not specifically evaluated for an effect on mitochondria. Jaquet et al. (2011) found that in PLB cells, celastrol inhibited oxygen consumption to an equal level as DPI, producing an almost flat trace. PLB cells do not contain many mitochondria, and the oxygen consumption was almost exclusively produced by NOX2. In the other NOX-expressing cells, an overexpression system in HEK cells was used, and although DPI continued to produce an almost complete inhibition of oxygen consumption, some residual consumption appears to be present in celastrol-treated cells. Since HEK cells have more mitochondria, we wanted to explore the possibility that celastrol was a more selective inhibitor of NOX than DPI, and could be a useful tool to use when one is trying to determine if a ROS mediated effect is to be attributed to NOX or mitochondrial derived ROS.

Our result of celastrol increasing mitochondrial ROS generation is surprising, since based on previous work regarding celastrol as a ROS inhibitor and antioxidant, and we might have expected celastrol to have no effect, or might have expected celastrol to cause a decrease in ROS levels. When tumor cells and their mitochondria were analyzed via spectrophotometery, and a fluorescent dye coupled with flow cytometry, it was

determined that celastrol can inhibit complex I activity of the mitochondrial electron transport chain (mETC) and increase the amount of ROS produced (Chen et al., 2011). This result agrees with the trend we observed from our experiment measuring H_2O_2 levels produced by mitochondria treated with celastrol. Inhibiting complexes of the mETC increases ROS production by promoting leakage of electrons from the system (Li et al., 2003; Dias & Bailly, 2003). The effect celastrol has on mitochondria may help explain the increase in ROS production at the 50 μM and 100 μM celastrol concentrations in Figure 21. The antioxidant and NOX-inhibiting effects of celastrol at 10 μM and lower may overcome the increase in mitochondrial ROS, but at 50 μM and above those effects may be overwhelmed by the mitochondrial ROS production.

4.9 Future Directions

Collectively, these results suggest that the $p22^{phox}$ genetic polymorphisms investigated in this study may not have an impact on the amount of ROS produced by NOX1, and there may be a disconnect between mRNA levels, protein expression, and functional results. While I was unable to establish a cell line that could conclusively determine the effect of the $p22^{phox}$ polymorphisms, I was able to establish a novel protocol that could be used to generate a cell line capable of doing so in the future. In order to determine the effect of SNPs on mRNA stability I could incorporate actinomycin D, a compound known for inhibiting transcription, into qRT-PCR experiments to examine if the rate of mRNA degradation differs for SNPs found in the 3'UTR (Schneider-Poetschet al., 2010).

NOX4 is involved in cell growth, differentiation, and vascular disease (Touyz & Montezano, 2012). It would be interesting to conduct similar $p22^{phox}$ polymorphism studies in NOX4-containing cells, as the $p22^{phox}$ variants may influence the level of ROS generated by NOX4.

To further investigate the inhibitory effects of celastrol and resveratrol, it may prove useful to determine oxygen consumption in the presence of these compounds through the use of an oximeter. If celastrol does not inhibit mitochondria ROS production, and resveratrol does not inhibit NOX-mediated ROS production, then oxygen consumption will be observed when measured via an oximeter. Furthermore, in order to help determine if celastrol truly is increasing mitochondrial ROS production, it would be useful to determine the ideal conditions and reagents to stimulate a positive control compared to a negative control.

4.10 Conclusion

As determined through this study, the seven common variants of $p22^{phox}$ are all able to support NOX1 activity; however, these variations did not cause significant differences in overall NOX1 activity. Interestingly, the levels of $p22^{phox}$ mRNA did not correlate with NOX1 activity, or with $p22^{phox}$ protein expression. The novel technique of quantifying lentiviral particles via qRT-PCR was effective in achieving equal transduction, although cells with low levels of transduction may be prone to spontaneous gene silencing.

Celastrol and resveratrol appear to be working as strong antioxidants towards H_2O_2 in a dose-dependent manner, and while celastrol is a mild antioxidant towards

superoxide, it appears that resveratrol is not. Celastrol is confirmed as an inhibitor of NOX1 and NOX2, but a 10 μM concentration appears to have the effect of increasing ROS generated by mitochondria isolated from HEK cells, although further studies are required to confirm this finding.

REFERENCES

Abate C, Patel L, Rauscher FJ III, Curran T. 1990. Redox regulation of Fos and Jun DNA-binding activity in vitro. Science. 249:1157–1161.

Abdel-Sattar, E., Maes, L., & Salama, M. M. 2010. In vitro activities of plant extracts from Saudi Arabia against malaria, leishmaniasis, sleeping sickness and Chagas disease. Phytotherapy Research. 24:1322-1328.

Adimora NJ, Jones DP, Kemp ML. 2010. A model of redox kinetics implicates the thiol proteome in cellular hydrogen peroxide responses. Antioxid. Redox. Signal. 13:731–743.

Aharoni-Simon M.; Reifen R.; Tirosh O. 2006. ROS-production-mediated activation of AP-1 but not NFκB inhibits glutamate-induced HT4 neuronal cell death. Antioxid. Redox. Signal. 8:1339-49.

Al-Shaal,L., R. Shegokar, and R. H. Muller. 2011. Production and characterization of antioxidant apigenin nanocrystals as a novel UV skin protective formulation, International Journal of Pharmaceutics. 420:133–140.

Allison AC, Cacabelos R, Lombardi VR, Alvarez XA, Vigo C. 2001. Celastrol, a potent antioxidant and anti-inflammatory drug, as a possible treatment for Alzheimer's disease. Prog Neuropsychopharmacol Biol Psychiatry. 25:1341–57.

Altenhofer, S., P. Kleikers, K. Radermacher, P. Scheurer, J. Hermans, P. Schiffers, H. Ho, K. Wingler, and H. Schmidt. 2012. The NOX toolbox: validating the role of NADPH oxidases in physiology and disease. Cellular and Molecular Life Sciences. 69:2327–2343.

Ambasta, R. K., Kumar, P., Griendling, K. K., Schmidt, H. H., Busse, R., & Brandes, R. P. 2004. Direct interaction of the novel Nox proteins with p22phox is required for the formation of a functionally active NADPH oxidase. Journal of Biological Chemistry. 279: 45935-45941.

Antoniades C, Bakogiannis C, Tousoulis D, Reilly S, Zhang MH, Paschalis A, Antonopoulos A, Demosthenous M, Miliou A, Psarros C, Marinou K, Sfyras N, Economopoulos G, Casadei B, Channon KM, Stefanadis C. 2010. Preoperative atorvastatin treatment in CABG patients rapidly improves vein graft redox state by inhibition of Rac1 and NADPH-oxidase activity preoperative atorvastatin treatment in CABG patients rapidly improves vein. Circulation. 122:S66–S73.

Antunes F and E. Cadenas. 2004. Estimation of H_2O_2 gradients across biomembranes. FEBS Lett 475: 121–126.

Apel, K. and H. Hirt. 2004. Reactive oxygen species: Metabolism, oxidative stress, and signal transduction. Annu. Rev. Plant Biol. 55:373-399.

Aqil F, Ahmed I, Mehmood Z. 2006. Antioxidant and free radical scavenging properties of twelve traditionally used Indian medicinal plants. Turk J Biol. 30: 177-183.

Babior, B.M., Kipnes, R.S., and J.T. Curnutte. 1973. Biological defense mechanisms: the production by leukocytes of superoxide, a potential bactericidal agent. J. Clin. Invest., 52:741–744.

Baldridge, C.W. and R.W. Gerard. 1932. The extra respiration of phagocytosis. AJP Legacy, 103:235–236.

Banfi B, Clark RA, Steger K, Krause KH. 2003. Two novel proteins activate superoxide generation by the NADPH oxidase NOX1. J Biol Chem. 278:3510–3513

Barde I, Salmon P, Trono D. 2010. Production and titration of lentiviral vectors. Curr Protoc Neurosci 53:4.21.1–4.21.23.

Basset O, Deffert C, Foti M, Bedard K, Jaquet V, Ogier-Denis E, Krause KH. 2009. NADPH oxidase 1 deficiency alters caveolin phosphorylation and angiotensin II receptor localization in vascular smooth muscle. Antioxid Redox Signal. 2371–2384.

Bedard K, Attar H, Bonnefont J, Jaquet V, Borel C, Plastre O, Stasia MJ, Antonarakis SE,and KH Krause. 2009. Three common polymorphisms in the CYBA gene form a haplotype associated with decreased ROS generation. Hum Mutat. 30:1123–1133.

Bhat KP, Pezzuto JM. 2002. Cancer chemopreventive activity of resveratrol. Ann N Y Acad Sci. 957:210–29.

Bielski, B.H.J., Cabelli, D.E., Arudi, R.L., and A.B. Ross. 1985. Reactivity of HO_2/O_2-radicals in aqueous solution. J. Phys. 14:1041–1102.

Bjelakovic G, Nikolova D, Gluud LL, Simonetti RG, Gluud C. 2008. Antioxidant supplements for prevention of mortality in healthy participants and patients with various diseases. Cochrane Database Syst Rev. 2008;16:CD007176.

Block K, and Y Gorin. 2012. Aiding and abetting roles of NOX oxidases in cellular transformation. Nature. 12:627-637.

Bokoch GM. 1994. Regulation of the human neutrophil NADPH oxidase by the rac gtp-binding proteins. Current Opinion in Cell Biology. 6:212–218.

Boveris, A., Oshino, N., and B. Chance. 1972. The cellular production of hydrogen peroxide. Biochem. J. 128:617–630.

Brandes RP, Kreuzer J. 2004. Vascular NADPH oxidases: molecular mechanisms of activation. Cardiovasc Res. 65: 16–27.

Brandes RP, Schroder K. 2008. Composition and functions of vascular nicotinamide adenine dinucleotide phosphate oxidases. Trends Cardiovasc Med. 18:15-19

Brandes, R. P., Weissmann, N., & Schröder, K. 2010. NADPH oxidases in cardiovascular disease. Free Radical Biology and Medicine. 49: 687-706.

Brewer MS. 2011. Natural antioxidants: Sources, compounds, mechanisms of action, and potential applications. Compr Rev Food Sci Food Safety. 10:221-247.

Brittes, J., M. L´ucio, C. Nunes, J. L. F. C. Lima, and S. Reis. 2010. Effects of resveratrol on membrane biophysical properties: relevance for its pharmacological effects. Chemistry and Physics of Lipids. 163: 747–754.

Cabiscol, E., Tamarit, J., & Ros, J. 2010. Oxidative stress in bacteria and protein damage by reactive oxygen species. International Microbiology. 3:3-8.

Cadenas, E. 1989. Biochemistry of oxygen toxicity. Annu. Rev. Biochem. 58:79–110.

Canter, P.H., H.S. Lee, E. Ernst. 2006. A systematic review of randomised clinical trials of Tripterygium wilfordii for rheumatoid arthritis. Phytomedicine. 13:371–377.

Cave, A. 2009. Selective targeting of NADPH oxidase for cardiovascular protection. Curr Opin Pharmacol. 9:208-213.

Chelikani P., Carpena X., Fita I, and P.C. Loewen. 2003. An electrical potential in the access channel of catalases enhances catalysis. J. Biol. Chem. 278: 31290–31296.

Chen G, Zhang X, Zhao M, Wang Y, Cheng X, Wang D, Xu Y, Du Z, Yu X. 2011. Celastrol targets mitochondrial respiratory chain complex I to induce reactive oxygen species-dependent cytotoxicity in tumor cells. BMC Cancer. 11:170.

Chen M. L., Li J., Xiao W. R., Sun L., Tang H., Wang L., Wu L. Y., Chen X., Xie H. F. 2006. Protective effect of resveratrol against oxidative damage of UVA irradiated HaCaT cells. Zhong Nan Da Xue Xue Bao Yi Xue Ban 31:635–639.

Cheng G, Lambeth JD. 2004a. NOXO1, regulation of lipid binding, localization, and activation of Nox1 by the Phox homology (PX) domain. J Biol Chem. 279:4737–4742.

Cheng, G., Ritsick, D., & Lambeth, J. D. 2004b. Nox3 regulation by NOXO1, p47phox, and p67phox. Journal of Biological Chemistry. 279:34250-34255.

Clark R, Malech H, Galin J et al. 1989. Genetic variants of chronic granulomatous disease: prevalence of deficiencies of two cytosolic components of the NADPH oxidase system. N Engl J Med. 321:647–65.

Cleren C, Calingasan NY, Chen J, Beal MF. 2005. Celastrol protects against MPTP- and 3-nitropropionic acid-induced neurotoxicity. J Neurochem. 94:995–1004.

Conference Board of Canada. The Canadian Heart Health Strategy: Risk Factors and Future Cost Implications. Report February 2010.

Cross, A. R. 1987. The inhibitory effects of some iodonium compounds on the superoxide generating system of neutrophils and their failure to inhibit diaphorase activity. Biochemical pharmacology. 36:489.

Csiszar A, Labinskyy N, Olson S, Pinto JT, Gupte S, Wu JM, Hu F, Ballabh P, Podlutsky A, Losonczy G, de Cabo R, Mathew R, Wolin MS, Ungvari Z. 2009. Resveratrol prevents monocrotaline-induced pulmonary hypertension in rats. Hypertension. 54:668–675.

Cuzzocrea S, Mazzon E, Dugo L, Di Paola R, Caputi AP, and D. Salvemini. 2004. Superoxide: a key player in hypertension. FASEB J. 18:94-101.
Deby-Dupont G, Mouithys-Mickalad A, Serteyn D, Lamy M, and Deby C. 2005. Resveratrol and curcumin reduce the respiratory burst of Chlamydia-primed THP-1 cells. Biochem Biophys Res Commun 333:21–27.

de Mendez, I., Homayounpour, N. and Leto, T. 1997. Specificity of p47 phox SH3 domain interactions in NADPH oxidase assembly and activation. Mol. Cell. Biol. 17:2177- 2185.

Della-Morte, D., Dave, KR., Defazio, RA., Bao, YC., Raval, AP. and Perez-Pinzon, MA. 2009. Resveratrol pretreatment protects rat brain from cerebral ischemic damage via Sirt1 – UCP2 pathway. Neuroscience. 159:993-1002.

den Dunnen JT, Antonarakis SE. 2000. Mutation nomenclature extensions and suggestions to describe complex mutations: a discussion. Hum Mutat. 15:7–12.

Denu, J.M., and Dixon, J.E. 1998. Protein tyrosine phosphatases: Mechanisms of catalysis and regulation. Curr. Opin. Chem. Biol. 2: 633-641

Dias N, Bailly C. 2005. Drugs targeting mitochondrial functions to control tumor cell growth. Biochemical Pharmacology. 70:1-12.

Doonan R, McElwee JJ, Matthijssens F, et al. 2008. Against the oxidative damage theory of aging: superoxide dismutases protect against oxidative stress but have little or no effect on life span in Caenorhabditis elegans. Genes Dev. 22:3236–41.

Dröge, W. 200.. Free radicals in the physiological control of cell function. Physiological reviews. 82:47-95.

Droillard MJ and A. Paulin. 1990 Isozymes of superoxide dismutase in mitochondria and peroxisomes isolated from petals of carnation (Dianthus caryophyllus) during senescence. Plant Physiol. 94:1187-1192.

Ehret G.B. 2010. Genome-wide association studies: contribution of genomics to understanding blood pressure and essential hypertension. Curr Hypertens Rep. 12:17–25.

Lacy, F., D. T. O'Connor, and G. W. Schmid-Schönbein. 1998. Plasma hydrogen peroxide production in hypertensives and normotensive subjects at genetic risk of hypertension. Journal of Hypertension. 16:291–303.

Finley, LWS. and Haigis, MC. 2010. The coordination of nuclear and mitochondrial communication during aging and calorie restriction. Ageing Research Reviews. 8: 173-188.

Forman HJ, Fukuto JM, Torres M. 2004. Redox signaling: thiol chemistry defines which reactive oxygen and nitrogen species can act as second messengers. Am J Physiol Cell Physiol. 287:C246–256.

Forman HJ, Torres M, and Fukuto J. 2002. Redox signaling. Mol Cell Biochem. 234-235:49-62.

Forman JP, Stampfer MJ, Curhan GC. 2009. Diet and lifestyle risk factors associated with incident hypertension in women. JAMA. 302:401–11.

Gavazzi G, Banfi B, Deffert C, Fiette L, Schappi M, Herrmann F, and K.H. Krause. 2006. Decreased blood pressure in NOX1-deficient mice. FEBS Lett. 580:497–504.

Gavazzi G, Deffert C, Trocme C, Schappi M, Herrmann FR, and K.H. Krause. 2007. NOX1 deficiency protects from aortic dissection in response to angiotensin II. Hypertension. 50:189–196.

Gülçin, I. 2010. Antioxidant properties of resveratrol: a structure–activity insight. Innov. Food Sci. Emerg. 11:210–218.

Gu, Y., Wang, X., Wu, G., Wang, X., Cao, H., Tang, Y., & Huang, C. 2012. Artemisinin suppresses sympathetic hyperinnervation following myocardial infarction via anti-inflammatory effects. Journal of Molecular Histology. 1-7.

Gupta, D., K. K. Griendling, W. R. Taylor. 2010. Oxidative Stress and Cardiovascular Disease in Diabetes Mellitus. Studies on Cardiovascular Disorders. Oxidative Stress in Applied Basic Research and Clinical Practice 2010, pp 263-279.

Gurusamy N, Ray D, Lekli I, Das DK. 2010. Red wine antioxidant resveratrol-modified cardiac stem cells regenerate infarcted myocardium. J Cell Mol Med. 14:2235–2239.

Guzik, T.J., W. Chen, M.C. Gongora, B. Guzik, H.E. Lob, D. Mangalat, N. Hoch, S. Dikalov, P. Rudzinski, B. Kapelak, J., and D.G. Sadowski. 2008. Harrison Calcium-dependent NOX5 nicotinamide adenine dinucleotide phosphate oxidase contributes to vascular oxidative stress in human coronary artery disease J. Am. Coll. Cardiol. 52:1803–1809.

Hanna, I. R., Hilenski, L. L., Dikalova, A., Taniyama, Y., Dikalov, S., Lyle, A., ... & Griendling, K. K. 2004. Functional association of nox1 with p22phox in vascular smooth muscle cells. Free Radical Biology and Medicine. 37:1542-1549.

Helmcke I, Heumuller S, Tikkanen R, Schroder K, Brandes RP. 2008. Identification of structural elements in Nox1 and Nox4 controlling localization and activity. Antioxid Redox Signal. 11:1279–1287.

Ho, W.E., Cheng C., Peh HY, Xu F, Tannenbaum SR, Ong CN et al. 2012. Anti-malarial drug artesunate ameliorates oxidative lung damage in experimental allergic asthma. Free Radic Biol Med. 53:498–507.

Huang J, Hitt, N.D, Kleinberg ME. 1995. Stoichiometry of p22-phox and gp91-phox in phagocyte cytochrome b558. Biochemistry. 34:16753–16757

Hung L.M., M.J. Su, W.K. Chu, C.W. Chiao, W.F. Chan, and J.K. Chen. 2002. The protective effect of resveratrols on ischaemia-reperfusion injuries of rat hearts is correlated with antioxidant efficacy Br. J. Pharmacol. 135:1627–1633.

Iyer, G.Y.N., M.F. Islam, and H. Quastel. 1961. Biochemical aspects of phagocytosis. Nature. 192:535–541.

Jagdale, S. C., Kuchekar, B. S., Chabukswar, A. R., Lokhande, P. D., & Raut, C. G. 2009. Anti-oxidant activity of Piper longum Linn. International Journal of Biological Chemistry. 3:119-125.

Jaquet V, Marcoux J, Forest E, Leidal KG, McCormick S, Westermaier Y, Perozzo R, Plastre O, Fioraso-Cartier L, Diebold B, Scapozza L, Nauseef WM, Fieschi F, Krause KH, and Bedard K. 2011. NOX NADPH oxidase isoforms are inhibited by celastrol with a dual mode of action. Br J Pharmacol 164:507–520.

Johnson, J.J., M. Nihal, I.A. Siddiqui, C.O. Scarlett, H.H. Bailey, H. Mukhtar, N. Ahmad. 2011. Enhancing the bioavailability of resveratrol by combining it with piperine Mol. Nutr. Food Res. 55:1169–1176.

Kamaraj, S., Ramakrishnan, G., Anandakumar, P., Jagan, S., & Devaki, T. 2009. Antioxidant and anticancer efficacy of hesperidin in benzo (a) pyrene induced lung carcinogenesis in mice. Investigational new drugs. 27: 214-222.

Kannel WB. 1996. Blood pressure as a cardiovascular risk factor: prevention and treatment. JAMA. 275:1571-1576.

Khanduja KL. 2003. Stable free radical scavenging and antiperoxidative properties of resveratrol in vitro compared with some other bioflavonoids. Ind J Biochem Biophys. 40:416–22.

Klotz L. O., 2002. Oxidant-induced signaling: effects of peroxynitrite and singlet oxygen. Biol. Chem. 383:443–56.

Knez WL, Jenkins DG, Coombes JS. 2007. Oxidative stress in half and full Ironman triathletes. Med Sci Sports Exerc. 39:283-288.

Kristian, T., I. B. Hopkins, M. C. McKenna, and G. Fiskum. 2006. Isolation of mitochondria with high respiratory control from primary cultures of neurons and astrocytes using nitrogen cavitation. J Neurosci Methods. 152: 136-143.

Lambeth JD. 2000. Regulation of the phagocyte respiratory burst oxidase by protein interactions. Biochem Mol Biol. 33:427-439.

Lacy F, Kailasam MT, O'Connor DT, Schmid-Schonbein GW, Parmer RJ. 2000. Plasma hydrogen peroxide production in human essential hypertension: role of heredity, gender, and ethnicity. Hypertension. 36:878–884.

Lancon A., Delma D., Osman H., Thenot J.P., Jannin B., and N. Latruffe. 2004. Human hepatic cell uptake of resveratrol: involvement of both passive diffusion and carrier-mediated process, Biochem Biophys Res Commun. 316:1132-1137

Lania-Pietrzak B., A.B. Hendrich, and K. Michalak. 2004. Perturbation of model lipid membrane structure by resveratrol Curr. Topics Biophys. 28:17–60.

Lee MY, San Martin A, Mehta PK, et al. 2009. Mechanisms of vascular smooth muscle NADPH oxidase 1 (Nox1) contribution to injury-induced neointimal formation. Arterioscler Thromb Vasc Biol. 29:480–487.

Leiro J, Alvarez E, Arranz JA, Laguna R, Uriarte E, Orallo F. 2004. Effects of cis-resveratrol on inflammatory murine macrophages: antioxidant activity and down-regulation of inflammatory genes. J Leukoc Biol 75:1156–1165.

Lekli, I., Ray, D. and Das, DK. 2010. Longevity nutrients resveratrol, wines and grapes. Genes & Nutrition. 5:55-60.

Leonard S.S., C. Xia, B.H. Jiang, B. Stinefelt, H. Klandorf, G.K. Harris, X. Shi. 2003. Resveratrol scavenges reactive oxygen species and effects radical-induced cellular responses Biochem. Biophys. Res. Commun. 309:1017–1026

Li H., Xia N., Forstermann U. 2012. Cardiovascular effects and molecular targets of resveratrol. Nitric Oxide 26:102–110.

Li N, Ragheb K, Lawler G, Sturgis J, Rajwa B, Melendez JA, Robinson JP. 2003. Mitochondrial complex I inhibitor rotenone induces apoptosis through enhancing mitochondrial reactive oxygen species production. J Biol Chem. 278:8516-8525.

Li, N and M. Karin. 1999. Is NF-kappaB the sensor of oxidative stress? FASEB J, 13:1137–1143.

Lim JC, Choi HI, Park YS, Nam HW, Woo HA, Kwon KS, Kim YS, Rhee SG, Kim K, Chae HZ. 2008. Irreversible oxidation of the active-site cysteine of peroxiredoxin to cysteine sulfonic acid for enhanced molecular chaperone activity. J Biol Chem. 283:28873–28880.

Liu B, Chen Y, St Clair DK. 2008. ROS and p53: a versatile partnership. Free Radic Biol Med. 44:1529–1535.

Liu, F., Gomez Garcia, A.M., and Meyskens Jr, F.L. 2012. NADPH oxidase 1 overexpression enhances invasion via matrix metallopro- teinase-2 and epithelial-mesenchymal transition in melanoma cells. J. Invest. Dermatol. 132:2033–2044.

Lloyd R.V., Hanna P.M., and R.P. Mason. 1997. The origin of the hydroxyl radical oxygen in the Fenton reaction. Free Rad Biol Med. 22:885–888.

Lodge, J.K. 2005.Vitamin E bioavailability in humans. J. Plant Physiol. 162:790–796.

Lois C, Hong E, Pease JS, Brown E J, Baltimore D. 2002 Germline transmission and tissue-specific expression of transgenes delivered by lentiviral vectors. Science. 295:868–872.

Lu X, Dang CQ, Guo X, Molloi S, Wassall CD, Kemple MD, and G.S. Kassab. 2011. Elevated oxidative stress and endothelial dysfunction in right coronary artery of right ventricular hypertrophy. J Appl Physiol (March 17, 2011). doi:10.1152/japplphysiol.00744.2009.2011.

Kiaei, M., K. Kipiani, S. Petri, J. Chen, N.Y. Calingasan, M.F. Beal. 2005. Celastrol blocks neuronal cell death and extends life in transgenic mouse model of amyotrophic lateral sclerosis, Neurodegener. Dis. 2:246–254.

Korn, S.H., E.F. Wouters, N. Vos, Y.M. Janssen-Heininger. 2001. Cytokine-induced activation of nuclear factor-kappa B is inhibited by hydrogen peroxide through oxidative inactivation of IkappaB kinase J Biol Chem. 276:35693–35700

Magnani E, Bartling L, Hake S. 2006. From Gateway to MultiSite Gateway in one recombination event. BMC Mol Biol 7: 46.

Makino N, Sasaki K, Hashida K, and Y. Sakakura. 2004. A metabolic model describing the H2O2 elimination by mammalian cells including H2O2 permeation through cytoplasmic and peroxisomal membranes: comparison with experimental data. Biochim Biophys Acta 1673:149–159.

Mancia, G., de Backer, G., Dominiczak, A., Cifkova, R., Germano, G., Grassi, G., Heagerty, A. M., Kjeldsen, S. E., Laurent, S., Narkiewitcz, K. et al. 2007. 2007 Guidelines for the Management of Arterial Hypertension: the Task Force for the Management of Arterial Hypertension of the European Society of Hypertension (ESH) and of the European Society of Cardiology (ESC). J. Hypertens. 6:1105–118.

Marino S. M., and V.N. Gladyshev. 2012. Analysis and functional prediction of reactive cysteine residues. J. Biol. Chem. 287:4419–4425.

Markus, MA. and Morris, BJ. 2008, Resveratrol in prevention and treatment of common clinical conditions of aging. Clinical Interventions in Aging. 3:331-339.

Martindale JL, Holbrook NJ. 2002. Cellular response to oxidative stress: Signaling for suicide and survival. Journal of Cellular Physiology. 192:1–15.

Matsuno K, Yamada H, Iwata K, Jin D, Katsuyama M, Matsuki M, Takai S, Yamanishi K, Miyazaki M, Matsubara H, Yabe- Nishimura C. 2005. Nox1 is involved in angiotensin II-mediated hyper- tension: a study in Nox1-deficient mice. Circulation. 112:2677– 2685.

McClain D E, Kalinich J F, and N. Ramakrishnan. 1995. Trolox inhibits apoptosis in irradiated MOLT-4 lymphocytes. FASEB J. 9:1345–1354.

Meng TC, Lou YW, Chen YY, Hsu SF, Huang YF. 2006. Cys-oxidation of protein tyrosine phosphatases: Its role in regulation of signal transduction and its involvement in human cancers. J Cancer Mol 2:9–16.

Menon SG, Goswami PC. 2007. A redox cycle within the cell cycle: Ring in the old with the new. Oncogene. 26:1101–1109.

Minder CM, Blaha MJ, Horne A, Michos ED, Kaul S, Blumenthal RS. 2012. Evidence-based use of statins for primary prevention of cardiovascular disease. Am J Med. 125:440-6.

Miyano K and H. Sumimoto. 2012. Assessment of the role for Rho family GTPases in NADPH oxidase activation. Methods Mol Biol 827: 195–212.

Moosmann B, Behl C. 2004. Selenoprotein synthesis and side-effects of statins. Lancet. 363:892-894.

Morgan MJ, Liu ZG. 2011. Crosstalk of reactive oxygen species and NF-κB signaling. Cell Res 21:103–115.

Morré, D. J. 2002. Preferential inhibition of the plasma membrane NADH oxidase (NOX) activity by diphenyleneiodonium chloride with NADPH as donor. Antioxidants and Redox Signaling. 4:207-212.

Morrell, C. N. 2008. Reactive Oxygen Species Finding the Right Balance. Circulation research, 103(6). 571-572.

Nathan, C. 2003. Specificity of a third kind: Reactive oxygen and nitrogen intermediates in cell signaling. Journal of Clinical Investigation. 111:769–778.

Nei M., Suzuki Y., Nozawa M. 2010. The neutral theory of molecular evolution in the genomic era. Annu. Rev. Genomics Hum. Genet. 11:265–289.

Nordberg J, Arner ES. 2001. Reactive oxygen species, antioxidants, and the mammalian thioredoxin system. Free Radic. Biol. Med. 31:1287–1312.

O'Donnell, V.B., and A. Azzi. 1996. High rates of extracellular superoxide generation by cultured human fibroblasts: involvement of a lipid-metabolizing enzyme. Biochem. J. 318:805–812.

Ozsoy N, Candoken E, Akev N. 2009. Implications for degenerative disorders: antioxidative activity, total phenols, flavonoids, ascorbic acid, beta-carotene and beta-tocopherol in Aloe vera. Oxid Med Cell Long. 2:99–106.

Paravicini T.M. and R.M. Touyz. 2008. NADPH oxidases, reactive oxygen species, and hypertension: clinical implications and therapeutic possibilities. Diabetes Care. 3:170-80.

Park DW, Baek K, Kim JR, Lee JJ, Ryu SH, Chin BR, and SH Baek. 2009. Resveratrol inhibits foam cell formation via NADPH oxidase 1- mediated reactive oxygen species and monocyte chemotactic protein-1. Exp Mol Med. 41:171–179

Pfeifer A, Ikawa M, Dayn Y., and M.I. Verma. 2002. Transgenesis by lentiviral vectors: Lack of gene silencing in mammalian embryonic stem cells and preim- plantation embryos. Proc Natl Acad Sci USA. 99:2140–2145.

Pignatelli P, Pulcinelli FM, Celestini A, Lenti L, Ghiselli A, Gazzaniga PP, Violi F. 2000. The flavonoids quercetin and catechin synergistically inhibit platelet function by antagonizing the intracellular production of hydrogen peroxide. Am J Clin Nutr. 72:1150–1155.

Poolman TM, Ng LL, Farmer PB, Manson MM. 2005. Inhibition of the respiratory burst by resveratrol in human monocytes: correlation with inhibition of PI3K signaling. Free Radic Biol Med 39:118–132.

Qiu, D., P.N. Kao. 2003. Immunosuppressive and anti-inflammatory mechanisms of triptolide, the principal active diterpenoid from the Chinese medicinal herb Tripterygium wilfordii Hook. F. Drugs R D 4:1–18.

Quie P.G., White J.G., Holmes B., and R.A. Good. 1967. In vitro bactericidal capacity of human polymorphonuclear leukocytes: diminished activity in chronic granulomatous disease of childhood. J Clin Invest. 46:668–679

Ray, P. D., Huang, B. W., & Tsuji, Y. 2012. Reactive oxygen species (ROS) homeostasis and redox regulation in cellular signaling. Cellular signalling.

Reuter, S., Gupta, S. C., Chaturvedi, M. M., & Aggarwal, B. B. 2010. Oxidative stress, inflammation, and cancer: how are they linked?. Free Radical Biology and Medicine. 49: 1603-1616.

Rhee SG, Jeong W, Chang TS, Woo HA. 2007. Sulfiredoxin, the cysteine sulfinic acid reductase specific to 2-Cys peroxiredoxin: its discovery, mechanism of action, and biological significance. Kidney Int Suppl. S3–8.

Roos, D. 1994. The genetic basis of chronic granulomatous disease. Immunol. Rev. 138:121–157.

Roos, D., Kuhns, D. B., Maddalena, A., Bustamante, J., Kannengiesser, C., de Boer, M., & Stasia, M. J. 2010. Hematologically important mutations: the autosomal recessive forms of chronic granulomatous disease (second update). Blood Cells, Molecules, and Diseases. 44: 291-299

Royer-Pokora, Brigitte, Louis M. Kunkel, Anthony P. Monaco, Sabra C. Goff, Peter E. Newburger, Robert L. Baehner, F. Sessions Cole, John T. Curnutte, and Stuart H. Orkin. 1986. Cloning the gene for an inherited human disorder—chronic granulomatous disease—on the basis of its chromosomal location. Nature. 322:32-38.

San Jose, G., Fortuno, A., Diez, J., & Zalba, G. 2008. NADPH oxidase CYBA polymorphisms, oxidative stress and cardiovascular diseases. Clinical Science. 114:173-182.

Sassa H, Takaishi Y, Terada H. 1990. The triterpene celastrol as a very potent inhibitor of lipid peroxidation in mitochondria. Biochem Biophys Res Commun. 172:890–897.

Sassa, H., K. Kogure, Y. Takaishi, H. Terada 1994. Structural basis of potent antiperoxidation activity of the triterpene celastrol in mitochondria: effect of negative membrane-surface charge on lipid peroxidation Free Radic. Biol. Med. 17:201–207.

Scherr M, Battmer K, Bloemer U, Ganser A, Grez M. 2001. Determination of lentiviral vector particles using quantitative real-time PCR. Biotechniques. 31:520-526.

Schneider-Poetsch, T., Ju, J., Eyler, D. E., Dang, Y., Bhat, S., Merrick, W. C., & Liu, J. O. 2010. Inhibition of eukaryotic translation elongation by cycloheximide and lactimidomycin. Nature chemical biology. 6:209-217.

Schreck, R., P. Rieber, P.A. 1991. Baeuerle Reactive oxygen intermediates as apparently widely used messengers in the activation of the NF-kappa B transcription factor and HIV-1 EMBO J, 10:2247–2258

Sharma G, Berger JS. 2011. Platelet activity and cardiovascular risk in apparently healthy individuals: a review of the data. J Thromb Thrombolysis. 32:201-208.

Shaulian, E., and M. Karin. 2002. AP-1 as a regulator of cell life and death. Nat. Cell Biol. 4:E131-E136.

Shen M.Y., G. Hsiao, C.L. Liu, T.H. Fong, K.H. Lin, D.S. Chou and, J.R. Sheu. 2007. Inhibitory mechanisms of resveratrol in platelet activation: pivotal roles of p38 MAPK and NO/cyclic GMP Br. J. Haematol. 139:475–485

Shukla S, Gupta S. 2010. Apigenin: a promising molecule for cancer prevention. Pharm Res 27:962–978.

Sies H. 1993. Strategies of antioxidant defense. Eur J Biochem. 215:213–219.

Souri, E., Amin, G., Farsam, H., Jalalizadeh, H., & Barezi, S. 2010. Screening of thirteen medicinal plant extracts for antioxidant activity. Iranian Journal of Pharmaceutical Research. 7: 149-154.

Spanier G, Xu H, Xia N, Tobias S, Deng S, Wojnowski L, Forstermann U, Li H. 2009. Resveratrol reduces endothelial oxidative stress by modulating the gene expression of superoxide dismutase 1 (SOD1), glutathione peroxidase 1 (GPx1) and NADPH oxidase subunit (Nox4). J Physiol Pharmacol 60:111–116.

Starkov, A.A., 2008. The role of mitochondria inreactive oxygen species metabolism and signaling. Ann. NY Acad. Sci. 1147:37–52.

Statistics Canada. Morality, Summary List of Causes 2008. Released October 18, 2011.

Steffen Y, Schewe T, Sies H. 2007. (-)-Epicatechin elevates nitric oxide in endothelial cells via inhibition of NADPH oxidase. Biochem Biophys Res Comm. 359:828–33.

Sun Y and LW Oberley. Redox regulation of transcriptional activa-tors. 1996. Free Radical Biol Med. 21:335–348.

Sundaresan, M., Z.X. Yu, V.J. Ferrans, K. Irani, and T. Finkel. 1995. Requirement for generation of H2O2 for platelet-derived growth factor signal transduction. Science. 270:296–299.

Sumimoto, H., Kage, Y., Nunoi, H., Sasaki, H., Nose, T., Fukumaki, Y., Ohno, M., Minakami, S. and Takeshige, K. 1994. Role of Src homology 3 domains in assembly and activation of the phagocyte NADPH oxidase. Proc. Natl. Acad. Sci. USA. 91:5345-5349.
Sumimoto, H., Hata, K., Mizuki, K., Ito, T., Kage, Y., Sakaki, Y., Fukumaki, Y., Nakamura, M. and Takeshige, K. 1996. Assembly and activation of the phagocyte NADPH oxidase: Specific Interaction of the N-terminal Src homology 3 domain of p47phox with p22phox is required for activation of the NADPH oxidase complex. J. Biol. Chem. 36:2152- 22158.

Suter D. M., Cartier L., Bettiol E., Tirefort D., Jaconi M. E., Dubois-Dauphin M., Krause K. H. 2005. Rapid generation of stable transgenic embryonic stem cell lines using modular lentivectors. Stem Cells 24:615–623.

Szkudelski T, Szkudelska K. 2011. Anti-diabetic effects of resveratrol. Ann N Y Acad Sci. 1215:34–39.

Terada LS. 2006. Specificity in reactive oxidant signaling: Think globally, act locally. Journal of Cell Biology. 174:615–623.

Tonks NK. 2006. Protein tyrosine phosphatases: from genes, to function, to disease. Nat Rev Mol Cell Biol. 7:833–846.

Touyz, R.M., A.C. Montezano. 2012. Vascular NOX4: a multifarious NADPH oxidase Circ. Res., 110:1159–1161.

Trachootham, D., Lu, W., Ogasawara, M. A., Valle, N. R. D., & Huang, P. 2008. Redox regulation of cell survival. Antioxidants & redox signaling. 10:1343-1374.

Ueno, N., Takeya, R., Miyano, K., Kikuchi, H., & Sumimoto, H. 2005. The NADPH Oxidase Nox3 Constitutively Produces Superoxide in a p22phox-dependent Manner. Journal of Biological Chemistry. 280:23328-23339.

Ungvari Z, Labinskyy N, Mukhopadhyay P, Pinto JT, Bagi Z, Ballabh P, Zhang C, Pacher P, Csiszar A. 2009. Resveratrol attenuates mitochondrial oxidative stress in coronary arterial endothelial cells. Am J Physiol Heart Circ Physiol. 297:H1876–H1881.

Ungvari Z., Z. Orosz, A. Rivera, N. Labinskyy, Z. Xiangmin, S. Olson, A. Podlutsky, A. Csiszar. 2007. Resveratrol increases vascular oxidative stress resistance Am. J. Physiol. Heart Circ. Physiol., 292:H2417–2424

van Rijn, M. J., Schut, A. F., Aulchenko, Y. S., Deinum, J., Sayed-Tabatabaei, F. A., Yazdanpanah, M., Isaacs, A., Axenovich, T. I., Zorkoltseva, I. V., Zillikens, M. C. et al. 2007. Heritability of blood pressure traits and the genetic contribution to blood pressure variance explained by four blood pressure-related genes. J. Hypertens. 25:565–570

Vang O, Ahmad N, Baile CA, Baur JA, Brown K, Csiszar A, Das DK, Delmas D, Gottfried C, Lin HY, Ma QY, Mukhopadhyay P, Nalini N, Pezzuto JM, Richard T, Shukla Y. 2011. What is new for an old molecule? Systematic review and recommendations on the use of resveratrol. PLoS One. 6:e19881.

Vaziri ND, Wang XQ, Oveisi F, Rad B. 2000. Induction of oxidative stress by glutathione depletion causes severe hypertension in normal rats. Hypertension. 36:142–146.

Vinck, W. J., Fagard, R. H., Loos, R. and Vlietinck, R. 2001. The impact of genetic and environmental influences on blood pressure variance across age-groups. J. Hypertens. 19: 1007–1013

Vogel C, Marcotte EM .2012. Insights into the regulation of protein abundance from proteomic and transcriptomic analyses. Nat Rev Genet 13:227–232.

Volpp, B. D., Nauseef, W. M., & Clark, R. A. 1988. Two cytosolic neutrophil oxidase components absent in autosomal chronic granulomatous disease. Science (New York, NY). 242:1295.

Vroemen M, Weidner N, and A. Blesch. 2005. Loss of gene expression in lentivirus- and retrovirus-transduced neural progenitor cells is correlated to migration and differentiation in the adult spinal cord. Exp Neurol. 195:127-39.

Wagner AH, Kohler T, Ruckschloss U, Just I, Hecker M. 2000. Improvement of nitric oxide-dependent vasodilatation by HMG-CoA reductase inhibitors through attenuation of endothelial superoxide anion formation. Arterioscler Thromb Vasc Biol. 20:61–69.

Wind, S., K. Beuerlein, M.E. Armitage, A. Taye, A.H. Kumar, D. Janowitz. 2010. Oxidative stress and endothelial dysfunction in aortas of aged spontaneously hypertensive rats by NOX1/2 is reversed by NADPH oxidase inhibition Hypertension. 56:490–497

Wong, W. S. F., Cheng, C., & Ho, W. E. 2012. Anti-malarial drug artesunate is an effective drug for allergy and asthma. Zhongguo Yaolixue yu Dulixue Zazhi- Chinese Journal of Pharmacology and Toxicology. 26: 718.

Woo HA, Chae HZ, Hwang SC, Yang KS, Kang SW, Kim K, and Rhee SG. 2003. Reversing the inactivation of peroxiredoxins caused by cysteine sulfinic acid formation. Science 300:653–656.

Wu JM, Hsieh TC, Wang Z. 2011. Cardioprotection by resveratrol: a review of effects/targets in cultured cells and animal tissues. Am J Cardiovasc Dis. 1:38-47.

Wyche KE, Wang SS, Griendling KK, Dikalov SI, Austin H, Rao S, Fink B, Harrison DG, Zafari AM. 2004. C242T CYBA polymorphism of the NADPH oxidase is associated with reduced respiratory burst in human neutrophils. Hypertension. 43:1246–1251

Xia, E., Deng, G-F., Guo, Y-J. and LI, HB. 2010. Biological active of polyfenols from grapes. Int. J. Mol. Sciences. 11:622-646.

Xu, L, Zhang, L, Bertucci, AM. 2008. Apigenin a dietary flavonoid sensitizes human T cells for activation-induced cell death by inhibiting PKB/Akt and NF-κB activation pathway. Immunol Lett. 121:74–83.

Yaffe, P. B., Doucette, C. D., Walsh, M., & Hoskin, D. W. 2012. Piperine impairs cell cycle progression and causes reactive oxygen species-dependent apoptosis in rectal cancer cells. Experimental and molecular pathology. 94: 109–114.

Yorek, M. A. 2003. The role of oxidative stress in diabetic vascular and neural disease. Free Radic. Res. 37:471–480.

Zafari AM, Davidoff MN, Austin H, Valppu L, Cotsonis G, Lassegue B, Griendling KK. 2002. The A640G and C242T p22phox polymorphisms in patients with coronary artery disease. Antioxid Redox Signal. 4:675–680.

Zhang H, Zhang J, Ungvari Z, and C. Zhang. 2009. Resveratrol improves endothelial function: role of TNF{alpha} and vascular oxidative stress. Arterioscler Thromb Vasc Biol. 29:1164–71

Zhou Q, Liao JK. 2010. Pleiotropic effects of statins. Basic research and clinical perspectives. Circ J. 74:818–826.